Low-cost Interference Mitigation and Relay Processing for Cooperative DS-CDMA Systems

Jiaqi Gu

Doctor of Philosophy

University of York

Electronics

August 2016

Abstract

In wireless communications, propagation aspects such as fading, shadowing and path loss are the major constraints that seriously limit the overall performance of systems. Indeed, severe fading has a detrimental effect on the received signals and can lead to a degradation of the transmission of information and the reliability of the network. In this case, diversity techniques are introduced in order to mitigate fading. Among various kinds of diversity techniques, cooperative diversity with relaying nodes is a modern technique that has been widely considered in recent years as an effective tool to deal with this problem. Several cooperative protocols have been proposed in the literature, and among the most effective ones are Amplify-and-Forward (AF) and Decode-and-Forward (DF).

Cooperative diversity can be combined with direct sequence code division multiple access (DS-CDMA) systems to further enhance the information security. However, due to the multiple access interference (MAI) that arises from nonorthogonal received waveforms in the DS-CDMA systems, the system performance may easily be affected. To deal with this issue, novel multiuser detection (MUD) technique is introduced as a useful relay processing strategy for the uplink of cooperative DS-CDMA systems. Apart from that, distributed space-time coding (DSTC) is another effective approach that can be combined with cooperative diversity to further improve the transmission performance. Moreover, in order to increase the throughput of the cooperative DS-CDMA network, physical-layer network coding (PNC) scheme is then adopted together with the cooperative DS-CDMA network. Clearly, better performance gain and lower power consumption can be obtained when appropriate relaying strategies are applied.

Contents

List of Tables

List of Algorithms

List of Figures

Acknowledgements

I would like to show my sincere gratitude to my supervisor, Prof. Rodrigo C. de Lamare, for his support and encouragement during my PhD study.

I am very grateful to my thesis advisor, Dr. Yuriy Zakharov, whose insightful discussions and suggestions have benefited me.

I would also like all may friends and colleagues in the Communications and Signal Processing Research Group.

The research presented in this thesis has been funded jointly funded by ESII and University of York.

This thesis is dedicated to my parents.

Declaration

All work presented in this thesis as original is so, to the best knowledge of the author. References and acknowledgements to other researchers have been given as appropriate.

Elements of the research presented in this thesis have resulted in some publications. A list of these publications can be found below.

Journal Papers

1. J. Gu and R. C. de Lamare, "Buffer-Aided Distributed Space-Time Coding Schemes and Algorithms for Cooperative DS-CDMA Systems", *Eurasip Journal on wireless communication and networking.* (accepted)

2. J. Gu and R. C. de Lamare, "Joint Interference Cancellation and Relay Selection Algorithms Based on Greedy Techniques for Cooperative DS-CDMA Systems", *Eurasip Journal on wireless communication and networking.*, pp. 1-19, Feb. 2016

Conference Papers

1. J. Gu and R. C. de Lamare, "Buffer-aided Distributed Space Time Coding Techniques for Cooperative DS-CDMA Systems", *Proc. IEEE International Conference on Acoustics, Speech and Signal Processing (ICASSP)*, pp. 3626-3630, Shanghai, China, March, 2016.

2. J. Gu and R. C. de Lamare, "Dynamic Buffer-aided Distributed Space Time Coding Technique for Cooperative DS-CDMA Systems", *ITG/IEEE Workshop on Smart Antennas (WSA)*, pp. 1-6, Munich, Germany, March, 2016.

3. J. Gu and R. C. de Lamare, “Joint SIC and Multi-relay Selection Algorithms for Cooperative DS-CDMA Systems”, *European Signal. Processing Conference (EUSIPCO)*, pp. 556-560, Lisbon, Portugal, September, 2014.

4. J. Gu and R. C. de Lamare, “Joint Parallel Interference Cancellation and Relay Selection Algorithms Based on Greedy technique for Cooperative DS-CDMA Systems”, *Proc. IEEE International Conference on Acoustics, Speech and Signal Processing (ICASSP)*, pp. 2754-2758, Florence, Italy, May, 2014.

Chapter 1

Introduction

Contents

1.1 Overview

Initially demonstrated in 1896 by Guglielmo Marconi [2, 3], wireless communication is, by any measure, the fastest growing segment of the communication industry. With over 100 years' rapid evolution of communication engineering, it has become an essential part in every aspect of modern life ranging from smart phones to computers, bluetooth, GPS, Wi-Fi technologies and satellite communications. The increasing demand for high-quality transmission, secure information and substantial system capacity, however, present key challenges to modern wireless communication systems.

In order to overcome these challenges, one potential solution is code division multiple-access (CDMA) implemented with direct-sequence (DS) spread spectrum.

DS-CDMA is among the most promising multiple acess technologies for current and future telecommunications services such as ad-hoc wireless communications, military communication and sensor networks. The advantages of DS-CDMA include superior capabilities in multipath environments, flexibility in the allocation of channels, increased capacity in burst and fading situations, and the ability to share bandwidth with narrowband communication systems without deterioration of either's systems performance [4]. However, due to the multiple access interference (MAI) effect that arises from nonorthogonal received waveforms and narrowband interfering signals in DS-CDMA systems, the system performance may easily be affected. To deal with this issue, multiuser detection (MUD) techniques have been developed [5] as an effective approach to suppress MAI. The optimal detector, known as maximum likelihood (ML) detector, has been proposed in [6]. However, this method is infeasible for ad hoc and sensor networks considering its computational complexity. Motivated by this fact, several sub-optimal strategies have been developed, including the linear detector [7], the successive interference cancellation (SIC) [8], the parallel interference cancellation (PIC) [9] and the minimum mean-square error (MMSE) decision feedback detector [10].

Another effective solution to meet these challenges is the employment of diversity techniques [4, 11]. Specifically, diversity is one of the most powerful communication techniques that is able to mitigate the effect of fading arising from the propagation effect. Among various forms of diversity techniques, cooperative diversity is particularly attractive as it exploits the broadcast nature and the inherent spatial diversity of the channel. It allows terminals to share their antennas and relay messages to each other to create a distributed array through distributed transmissions and signal processing [12]. There are two main cooperative protocols, Amplify-and-Forward (AF) [13] and Decode-and-Forward (DF) [12]. For an AF protocol, relays amplify the received signals with a given transmit power, this method is simple except for the fact that the relays also amplify their own noise. For a DF protocol, relays decode the received signals and then forward the re-encoded message to the destination. Naturally, in order to reduce the error propagation and achieve more accurate detection results, MUD techniques can be applied at both the relays and the destination of an uplink of a cooperative DS-CDMA system.

In addition to that, distributed space-time coding (DSTC) [14–18] is another diversity

technique that can be applied at the relays of cooperative DS-CDMA systems. It exploits spatial and temporal transmit diversity by using a set of distributed antennas. Specifically, with DSTC, multiple redundant copies of data are sent to the receiver to improve the quality and reliability of data transmission. Applying DSTC at the relays in cooperative systems provides multiple processed signal copies to compensate for the fading and noise, helping to achieve the attainable diversity and coding gains so that the interference can be more effectively mitigated. Among various DSTC techniques, Alamouti [19] proposed a simple and useful transmit diversity scheme to improve the overall performance of wireless communication systems.

Moreover, since better performance can be achieved when appropriate signal processing and relay selection strategies are applied, another alternative relay processing technique that can be corporated with the cooperative scenario is physical-layer network coding (PNC) schemes [20–23]. PNC schemes have significant advantages in wireless multi-hop networks, where multiple relay nodes are provided to assist multiple source nodes to transfer data to one or more destinations. More precisely, they allow a node to exploit as far as possible all signals that it receives simultaneously, rather than treating them as interference [24]. Instead of decoding each incoming data stream separately, a node detects and forwards some function of the incoming data streams [24, 25]. This technique is a newly-emerged tool which helps to improve the potential network throughput and the degree of system robustness.

In summary, the exponential growth of development in overcoming these challenges with low cost and near ML performance is the current general trend of wireless communication systems.

1.2 Motivation

In this thesis, a number of innovative relay processing techniques for dealing with interference cancellation, multipath fading mitigation and network throughput enhancement are proposed for cooperative DS-CDMA systems in wireless sensor networks, which require low computational complexity and high transmission

performance. However, the conflict between high performance transmission, delay requirements, throughput and computational complexity becomes a limitation, which has motivated us to seek different relay processing techniques in order to balance and satisfy.

When investigating the MUD techniques that are employed at both the relays and the destination of a cooperative DS-CDMA system, it is not difficult to find that the existing successive interference cancellation (SIC) and parallel interference cancellation (PIC) algorithms often require matrix inversions and have a performance that is not close to the optimal ML detector. Inspired by that, based on the traditional SIC and PIC strategies, a greedy list-based design that splits users into either reliable or unreliable groups for further examination is developed and used at both the relays and the destination in order to obtain improved detection results. In particular, the proposed MUD techniques, along with an innovative greedy relay selection algorithm, provide a good balance between low cost and high quality performance.

There is a high possibility that the transmission performance may easily be influenced by the outside environment. In this case, a selection between received information at each relay is required as seriously affected data may cause error propagation in the next phase of transmission. Motivated by that, the idea of using buffer to store data prior to transmission at suitable times is introduced. In particular, in the cooperative DS-CDMA system, each relay is equipped with a dynamic buffer to accommodate enough candidate data. After that, in order to obtain further diversity gain and combat fading, a DSTC scheme is performed in the following relay-destination phase. Specifically, the proposed algorithm begins with a channel combination selection between both the source-relay links and relay-destination links to further improve the transmission reliability. With the help of buffers, information is sent under good conditions to guarantee that the loss and damage is minimized to an acceptable level. In addition, with the dynamic design of buffers, the proposed schemes take advantage of the high storage capacity where multiple blocks of data can be stored so that the most appropriate ones can be selected at a suitable time instant. On the other hand, with DSTC, multiple redundant copies of data are sent to the receiver to improve the quality and reliability of data transmission. Applying DSTC at the relays provides multiple processed signal copies to compensate for the fading and noise, helping to achieve the attainable diversity and coding gains so that the interference can be more effectively mitigated.

Finally, a buffer-aided physical-layer network coding (PNC) scheme is proposed for cooperative DS-CDMA networks. Similarly, the idea of using a buffer is introduced to effectively exploit the extra degrees of freedom allowed by extra storage and delay. The buffer-aided approach starts with a channels selection procedure among all link combinations and the selected relays associated with the optimum link combination are then used and prepared for either transmission or reception, each relay in this system is equipped with a buffer so that a reduced amount of data needs to be stored. After that, the PNC scheme is performed and the network coded symbol (NCS) at each relay is sent to the destination. Unlike traditional strategies that treat interference as a nuisance to be avoided, PNC techniques take the advantage of superposition of signals and embrace the interference to improve the system throughput.

1.3 Contributions

The main contributions of this thesis can be summarized as follows:

- a low-cost greedy list-based successive interference cancellation (GL-SIC) multiuser detection method that can be applied at both the relays and the destination of cooperative systems is proposed. This strategy adopts RAKE receivers as the front-end, which reduces computational complexity by avoiding the matrix inversion required when MMSE filters are applied. Unlike prior art, the proposed GL-SIC algorithm exploits the Euclidean distance between the signals associated with the users of interest and their nearest constellation points, together with multiple ordering at each stage, GL-SIC examines all tentative lists of detection candidates so that the optimum or near-optimum detection can be achieved.

- A low-cost greedy list-based parallel interference cancellation (GL-PIC) strategy which employs RAKE receivers as the front-end and can approach the ML detector performance is also developed. This algorithm automatically divides all users into two candidate groups by comparing the Euclidean distance between the signals associated with the users of interest and their nearest constellation points

with a given threshold. The GL-PIC method then re-examines the reliability of some chosen estimates to ensure relevant lists of tentative decisions are checked.

- A low-complexity multi-relay selection algorithm based on greedy techniques that can approach the performance of an exhaustive search is then presented. In the proposed greedy algorithm, a selection rule is employed via several stages. At each stage, a limited number of relay combinations is examined and compared, resulting in a low-cost strategy to approach the performance of an exhaustive search.

- A buffer-aided distributed space-time coding (DSTC) scheme that can store enough data packets in the corresponding buffer entries according to different criteria so that more appropriate symbols can be selected in a suitable time instant is introduced. Furthermore, the computational complexity required by the proposed relay pair selection algorithm, the problem of the average delay brought by the proposed schemes and algorithms is analyzed, followed by the discussion of the proposed greedy algorithm.

- A buffer-aided physical-layer network coding (PNC) technique that is able to encode the detected symbols with an exclusive-or (XOR) mapping and linear network coding techniques and then forward the encoded signals to the destination is presented. In this design, each relay is equipped with a buffer so that the most suitable symbols are sent to the encoding process when relays are under the reception mode. Similarly, the selected encoded symbols are sent to the destination when the relays are under transmission mode. Additionally, the analysis of the computational complexity and sum-rate are then presented.

1.4 Thesis Outline

The rest of the thesis is organized as follows:

- Chapter 2 presents a literature review of the techniques that are used at the relays in cooperative DS-CDMA systems. These techniques include multiuser detection (MUD), space-time coding (STC) schemes and physical-layer network coding (PNC) strategies.

- Chapter 3 presents a joint interference cancellation and greedy relay selection techniques in cooperative DS-CDMA system. The computational complexity of different relay selection algorithms is detailed and compared. Additionally, a cross-layer design strategy that combines the proposed MUD techniques with the proposed greedy multi-relay selection algorithm is also introduced.

- Chapter 4 presents a buffer-aided DSTC schemes and algorithms for cooperative DS-CDMA systems. Buffers with dynamic size are equipped at each relay to increase the reliability of transmission, additional performance gain is achieved when relay selection technique is operated in the relay-destination links. Then the analysis of the computational complexity required by the proposed relay pair selection algorithm, the problem of the average delay brought by the proposed schemes and the proposed greedy relay pair selection algorithms are discussed.

- Chapter 5 presents a buffer-aided PNC schemes for the uplink of the cooperative DS-CDMA systems. Similarly, each relay is equipped a buffer to ensure that the information is transmitted at the most appropriate time instant. The XOR mapping and a novel linear PNC scheme are employed at the relay to process the information received from the sources.

- Chapter 6 presents the conclusions and discussions of possible future work based on the content of the thesis.

1.5 Notation

In this thesis, we use boldface upper and boldface lower fonts to denote matrices and vectors, respectively. $(.)^T$ and $(.)^H$ represent the transpose and Hermitian transpose, respectively. $(.)^{-1}$ stands for the matrix inversion, $E[.]$ denotes the expected value, $|\ .\ |$ indicates the absolute value of a scalar and $\|\ .\ \|$ implies the norm of a vector.

Chapter 2

Literature Review

Contents

2.1 Introduction

This chapter presents the backgrounds of the conventional techniques that are used throughout the associated system models, namely, DS-CDMA and cooperative relaying systems. We first describe the spread spectrum technique where CDMA is derived from, then some existing MUD techniques that are used for mitigating interference are carefully discussed. Consequently, an overview and description of the specific transmission process together with different protocols utilized in the cooperative networks is introduced. At last, an introduction of distributed space-time coding (DSTC) techniques and physical-layer network coding (PNC) are detailed [26].

2.2 Direct Sequence Spread Spectrum System

Initially developed for communication security and military antijamming applications in mid-1950s, spread spectrum (SS) has then gradually occupied a dominant role in commercial services due to its flexibility and multiuser properties [5, 26]. The underlying idea of spread spectrum is to expand the transmission bandwidth while maintaining the same signal power, resulting the power spectrum density (PSD) reduces to a lower level and makes the received spread spectrum signal hardly to be distinguished from the spectrum. As a result, these characteristics make the signal more resistant to the attacks from narrow band jamming, radio interference and hostile eavesdropping [27]. Among various ways of spreading the content of data over a given bandwidth, direct sequence (DS) spread spectrum [28] is one of the most effectively available techniques [26].

DS spread spectrum executes the spreading process by modulating the transmitted symbol stream with a higher rate binary chip sequence. Assume that each symbol of duration T_s is spread into multiple chips of duration T_c, where $T_c < T_s$ and $N = T_s/T_c$ represents the processing gain or the spreading factor. In practice, the entire spreading process is controlled by a pseudorandom noise (PN) code, where the PN code is a binary pseudo-random sequence. After spreading, a chip pulse shaping filter $p(t)$ is employed to shape the chip sequence so that the bandwidth of the output can be limited [26]. Mathematically, the spread spectrum modulated signal can be expressed by:

$$x(t) = A \sum_{i=-\infty}^{+\infty} b(i) s_i(t - iT), \tag{2.1}$$

where $b(i) \in \{\pm 1\}$ denotes the i-th symbol, A stands for the amplitude and

$$s_i(t) = \frac{1}{\sqrt{N}} \sum_{n=1}^{N} a_i(n) p(t - nT_c + T_c) \tag{2.2}$$

represents the real-valued spreading waveform for the i-th symbol, $a_i(n) \in \{\pm 1\}$, $p(t)$ is the chip waveform.

The desired signal is filtered by a matched filter causing the narrow band noise to be spread and the wideband information to be de-spread (recovered). In other words, the interference power is reduced by N, which, obviously, made it easier to extract the signal of interest from the background noise or interference.

2.3 Multiuser Detection for DS-CDMA System

Multiuser detection (MUD) helps to demodulate the mutually interfering signals and it is widely used in various aspects of communications. In this section, we mainly focus on the development of multiuser detection techniques for the DS-CDMA systems. We introduce the optimum maximum likelihood detector at the first stage, followed by the linear minimum mean-square error (MMSE) detector. Interference cancellations including the successive interference cancellation (SIC) and parallel interference cancellation (PIC) are presented at last.

2.3.1 Optimum Multiuser Detector

The optimum MUD is performed based on the maximum likelihood (ML) detection algorithm. Unlike the conventional single-user matched filter, which is regarded as the optimal detector in single-user CDMA channel that requires no prior knowledge beyond the signature waveforms and user timing information, the ML receiver needs to know not only the signature waveforms, but also the received amplitudes for all users and the noise power. Since the transmitted data are equiprobable and independent, the received signal can be expressed by

$$\mathbf{y}(i) = \sum_{k=1}^{K} A_k b_k(i) h_k(i) \mathbf{s}_k(i) + \mathbf{n}(i) \tag{2.3}$$

and the likelihood function is equivalent to obtain the minimum Euclidean distance as expressed by [5]:

$$[\hat{b}_1(i), \hat{b}_2(i), ..., \hat{b}_k(i)] = \min_{b_1(i),...,b_k(i)\in\{\pm 1\}} \left\| \mathbf{y}(i) - \sum_{k=1}^{K} A_k b_k(i) h_k(i) \mathbf{s}_k(i) \right\|^2 \tag{2.4}$$

where i denotes the symbol index, A_k is the received amplitude of the k-th user, $h_k(i)$ is the channel coefficient for user k and the $N \times 1$ vector $\mathbf{s}_k(i)$ represents the signature waveform assigned to the k-th user. It is not difficult to realize that the optimal solution to (2.4) is attained through an exhaustive search of all possible combinations of the user symbols, namely, computes $(\left\| \mathbf{y}(i) - \sum_{k=1}^{K} A_k b_k(i) h_k(i) \mathbf{s}_k(i) \right\|^2)$ for every possible combination and picks one with the lowest cost. With K users involved in the

transmission, an exponential complexity of 2^K need to be experienced, limiting its application in practical communication systems.

2.3.2 Linear Minimum Mean-Square Error (MMSE) Detector

Motivated by the fact that the ML receiver requires a considerable complexity, other alternative sub-optimal strategies have been proposed to provide a good trade-off between the computational complexity and the performance. Minimum mean-square error (MMSE) parameter estimation is a common approach in estimation theory where we estimate a random variable W based on the observations Z, this is equivalent to find a $\hat{W}(Z)$ that can approach W as close as possible, therefore, we are able to minimize the following mean-square error (MSE) [5]:

$$E[(W - \hat{W}(Z))^2] \tag{2.5}$$

In real signal transmissions, (2.5) can be further extended as $E[|b_k(i) - \hat{b}_k(i)|^2]$, this problem thus can be cast as the following optimization:

$$\mathbf{w}_{\text{k,opt}}(i) = \arg \min_{\mathbf{w}_k} E[\mid b_k(i) - \mathbf{w}_k^H(i)\mathbf{y}(i) \mid^2], \tag{2.6}$$

where i denotes the symbol index, $\mathbf{y}(i) = \sum_{k=1}^{K} A_k b_k(i) h_k(i) \mathbf{s}_k(i) + \mathbf{n}(i)$ denotes a $N \times 1$ received signal vector, $\mathbf{s}_k(i)$ is a $N \times 1$ signature waveform and $\mathbf{n}(i)$ is a $N \times 1$ noise vector. $\mathbf{w}_k(i)$ represents a $N \times 1$ filter for user k. By taking the gradient with respect to $\mathbf{w}_k(i)$ and equating to zero, we can obtain the follows:

$$E[b_k(i)\mathbf{y}(i) - \mathbf{y}(i)\mathbf{y}(i)^H \mathbf{w}_k] = 0. \tag{2.7}$$

On the left-hand side we have

$$E[b_k(i)\mathbf{y}(i)] = A_k h_k(i) \mathbf{s}_k(i), \tag{2.8}$$

$$E[\mathbf{y}(i)\mathbf{y}^H(i)] = \sigma^2 \mathbf{I} + \sum_{k=1}^{K} A_k^2 |h_k|^2(i) \mathbf{s}_k(i) \mathbf{s}_k^H(i), \tag{2.9}$$

where $\mathbf{I}$ denotes the $N \times N$ identity matrix. Therefore, the expression of the linear MMSE filter is formed as:

$$\begin{aligned} \mathbf{w}_{\text{k,opt}}(i) =& E[\mathbf{y}(i)\mathbf{y}^H(i)]^{-1} E[b_k(i)\mathbf{y}(i)] \\ =& A_k [\sigma^2 \mathbf{I} + \sum_{k=1}^{K} A_k^2 |h_k|^2(i) \mathbf{s}_k(i) \mathbf{s}_k^H(i)]^{-1} h_k(i) \mathbf{s}_k(i). \end{aligned} \tag{2.10}$$

Following that, an linear estimate of the transmitted symbol can be computed as:

$$\hat{b}_k(i) = Q(\mathbf{w}_{\text{k,opt}}(i)^H \mathbf{y}(i)), \tag{2.11}$$

where $Q(\cdot)$ is a slicer (a basic decision-making operator that maps the soft output into 1 when the corresponding result is greater than 1, and map it to -1 when the corresponding result is less than 0). From the above equations, it can seen that the MMSE filter considers the effect of the background noise with a relatively lower complexity when compared with the ML detector, however, a matrix inversion of high complexity is still required.

2.3.3 Successive Interference Cancellation (SIC)

Successive interference cancellation (SIC) is one of the most popular non-linear MUD methods and it is ideal for the scenario where each user has a differential power gap [8]. This algorithm operates in a serial fashion, where at each successive stage, if a decision has been made about the current strongest user, then this interfering signal can be recreated and subtracted from the received waveforms at the next stage. The whole process is iteratively repeated for up to K interferers and a good performance can be achieved provided that the decision made on each user is correct. Therefore, the received signal at the j-th stage of SIC is given by:

$$\mathbf{y}^j(i) = \mathbf{y}(i) - \sum_{k=1}^{j-1} A_k \hat{b}_k(i) h_k(i) \mathbf{s}_k(i), \tag{2.12}$$

where $\mathbf{y}(i)$ is the total received signal, $\hat{b}_k(i)$ is the detected symbol from the previous stage and $h_k(i)$ is the channel coefficient for user k. Consequently, the detected result for the user k at the j-th stage is expressed as:

$$\hat{b}_k^j(i) = Q\big((\mathbf{w}_k^j)^H(i)\mathbf{y}^j(i)\big), \tag{2.13}$$

where $Q(\cdot)$ represents a slicer and $\mathbf{w}_k^j(i)$ is the filter for user k used at the j-th stage of the SIC process. The performance of SIC can be improved by optimizing the detected order for each user in terms of the power strength. Namely, mitigating the interference brought by the user with the current strongest power can help to approach the largest reduction in MAI and obtain a better detection performance.

2.3.4 Parallel Interference Cancellation (PIC)

An alternative method that works better than SIC in the situation when all of the users are received with equal power strength is the parallel interference cancellation (PIC) [9]. Unlike the conventional SIC algorithm, the conventional PIC is always performed in a multi-iteration way, where for each iteration, PIC attempts to simultaneously subtract off the interference for each user produced by all other users. The MAI generated by other users is reconstructed based on the tentative decisions from the previous iteration. Therefore, the accuracy of the previous iteration would highly affect the PIC performance as error propagation occurs when incorrect information imports. Mathematically, the received signal for the j-th user at the γ-th iteration is given by:

$$\mathbf{y}_j^{\gamma}(i) = \mathbf{y}(i) - \sum_{\substack{k=1 \\ k \neq j}}^{K} A_k \hat{b}_k^{\gamma-1}(i) h_k(i) \mathbf{s}_k(i), \tag{2.14}$$

where $\hat{b}_k^{\gamma-1}(i)$ is the k-th detected symbol from the $(\gamma - 1)$-th iteration. Similarly, the detected value for the j-th user at the γ-th iteration can be expressed as:

$$\hat{b}_j^{\gamma}(i) = Q(\mathbf{w}_j^H(i) \mathbf{y}_j^{\gamma}(i)), \tag{2.15}$$

where $\mathbf{w}_j(i)$ stands for the filter (e.g., matched filter or linear MMSE receiver) used for the j-th user of the PIC process. However, with the increase of the PIC iterations, the performance improvement can not be guaranteed as incorrect decisions made from previous iteration would spread and lead to a performance loss sometimes even more serious than that without interference cancellation [9].

2.4 Cooperative Networks

Conventional point-to-point communications have the shortcoming of being easily affected by severe multipath fading from the direct transmission between the source and the destination. In order to combat this effect, cooperative technique has arisen to deal with the channel degradation and mitigate the serious impairment on the received information. In a cooperative system, the whole transmission has been divided into two phases, where for the first phase, each user transmits its information to the corresponding

relaying node, after being processed at the relay, the data are then forwarded to the destination during the second phase. A key aspect of the cooperative transmission is the processing of signals received from the source node to the relay node. Different processing schemes result in different cooperative protocols [1]. Among various kinds of cooperative protocols, Amplify-and-Forward (AF) and Decode-and-Forward (DF) are the most common and effective ones.

2.4.1 Amplify-and-Forward (AF) Protocols

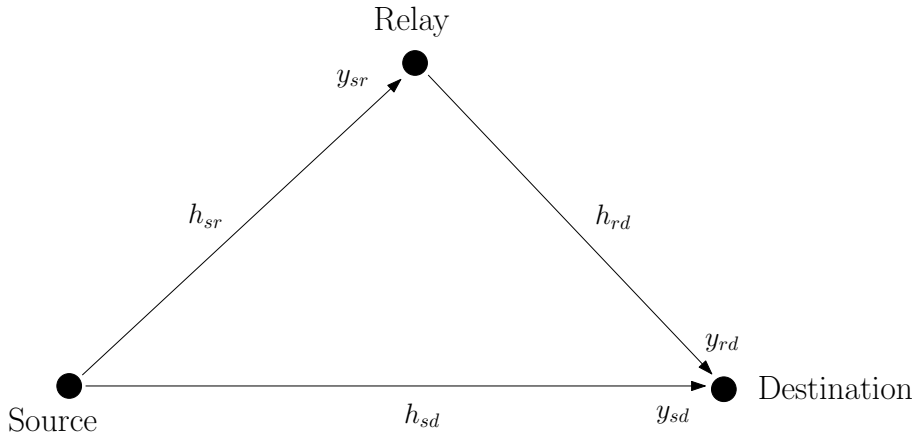

Figure 2.1: A simplified cooperation model [1]

For the AF protocol, each relay simply scales the received signal into an amplified version and subsequently, forwards the processed signal to the destination directly. This method is simple except that the relay has to amplify their own noise as well. Assume a signle user k is transmitted from the source to the destination through the cooperative network as shown by Fig. 2.1, the specific process can be described as the following, where for the first phase:

$$\mathbf{y}_{sd}(i) = A_k b_k(i) h_{sd} \mathbf{s}_k(i) + \mathbf{n}_{sd}(i), \tag{2.16}$$

$$\mathbf{y}_{sr}(i) = A_k b_k(i) h_{sr} \mathbf{s}_k(i) + \mathbf{n}_{sr}(i), \tag{2.17}$$

where $\mathbf{y}_{sd}(i)$ and $\mathbf{y}_{sr}(i)$ are the received signals from the source to the destination and the source to the relay, respectively. h_{sd} and h_{sr} are the channel coefficients from the source to the destination and the source to the relay, respectively. $\mathbf{n}_{sd}(i)$ and $\mathbf{n}_{sr}(i)$ are the

corresponding noise vectors. For the AF protocol, the relay amplifies the received signal and forwards it to the destination during the second phase, as given by:

$$\begin{aligned}\mathbf{y}_{rd}(i) =& h_{rd}\alpha\mathbf{y}_{sr}(i) + \mathbf{n}_{rd}(i) \\ =& \alpha A_k b_k(i) h_{sr} h_{rd}\mathbf{s}_k(i) + \alpha h_{rd}\mathbf{n}_{sr}(i) + \mathbf{n}_{rd}(i)\end{aligned} \tag{2.18}$$

where α is the amplify factor, $\mathbf{y}_{rd}(i)$ is the signal received from the relay to the destination, h_{rd} is the channel coefficient between the relay-destination link and $\mathbf{n}_{rd}(i)$ is the noise vector.

2.4.2 Decode-and-Forward (DF) Protocols

The DF protocol [1] is another kind of processing where relay decodes and re-encodes the received signal before being sent to the destination. Assuming a single user k is participate in the transmission. The resulting equations for the first phase transmission are given by:

$$\mathbf{y}_{sd}(i) = A_k b_k(i) h_{sd}\mathbf{s}_k(i) + \mathbf{n}_{sd}(i), \tag{2.19}$$

$$\mathbf{y}_{sr}(i) = A_k b_k(i) h_{sr}\mathbf{s}_k(i) + \mathbf{n}_{sr}(i), \tag{2.20}$$

The received signal at the destination for the second phase is then expressed by:

$$\mathbf{y}_{rd}(i) = A_k \hat{b}_{rd,k}(i) h_{rd}\mathbf{s}_k(i) + \mathbf{n}_{rd}(i), \tag{2.21}$$

where $\hat{b}_{rd}(i)$ is the decoded symbol at the output of the relay.

Both AF and DF protocols belong to the fixed relaying group of protocols, other alternative strategies including selection relaying and incremental relaying [12] have also been adopted widely in wireless networks. Specially, selection relaying performs the transmission according to a specific criterion, namely, if the channel gain falls below a certain threshold, the source simply sends the message to the destination repetitively, otherwise, the relay forwards the received information coming from the source to the destination after performing appropriate processing. When describing the incremental relaying, this protocol exploit limited feedback from the destination side. e.g., a single bit that indicate whether the direct transmission is successful or not. Consequently, this algorithm can be viewed as extensions of hybrid automatic-repeat-request (ARQ) [12].

2.5 Space-Time Coding

Apart from the DF and AF protocols, space-time coding (STC) schemes are another techniques that can be applied at the relays of the cooperative DS-CDMA system. These schemes exploit spatial and temporal transmit diversity between various antennas at various time periods. These techniques achieve transmit diversity and antenna gain over spatially encoded system without sacrificing bandwidth. With STC, multiple redundant copies of data are sent to the receiver to improve quality and reliability of data transmission. These strategies are usually used to combat the multipath fading and also to increase the diversity gain. During the past years, several STC schemes are investigated and applied in various scenarios, including vertical Bell Laboratories Layered Space-Time (V-BLAST) scheme [29], Alamouti STBC scheme [19], orthogonal STBC [30] and quasi-OSTBC (QOSTBC) [31]. In this thesis, we apply the simplest 2×1 Alamouti distributed space-time coding (DSTC) technique between the relay and destination phase in the cooperative DS-CDMA system.

2.5.1 Alamouti Distributed Space-Time Coding

The 2×1 Alamouti STC [19] scheme is the simplest and most important STC design that is employed in various scenarios. In this section, we expand the idea into a distributed scenario where we have two antennas that are located separately. The information bits are initially modulated so that for each transmit node, the modulated symbol vector $\mathbf{b} = [b(1), b(2), ...]$ is generated, after that, every two consecutive symbols are encoded with the following encoding matrix

$$\mathbf{B} = \begin{bmatrix} b(1) & -b^*(2) \\ b(2) & b^*(1) \end{bmatrix}. \tag{2.22}$$

where $b(i)$ denotes the i-th symbol. In DSTC design, the first column entry of $\mathbf{B}$ are sent by two different antennas in the first time slot while the second column entry is then sent by the same group of antennas in the next time slot.

For the simplest 2 transmitter 1 receiver (2×1) system, the received signal at the

destination from two consecutive time instants can be obtained as

$$\begin{aligned} \mathbf{y}_1 &= \mathbf{h}_1 b(1) + \mathbf{h}_2 b(2) + \mathbf{n}_1, \\ \mathbf{y}_2 &= \mathbf{h}_1\big(-b^*(2)\big) + \mathbf{h}_2 b^*(1) + \mathbf{n}_2, \end{aligned} \tag{2.23}$$

where $\mathbf{y}_i, i = 1, 2$ represents the $N \times 1$ received vector from the first and second time slots, $\mathbf{h}_k, k = 1, 2$ is the $N \times 1$ channel vector from the k-th transmitter to the destination, $\mathbf{n}_i, i = 1, 2$ is the noise vector generated at time slot i. These equations can then be rewritten in matrix form as

$$\mathbf{y} = \mathbf{H}\mathbf{b} + \mathbf{n}, \tag{2.24}$$

where $\mathbf{y} = [\mathbf{y}_1^T, (\mathbf{y}_2^*)^T]^T$ is the $2N \times 1$ received signal from the transmitters to the destination. The $2N \times 2$ Alamouti matrix with effective signatures is given by

$$\mathbf{H} = \begin{bmatrix} \mathbf{h}_1 & \mathbf{h}_2 \\ \\ \mathbf{h}_2^* & -\mathbf{h}_1^* \end{bmatrix}. \tag{2.25}$$

The 2×1 vector $\mathbf{b} = [b(1), b(2)]^T$ is the transmitted symbols and $\mathbf{n} = [\mathbf{n}_1^T, (\mathbf{n}_2^*)^T]^T$ is the noise vector. Consequently, at the destination side, various MUD techniques and the maximum likelihood (ML) decoding algorithms can be easily applied. For the MUD techniques, the detected symbols are achieved as given by

$$\hat{\mathbf{b}} = Q\big(\mathbf{w}^H \mathbf{y}\big), \tag{2.26}$$

where $\mathbf{w}$ denotes the receive filter (MF, MMSE, SIC, PIC, etc.) at the destination. As for the ML detector when Alamouti scheme is adopted, the decoding algorithm is computed as given by [19]

$$\begin{aligned} \tilde{b}(1) &= \mathbf{h}_1^H \mathbf{y}_1 + \mathbf{h}_2^T \mathbf{y}_2^* \\ &= (\mathbf{h}_1^H \mathbf{h}_1 + \mathbf{h}_2^T \mathbf{h}_2^*) b(1) + (\mathbf{h}_1^H \mathbf{n}_1 + \mathbf{h}_2^T \mathbf{n}_2^*) \\ \tilde{b}(2) &= \mathbf{h}_2^H \mathbf{y}_1 - \mathbf{h}_1^T \mathbf{y}_2^* \\ &= (\mathbf{h}_2^H \mathbf{h}_2 + \mathbf{h}_1^T \mathbf{h}_1^*) b(2) + (\mathbf{h}_2^H \mathbf{n}_1 - \mathbf{h}_1^T \mathbf{n}_2^*) \end{aligned} \tag{2.27}$$

Thus, after testing all possible symbols for ML decision, the most likely detection results are then selected.

2.6 Physical-layer Network Coding

The theoretical foundations of network coding were initially provided by Ahlswede et al. [21], where the idea of coding at intermediate nodes to general multi-node networks is presented. In particular, network coding allows nodes in the network to perform encoding and decoding operations on the received information, resulting in the re-transmission of messages that are a function of the incoming information. This technique has significant advantages in wireless multihop networks, where multiple relay nodes are provided to assist multiple source nodes to transfer data to one or more destinations. It allows a node to exploit as far as possible all signals that it receives simultaneously, rather than treating them as interference [24]. Instead of decoding each incoming data stream separately, a node detects and forwards some functions of the incoming data streams [24, 25].

In this section, we mainly focus on the fundamental concepts of several physical-layer network coding (PNC) schemes, namely, the bit-wise XOR mapping operation and the linear network coding technique [20–23].

2.6.1 PNC Using XOR Mapping

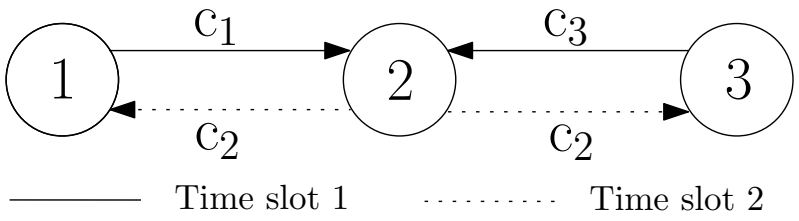

Figure 2.2: Physical-layer network coding (PNC)

The bit-wise XOR (the modulo-2 sum in the binary field) mapping operation [20] is one of the simplest cases of PNC, it is first designed to be employed in two-way relay channels for information exchange as shown in Fig. 2.2.

Let us assume the use of QPSK modulation in all nodes, and we further assume the transmission is synchronized. Fig. 2.2 illustrates that the physical-layer network coding scheme improves the transmission efficiency of time slot by 100% when compared with

the traditional network coding as the above physical-layer network coding is operated by node N_2 after the reception of superimposed signals that carry c_1 and c_3 from node N_1 and N_3 in the same time slot. Node N_2 deduces $c_2 = c_1 \bigoplus c_3$ ($\oplus$ is the bit-wise XOR operation) and in the next time instant, the coded information is forwarded back to nodes N_1 and N_3.

Specifically, the combined bandpass signal received at node N_2 from N_1 and N_3 during one time slot is given by [20]

$$\begin{aligned} r_2(t) &= c_1(t) + c_3(t) \\ &= [a_1 cos(\omega t) + b_1 sin(\omega t)] + [a_3 cos(\omega t) + b_3 sin(\omega t)] \\ &= (a_1 + a_3) cos(\omega t) + (b_1 + b_3) sin(\omega t) \end{aligned} \tag{2.28}$$

where $c_i, i = 1, 3$ is the bandpass signal transmitted from nodes N_i. a_i, b_i are the QPSK modulated information bits of N_i and ω is the carrier angular frequency. As shown by Fig. 2.2, node N_2 receives the bandpass signals from the other two nodes in both in-phase(I) and quadrature phase(Q) form as described below

$$\begin{aligned} I &= a_1 + a_3 \\ Q &= b_1 + b_3 \end{aligned} \tag{2.29}$$

Node N_2 cannot extract the individual information sent by nodes N_1 and N_3 as Eq. (2.29) has four unknowns (a_1, a_3, b_1, b_3). However, in this case, node N_2 works only as a relay node so that PNC mapping is performed as given by

$$\begin{aligned} c_2^I &= c_1^I \bigoplus c_3^I \\ c_2^Q &= c_1^Q \bigoplus c_3^Q \end{aligned} \tag{2.30}$$

Therefore, node N_2 then transmits

$$c_2(t) = a_2 cos(\omega t) + b_2 sin(\omega t) \tag{2.31}$$

Table 2.1 presents the PNC mapping for the in-phase component (the quadrature component is similar), where $c_i^I \in \{0, 1\}$ denotes the variable representing the in-phase data bits of N_i and $a_i \in \{-1, 1\}$ is the corresponding BPSK modulated bit of c_i^I $(a_i = 2c_i^I - 1)$.

Upon receiving $c_2(t)$, N_1 and N_3 can derive c_2^I and c_2^Q by ordinary QPSK demodulation. The successively derived c_2^I and c_2^Q bits within a time slot will then be

Modulation mapping at N_1 and N_3,				Demodulation mapping at N_2		
				Input	Output	
Input		Output			Modulation mapping at N_2	
					Input	Output
c_1^I	c_3^I	a_1	a_3	$a_1 + a_3$	c_2^I	a_2
1	1	1	1	2	0	-1
0	1	-1	1	0	1	1
1	0	1	-1	0	1	1
0	0	-1	-1	-2	0	-1

Table 2.1: PNC Mapping: modulation mapping at N_1, N_2 and N_3; demodulation at N_3

used to form the c_2. In other words, the operation $c_2 = c_1 \bigoplus c_3$ in straightforward network coding can now be realized through PNC mapping. Consequently, c_2 is then sent back to node N_1 and N_3 at the same time, after that, $c_3 = c_2 \bigoplus c_1$ is decoded at node N_1 and $c_1 = c_2 \bigoplus c_3$ is decode at node N_3, respectively. Therefore, with physical-layer network coding, we not only improves the transmission efficiency but also realize the information exchange.

As illustrated in Table 2.1, PNC requires only two time slots for the exchange of one frame (as opposed to three time slots in straightforward network coding and four time slots in traditional scheduling) [20].

2.6.2 Linear Network Coding

Linear network coding (LNC) is an important category that belongs to the area of network coding designs. The theory of LNC adopts a linear coding scheme at every node of the network and promises high data transmission rate from the source to all receivers. Specifically, instead of simply relaying the packets of received symbols, the intermediate nodes send out packets that are linear combinations of previously received information [32]. The development of this strategy leads to a wide applicability [23] including coding theory, computer science [33, 34], distributed data storage [35],

information security [36, 37], information theory [38], network tomography [39], optical networks [40], optimization theory [41], peer-to-peer (P2P) content delivery [42], switching theory [43], and wireless/satellite communications [44].

When signals propagate through the network using LNC scheme, they will transmit over every link of the network. Every outgoing signal from a non-source node is a linear combination of incoming signals to this node. The coefficients in the linear combination are the "linear gains" from incoming links to the outgoing link. Such coefficients determine the detailed LNC scheme employed by the data that transmit through the network [23]. The detailed process of LNC for a K source 1 destination network is shown in Fig. 2.3.

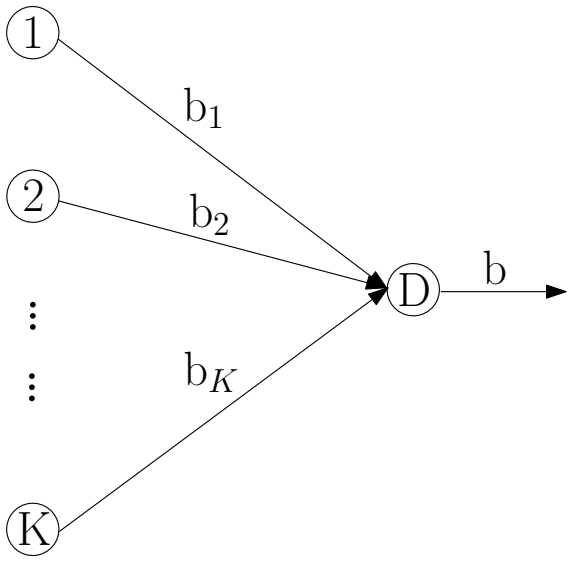

Figure 2.3: Linear Network Coding (LNC)

Clearly, as can be seen from Fig. 2.3, K sources generate K signals $b_1, b_2, ..., b_k$, and the output of the destination node D is a linear combination of every input source. Mathematically, the whole process can be descried as:

$$b = \sum_{k=1}^{K} g_k b_k \tag{2.32}$$

where b indicates the coded symbol and g_k are the coding coefficients often taken from a Galois field [20–23, 45, 46] for the link between the k-th user node and the destination node.

When expanding the above K users, 1 destination node network into a cooperative scenario that are equipped with K users, L relays and a single destination node, an independent coefficient g_{kl} is allocated for each user-relay link when LNC technique is used during the relay-destination phase, where m users and m relays are adopted and grouped. Therefore, these elements are grouped to form a $m \times m$ coefficient matrix $\mathbf{G}$ as given by

$$\mathbf{G} = \begin{bmatrix} g_{11} & g_{12} & \cdots & g_{1m} \\ g_{21} & g_{22} & \cdots & g_{2m} \\ & & \vdots & \\ g_{m1} & g_{m2} & \cdots & g_{mm} \end{bmatrix}, \tag{2.33}$$

where m suggests the size of the generated coefficient matrix ($m \leqslant L$)

This coefficient matrix is then stored at both the relay and the destination for the purposes of encoding and decoding operations. Specifically, after the detected symbols of interest are generated at relays, the detected user symbols are then multiplied by the coefficient matrix $\mathbf{G}$ to complete the encoding process. Consequently, the corresponding network coded symbol (NCS) is sent to the destination directly. At the destination side, since the coefficient matrix $\mathbf{G}$ is also stored here, the inversion of this matrix $\mathbf{G}^{-1}$ is then adopted for the decoding process.

2.7 Conclusions

In this chapter, we first introduce concept of the spread spectrum system where the DS-CDMA is derived from, followed by some existing MUD techniques that are usually employed in DS-CDMA systems to mitigate the MAI. After that, the system model of a cooperative transmission is detailed, along with the descriptions of some cooperative protocols. At last, an overview of the DSTC and PNC schemes are presented.

In the following chapters, the introduced concepts will be further developed and explored. In chapter 3, two novel MUD techniques are proposed and applied in the cooperative DS-CDMA system. After that, the DSTC scheme is adopted from the relay to the destination in the uplink of a cooperative DS-CDMA system in chapter 4. Finally,

novel PNC strategies are investigated and used at the relays in the cooperative networks in chapter 5.

Chapter 3

Joint Interference Cancellation and Relay Selection Algorithms Based on Greedy Techniques for Cooperative DS-CDMA Systems

Contents

3.1 Introduction

Multipath fading is a major constraint that seriously limits the performance of wireless communications. Indeed, severe fading has a detrimental effect on the received signals and can lead to a degradation of the transmission of information and the reliability of the network. Cooperative diversity is a technique that has been widely considered in recent years [4] as an effective tool to deal with this problem. Several cooperative schemes have been proposed in the literature [12, 47, 48], and among the most effective ones are Amplify-and-Forward (AF) and Decode-and-Forward (DF) [12]. For an AF protocol, relays cooperate and amplify the received signals with a given transmit power amplifying their own noise. With the DF protocol, relays decode the received signals and then forward the re-encoded message to the destination. Consequently, better performance and lower power consumption can be obtained when appropriate decoding and relay selection strategies are applied.

DS-CDMA system is a multiple access technique that can be incorporated with cooperative systems in ad hoc and sensor networks [49–51]. Due to the multiple access interference (MAI) effect that arises from nonorthogonal received waveforms, the system performance may be adversely affected. To deal with this issue, multiuser detection (MUD) techniques have been developed [5] as an effective approach to suppress MAI. The optimal detector, known as maximum likelihood (ML) detector, has been proposed in [6]. However, this method is infeasible for ad hoc and sensor networks considering its computational complexity. Motivated by this fact, several sub-optimal strategies have been developed: the linear detector [7], the successive interference cancellation (SIC) [8], the parallel interference cancellation (PIC) [9] and the minimum mean-square error (MMSE) decision feedback detector [10]. A key challenge is how to design interference cancellation techniques with low cost and near ML performance. Moreover, such interference cancellation algorithms should be suitable to cooperative relaying systems and feasible for deployment at the relays and small devices.

In cooperative relaying systems, different strategies that utilize multiple relays have

been recently introduced in [52–56]. Among these approaches, a greedy algorithm is an effective way to approach the global optimal solution. Greedy algorithms are important mathematical techniques that follow the approach of obtaining a locally optimal solution to complex problems with low cost in a step by step manner. Decisions at each step in the greedy process are made to provide the largest benefit based on improving the local state without considering the global situation. Greedy algorithms may fail to achieve the globally optimal choice as they do not execute all procedures exhaustively, however, they are still useful as they usually present a lower cost and can provide acceptable approximations. Greedy algorithms have been widely applied in sparse approximation [57], internet routing [58] and arithmetic coding [59]. In [57], orthogonal matching pursuit (OMP) and basis pursuit (BP) are two major greedy approaches that are used to approximate an arbitrary input signal with the near optimal linear combination of various elements from a redundant dictionary. In [58], greedy routing is mentioned as a routing strategy where messages are simply forwarded to the node that is closest to the destination. In order to reduce the computational complexity and improve the overall speed of arithmetic coding, a greedy re-normalization step that contains greedy thresholding and greedy outputting is proposed and analyzed in [59]. In relay-assisted systems, greedy algorithms are used in [54, 55] to search for the best set of relays, however, with insufficient numbers of combinations considered, a significant performance loss is experienced as compared to an exhaustive search.

This work presents cost-effective interference cancellation algorithms and multi-relay selection algorithms for cooperative DS-CDMA systems. The proposed interference cancellation algorithms do not require matrix inversions and rely on the RAKE receiver (suitable for frequency selective channels when multipath fading is introduced) as the front-end. A cross-layer optimization approach that jointly considers the proposed interference cancellation and relay selection algorithms for ad hoc and sensor networks is also proposed. The proposed techniques are not limited to DS-CDMA systems and could also be applied to multi-antenna and multi-carrier systems. Cross-layer designs that integrate different layers of the network have been employed in prior work [60, 61] to guarantee the quality of service and help increase the capacity, reliability and coverage of systems. However, MUD techniques with relay selection in cooperative relaying systems have not been discussed widely in the literature. In [48, 62], an MMSE-MUD technique has been applied to cooperative systems, where the results indicate that the

transmissions are more resistant to MAI and obtain a significant performance gain when compared with a single direct transmission. However, extra costs are introduced, as matrix inversions are required when an MMSE filter is deployed.

The contributions of this chapter are summarized as follows:

- A low-cost greedy list-based successive interference cancellation (GL-SIC) multiuser detection method that can be applied at both the relays and the destination of wireless systems is proposed.
- A low-cost greedy list-based parallel interference cancellation (GL-PIC) strategy which employs RAKE receivers as the front-end and can approach the ML detector performance is then developed.
- A low-complexity multi-relay selection algorithm based on greedy techniques that can approach the performance of an exhaustive search is presented.
- An analysis of the computational complexity, the greedy relay selection method and the cross-layer design is presented.
- A cross-layer design that incorporates the optimization of the proposed GL-SIC and GL-PIC techniques and the improved greedy multi-relay selection algorithm for the uplink of a cooperative DS-CDMA system is developed and evaluated.

3.2 Cooperative DS-CDMA System Model

Consider the uplink of a synchronous DS-CDMA system with K users $(k_1, k_2, ...k_K)$, L relays $(l_1, l_2, ...l_L)$, N chips per symbol and L_p $(L_p < N)$ multi paths for each link. Frequency selective channel for each link is experienced. The system is equipped with a DF protocol at each relay and we assume that the transmit data are organized in packets comprising P symbols. The received signals are filtered by a filter matched to the chip pulse, sampled at chip rate to obtain sufficient statistics and organized into $M \times 1$ vectors $\mathbf{y}_{sd}$, $\mathbf{y}_{sr}$ and $\mathbf{y}_{rd}$, which represent the signals received from the sources (users) to the destination, the sources to the relays and the relays to the destination, respectively (M

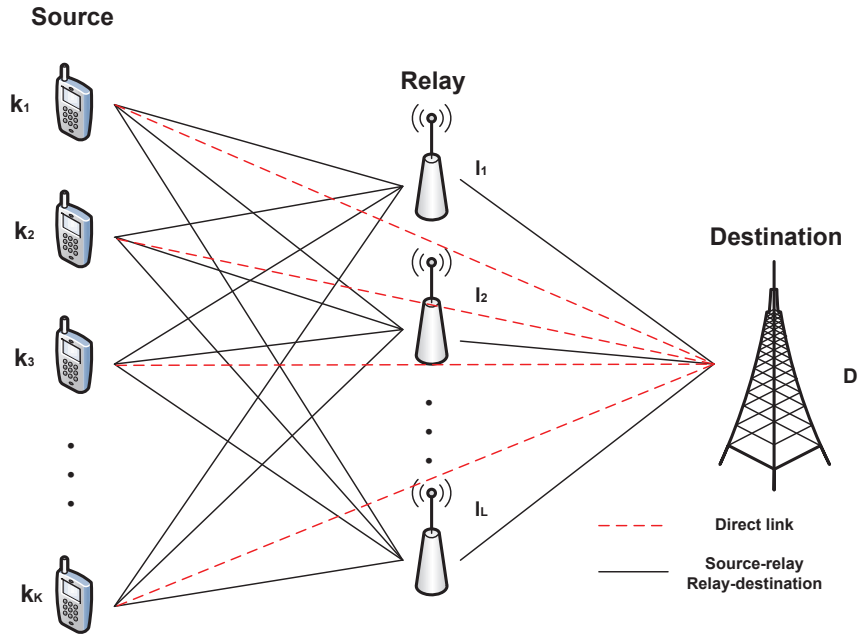

Figure 3.1: Uplink of a cooperative DS-CDMA system.

corresponds to the length of the receive filters). The proposed algorithms for interference mitigation and relay selection are employed at the relays and at the destination. As shown in Fig. 3.1, the cooperation takes place in two phases. During the first phase, the received data at the destination and the l-th relay can be described by

$$\mathbf{y}_{sd} = \sum_{k=1}^{K} a_{sd}^{k} \mathbf{S}_k \mathbf{h}_{sd,k} b_k + \boldsymbol{\eta}_{sd} + \mathbf{n}_{sd}, \tag{3.1}$$

$$\mathbf{y}_{sr_l} = \sum_{k=1}^{K} a_{sr_l}^{k} \mathbf{S}_k \mathbf{h}_{sr_l,k} b_k + \boldsymbol{\eta}_{sr_l} + \mathbf{n}_{sr_l}, \tag{3.2}$$

where $M = N + L_p - 1$, $b_k \in \{+1, -1\}$ correspond to the transmitted symbols, a_{sd}^{k} and $a_{sr_l}^{k}$ represent the k-th user's amplitude from the source to the destination and the source to relay l, clearly $a_{sd}^{k} = a_{sr_l}^{k}$. The vectors $\mathbf{h}_{sd,k}$, $\mathbf{h}_{sr_l,k}$ are the $L_p \times 1$ channel vectors for user k from the source to the destination and the source to relay l, respectively. The $M \times 1$ vectors $\boldsymbol{\eta}_{sd}$ and $\boldsymbol{\eta}_{sr_l}$ denote the intersymbol interference (ISI) arising from the source to the destination and source to the l-th relay. The $M \times 1$ noise vectors $\mathbf{n}_{sd}$ and $\mathbf{n}_{sr_l}$ contain samples of zero mean complex Gaussian noise with variance σ^2. The $M \times L_p$ matrix $\mathbf{S}_k$ contains the signature sequence of each user shifted down by one position at each column

that forms

$$\mathbf{S}_k = \begin{bmatrix} s_k(1) & & \mathbf{0} \\ \vdots & \ddots & s_k(1) \\ s_k(N) & & \vdots \\ \mathbf{0} & \ddots & s_k(N) \end{bmatrix}, \tag{3.3}$$

where $\mathbf{s}_k = [s_k(1), s_k(2), ...s_k(N)]^T$ is the signature sequence for user k. During the second phase of the transmission, each relay decodes and reconstructs the received signals using a DF protocol, then they forward the processed signals to the destination. It is assumed that each relay is perfectly synchronized and transmits at the same time, the signals received at the destination are then expressed by

$$\mathbf{y}_{rd} = \sum_{l=1}^{L} \sum_{k=1}^{K} a_{r_l d}^{k} \mathbf{S}_k \mathbf{h}_{r_l d,k} \hat{b}_{r_l d,k} + \sum_{l=1}^{L} \boldsymbol{\eta}_{r_l d} + \mathbf{n}_{rd}, \tag{3.4}$$

where $a_{r_l d}^{k}$ is the amplitude for source (user) k from the l-th relay to the destination, $\mathbf{h}_{r_l d,k}$ is the $L_p \times 1$ channel vector for user k from the l-th relay to the destination, the $M \times 1$ vector $\boldsymbol{\eta}_{r_l d}$ represents the ISI arising from the l-th relay to the destination, $\mathbf{n}_{rd}$ is the $M \times 1$ zero mean complex Gaussian noise with variance σ^2, $\hat{b}_{r_l d,k}$ is the decoded symbol at the output of relay l after using the DF protocol.

The received signal at the destination comprises the data transmitted during two phases that are jointly processed at the destination. Therefore, the received signal is described by a $2M \times 1$ vector formed by stacking the received signals from the relays and the sources as given by

$$\mathbf{y}_d = \begin{bmatrix} \mathbf{y}_{sd} \\ \mathbf{y}_{rd} \end{bmatrix} = \begin{bmatrix} \sum_{k=1}^{K} a_{sd}^{k} \mathbf{S}_k \mathbf{h}_{sd,k} b_k \\ \sum_{l=1}^{L} \sum_{k=1}^{K} a_{r_l d}^{k} \mathbf{S}_k \mathbf{h}_{r_l d,k} \hat{b}_{r_l d,k} \end{bmatrix} + \begin{bmatrix} \boldsymbol{\eta}_{sd} \\ \sum_{l=1}^{L} \boldsymbol{\eta}_{r_l d} \end{bmatrix} + \begin{bmatrix} \mathbf{n}_{sd} \\ \mathbf{n}_{rd} \end{bmatrix}. \tag{3.5}$$

By using the stacked received data from the source and the relays for joint processing and using i to denote the desired symbol in the transmitted packet and its received and relayed copies, we can rewrite the $2M \times 1$ vector $\mathbf{y}_d(i)$ in (3.5) in a compact form given by

$$\mathbf{y}_d(i) = \sum_{k=1}^{K} \mathbf{C}_k \mathbf{H}_k(i) \mathbf{A}_k(i) \mathbf{b}_k(i) + \boldsymbol{\eta}(i) + \mathbf{n}(i), \tag{3.6}$$

where i denotes the time instant corresponding to one symbol in the transmitted packet and its received and relayed copies. $\mathbf{C}_k$ is a $2M \times (L+1)L_p$ matrix comprising shifted

versions of $\mathbf{S}_k$ as given by

$$\mathbf{C}_k = \begin{bmatrix} \mathbf{S}_k & \mathbf{0} & \dots & \mathbf{0} \\ \mathbf{0} & \mathbf{S}_k & \dots & \mathbf{S}_k \end{bmatrix}, \tag{3.7}$$

where $\mathbf{0}$ here represents a $M \times L_p$ zero matrix. $\mathbf{H}_k(i)$ represents a $(L+1)L_p \times (L+1)$ channel matrix between the sources and the destination and the relays and the destination links as given by

$$\mathbf{H}_k(i) = \begin{bmatrix} \mathbf{h}_{sd,k} & \mathbf{0} & \dots & \mathbf{0} \\ \mathbf{0} & \mathbf{h}_{r_1 d,k} & \dots & \mathbf{h}_{r_L d,k} \end{bmatrix}, \tag{3.8}$$

where $\mathbf{0}$ in matrix $\mathbf{H}_k(i)$ denotes a $L \times L_p$ zero vector. The matrix $\mathbf{A}_k(i)$ is an $(L+1) \times (L+1)$ diagonal matrix of amplitudes for user k, $\mathbf{b}_k(i) = [b_k, \hat{b}_{r_1 d,k}, \hat{b}_{r_2 d,k}, ...\hat{b}_{r_L d,k}]^T$ is an $(L+1) \times 1$ vector for user k that contains the transmitted symbols at the source and the detected symbols at the output of each relay, $\boldsymbol{\eta}(i)$ is a $2M \times 1$ ISI term and $\mathbf{n}(i)$ is a $2M \times 1$ noise vector.

3.3 Proposed GL-SIC Multiuser Detection

In this section, we detail the GL-SIC multiuser detector that can be applied in the uplink of a cooperative system. The GL-SIC detector uses the RAKE receiver as the front-end, so that the matrix inversion required by the MMSE filter can be avoided. The GL-SIC detector exploits the Euclidean distance between the users of interest and their nearest constellation points, with multiple ordering at each stage, all possible lists of tentative decisions for each user are generated. When seeking appropriate candidates, a greedy-like technique is performed to build each list and all possible estimates within the list are examined when unreliable users are detected. Unlike prior work which employs the concept of Euclidean distance with multiple feedback SIC (MF-SIC) [63], GL-SIC does not require matrix inversions and jointly considers multiple numbers of users, constellation constraints and re-ordering at each detection stage to obtain an improvement in detection performance.

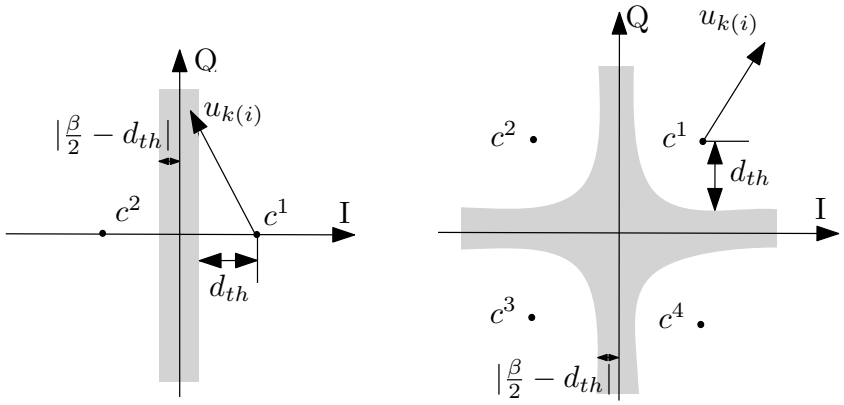

Figure 3.2: The reliability check in BPSK and QPSK constellations.

3.3.1 Proposed GL-SIC Design

In the following, we describe the process for initially detecting n users described by the indices $k_1, k_2, ..., k_n$ at the first stage. Other users can be obtained accordingly. As shown by Fig. 3.2, β is the distance between two nearest constellation points, d_{th} is the threshold. The soft output of the RAKE receiver for user k is then obtained by

$$u_k(i) = \mathbf{w}_{s_k r_l}^H \mathbf{y}_{sr_l}(i), \tag{3.9}$$

where $\mathbf{y}_{sr_l}(i)$ represents the received signal from the source to the l-th relay, $u_k(i)$ stands for the soft output of the i-th symbol for user k and $\mathbf{w}_{s_k r_l}$ denotes the RAKE receiver that corresponds to a filter matched to the effective signature at the receiver. After that, we order all users according to a decreasing power level and organize $[u_1, u_2, ..., u_k]$ into a $K \times 1$ vector $\mathbf{t}_a$. We choose the first n entries $[\mathbf{t}_a(1), \mathbf{t}_a(2), ..., \mathbf{t}_a(n)]$ which denote users $k_{\mathbf{t}_a(1)}, k_{\mathbf{t}_a(2)}, ..., k_{\mathbf{t}_a(n)}$. The reliability of each of the n users is examined by the corresponding Euclidean distance between the user of interest and its nearest constellation point c as explained next.

Reliable decision:

If all n users are considered reliable

$$u_{\mathbf{t}_a(t)}(i) \notin \mathbf{C}_{\text{grey}}, \quad \text{for } t \in [1, 2, ..., n], \tag{3.10}$$

these soft estimates will then be applied to a slicer $Q(\cdot)$ as

$$\hat{b}_{\mathbf{t}_a(t)}(i) = Q(u_{\mathbf{t}_a(t)}(i)), \text{ for } t \in [1, 2, ..., n], \tag{3.11}$$

where $\hat{b}_{\mathbf{t}_a(t)}(i)$ denotes the detected symbol for the $\mathbf{t}_a(t)$-th user, $\mathbf{C}_{\text{grey}}$ is the shadowed area in Fig. 3.2, it should be noted that the shadowed region would spread along both the vertical and horizontal directions. The cancellation is then performed in the same way as a conventional SIC where we mitigate the impact of MAI brought by these users

$$\mathbf{y}_{sr_l,s+1}(i) = \mathbf{y}_{sr_l,s}(i) - \sum_{t=1}^{n} \boldsymbol{h}_{sr_l,\mathbf{t}_a(t)}(i)\hat{b}_{\mathbf{t}_a(t)}(i), \tag{3.12}$$

where the italic font $\boldsymbol{h}_{sr_l,\mathbf{t}_a(t)}(i) = a_{sr_l}^{\mathbf{t}_a(t)}\mathbf{S}_{\mathbf{t}_a(t)}(i)\mathbf{h}_{sr_l,\mathbf{t}_a(t)}(i)$ stands for the desired user's channel vector associated with the link between the source and the l-th relay, $\mathbf{y}_{sr_l,s}$ is the received signal from the source to the l-th relay at the s-th $(s = 1, 2, ..., K/n)$ cancellation stage. The process is then repeated with another set of n users being selected from the remaining users at the following stage, and this algorithm changes to the unreliable mode when unreliable users are detected. Additionally, since the interference created by the previous users with the strongest power has been mitigated, improved estimates are obtained by reordering the remaining users.

Unreliable decision :

(a). If part of the n users are determined as reliable, while others are considered as unreliable, we have

$$u_{\mathbf{t}_p(t)}(i) \notin \mathbf{C}_{\text{grey}}, \quad \text{for } t \in [1, 2, ..., n_p], \tag{3.13}$$

$$u_{\mathbf{t}_q(t)}(i) \in \mathbf{C}_{\text{grey}}, \quad \text{for } t \in [1, 2, ..., n_q], \tag{3.14}$$

where $\mathbf{t}_p$ is a $1 \times n_p$ vector that contains n_p reliable users and $\mathbf{t}_q$ is a $1 \times n_q$ vector that includes n_q unreliable users, subject to $\mathbf{t}_p \cap \mathbf{t}_q = \varnothing$ and $\mathbf{t}_p \cup \mathbf{t}_q = [1, 2, ...n]$ with $n_p + n_q = n$. Consequently, the n_p reliable users are applied to the slicer $Q(\cdot)$ directly and the n_q unreliable ones are examined in terms of all possible constellation points c^m $(m \in [1, 2, ..., N_c])$ from the $1 \times N_c$ constellation points set $\mathbf{C} \subseteq F$, where F is a subset of the complex field, N_c is the number of constellation points and the index m is the index number from $\mathbf{C}$ that employed to search for the constellation points according to the modulation type. The detected symbols are given by

$$\hat{b}_{\mathbf{t}_p(t)}(i) = Q(u_{\mathbf{t}_p(t)}(i)), \text{for } t \in [1, 2, ..., n_p], \tag{3.15}$$

$$\hat{b}_{\mathbf{t}_q(t)}(i) = c^m, \ \text{ for } t \in [1, 2, ..., n_q], \tag{3.16}$$

At this point, $N_c^{n_q}$ combinations of candidates for n_q users are generated. The detection tree is then split into $N_c^{n_q}$ branches. After this processing, (3.12) is applied with its corresponding combination to ensure the interference caused by the n detected users is mitigated. Following that, $N_c^{n_q}$ numbers of updated $\mathbf{y}_{sr_l}(i)$ are generated as different re-created MAI is mitigated according to different branches, we reorder the remaining users at each cancellation stage and compute a conventional SIC with RAKE receivers for each branch.

The following $K \times 1$ different ordered candidate detection lists are then produced:

$$\mathbf{b}^j(i) = [\mathbf{s}_{\text{pre}}(i), \ \mathbf{s}_p(i), \ \mathbf{s}_q^j(i), \ \mathbf{s}_{\text{next}}^j(i)]^T, \ j \in [1, 2, ..., N_c^{n_q}], \tag{3.17}$$

where

$\mathbf{s}_{\text{pre}}(i) = [\hat{b}_{\mathbf{t}_a(1)}(i), \hat{b}_{\mathbf{t}_a(2)}(i), ...]^T$ stands for the previous stages detected reliable symbols,

$\mathbf{s}_p(i) = [\hat{b}_{\mathbf{t}_p(1)}(i), \hat{b}_{\mathbf{t}_p(2)}(i), ..., \hat{b}_{\mathbf{t}_p(n_p)}(i)]^T$ is a $n_p \times 1$ vector that denotes the current stage reliable symbols detected directly from slicer $Q(\cdot)$ when (3.13) occurs,

$\mathbf{s}_q^j(i) = [c^m_{\mathbf{t}_q(1)}, c^m_{\mathbf{t}_q(2)}, ..., c^m_{\mathbf{t}_q(n_q)}]^T, j \in [1, 2, ..., N_c^{n_q}]$ is a $n_q \times 1$ vector that contains the detected symbols deemed unreliable at the current stage as in (3.14), each entry of this vector is allocated a value from the constellation point set $\mathbf{C}$, therefore, since each entry goes through all possible constellation points, with n_q users contained in $\mathbf{s}_q^j(i)$, $N_c^{n_q}$ combinations need to be considered and examined. j is the index number from all $N_c^{n_q}$ combinations of $\mathbf{s}_q^j(i)$.

$\mathbf{s}_{\text{next}}^j(i) = [..., \hat{b}^{\mathbf{s}_q^j}_{\mathbf{t}'(1)}(i), ..., \hat{b}^{\mathbf{s}_q^j}_{\mathbf{t}'(n)}(i)]^T$ includes the corresponding detected symbols in the following stages after the j-th combination of $\mathbf{s}_q(i)$ is allocated to the unreliable user vector $\mathbf{t}_q$,

$\mathbf{t}'$ is a $n \times 1$ vector that contains the users from the last stage.

(b). If all n users are considered as unreliable, then we have

$$u_{\mathbf{t}_b(t)}(i) \in \mathbf{C}_{\text{grey}}, \quad \text{for } t \in [1, 2, ..., n], \tag{3.18}$$

where $\mathbf{t}_b = [1, 2, ..., n]$ and all n unreliable users can assume the values in $\mathbf{C}$. In this case, the detection tree will be split into N_c^n branches to produce

$$\hat{b}_{\mathbf{t}_b(t)}(i) = c^m, \text{ for } t \in [1, 2, ..., n]. \tag{3.19}$$

Similarly, (3.12) is then applied and a conventional SIC with different orderings at each cancellation stage is performed via each branch.

Since all possible constellation values are tested for all unreliable users, we have the candidate lists

$$\mathbf{b}^j(i) = [\mathbf{s}_{\text{pre}}(i),\ \mathbf{s}_b^j(i),\ \ \mathbf{s}_{\text{next}}^j(i)]^T,\ j \in [1, 2, ..., N_c^n], \tag{3.20}$$

where

$\mathbf{s}_{\text{pre}}(i) = [\hat{b}_{\mathbf{t}_a(1)}(i), \hat{b}_{\mathbf{t}_a(2)}(i), ...]^T$ are the reliable symbols that are detected from previous stages,

$\mathbf{s}_b^j(i) = [c^m_{\mathbf{t}_b(1)}, c^m_{\mathbf{t}_b(2)}, ..., c^m_{\mathbf{t}_b(n)}]^T, j \in [1, 2, ..., N_c^n]$ is a $n \times 1$ vector that represents the number of users n which are regarded as unreliable at the current stage as shown by (3.18), each entry of $\mathbf{s}_b^j$ is assigned a value from the constellation point set $\mathbf{C}$.

The vector $\mathbf{s}_{\text{next}}^j(i) = [..., \hat{b}^{\mathbf{s}_b^j}_{\mathbf{t}'(1)}(i), ..., \hat{b}^{\mathbf{s}_b^j}_{\mathbf{t}'(n)}(i)]^T$ contains the corresponding detected symbols in the following stages after the j-th combination of $\mathbf{s}_b(i)$ is allocated to all unreliable users.

After the candidates are generated, lists are built for each group of users, and the ML rule is used to choose the best candidate list as described by

$$\mathbf{b}^{\text{best}}(i) = \arg \min_{1 \le j \le N_c^{n_q} \text{or } N_c^n} \| \mathbf{y}_{sr_l}(i) - \mathbf{H}_{sr_l}(i)\mathbf{b}^j(i) \|^2, \tag{3.21}$$

where $\mathbf{H}_{sr_l}(i) = \begin{bmatrix} \boldsymbol{h}_{sr_l,1} & \boldsymbol{h}_{sr_l,2} & \dots & \boldsymbol{h}_{sr_l,K} \end{bmatrix}$ is an $M \times K$ channel matrix for all users from the source to the l-th relay, $\boldsymbol{h}_{sr_l,k} = a^k_{sr_l}\mathbf{S}_k(i)\mathbf{h}_{sr_l,k}(i)$ denotes a $M \times 1$ vector for user k from the source to the l-th relay.

Clearly, GL-SIC is a SIC receiver that is split at stage s into $N_c^{n_q}$ parallel SIC receivers (branches) where s is the first stage having unreliable users. The best branch is

Algorithm 1 The GL-SIC algorithm

$u_k(i) = \mathbf{w}_k^H \mathbf{y}_{sr_l}(i)$ % soft outputs of all candidates

order $u_k(i)$ according to a decreasing power level and organize them

into $\mathbf{t}_a$

for s = 1 **to** K/n

%Check whether unreliable users have already been detected

%from previous $s-1$ stages or not

if no unreliable users have been detected at previous $s-1$ stages

% Examine the reliability for each user for current stage s

for t=1: n

if $u_{\mathbf{t}_a(t)}(i) \notin \mathbf{C}_{\text{grey}}$ % **reliable**

$\hat{b}_{\mathbf{t}_a(t)}(i) = Q(u_{\mathbf{t}_a(t)}(i))$

else % **unreliable**

$\hat{b}_{\mathbf{t}_a(t)}(i) = c^m$

end

end

Do conventional SIC via each branch

else % unreliable users have already been detected at previous $s-1$ stages

Re-order the next n soft estimates for stage s and send them

to the slicer $Q(\cdot)$

Perform conventional SIC in each branch

end

end

% apply ML to choose the best candidates list $(1 \le j \le N_c^{n_q})$

$\mathbf{b}^{\text{best}}(i) = \arg\min_{1 \le j \le N_c^{n_q} \text{ or } N_c^n} \| \mathbf{y}_{sr_l}(i) - \mathbf{H}_{sr_l}(i)\mathbf{b}^j(i) \|^2$

decided at the end using the ML criterion (minimum residual energy). The optimum performance occurs when we examine the reliability for all users. However, in this work, once unreliable users are detected at stage s, for the following $s+1$, $s+2$,...,K/n stages, we process users directly through the conventional SIC detector to avoid further split of the detection tree as this would bring high complexity when large number of users are considered. Nevertheless, the performance gain can be compensated by increasing the number of users n that we have to consider per each stage.

The proposed GL-SIC algorithm is detailed in Algorithm 1.

3.3.2 GL-SIC with Multi-branch Processing

The multiple branch (MB) structure [10, 64] that employs multiple parallel processing branches can help to obtain extra detection diversity. Inspired by the MB approach [10, 64], we change the obtained best detection order for $\mathbf{b}^{\text{best}}$ with indices $\mathbf{O} = [1, 2, ..., K]$ into a group of different detection sequences to form a parallel structure with each branch sharing a different detection order. This approach generates multiple number of lists and can further improve the performance of GL-SIC. Since it is not practical to test all $L_b = K!$ possibilities due to the high complexity, a reduced number of branches is employed. Note that a small number of branches captures most of the performance gains and allow the GL-SIC with the MB technique to approach the ML performance. With each index number in $\mathbf{O}_{l_b}$ (the l_b-th branch) being the corresponding index number in $\mathbf{O}$ cyclically shifted to the right by one position as shown by

$$\mathbf{O}_{l_1} = [K, 1, 2, ..., K-2, K-1],$$

$$\mathbf{O}_{l_2} = [K-1, K, 1, ..., K-3, K-2],$$

$$\vdots$$

$$\mathbf{O}_{l_{K-1}} = [2, 3, 4, ..., K, 1],$$

$$\mathbf{O}_{l_K} = [K, K-1, K-2, ..., 2, 1] \text{(reverse order)}.$$

After that, each of the K parallel branches computes a GL-SIC algorithm with its corresponding order. After obtaining $K+1$ different candidate lists according to each branch, a modified ML rule is applied with the following steps:

1. Obtain the best candidate branch $\mathbf{b}^{O_{l_{\text{base}}}}(i)$ among all $K+1$ (**O** included) parallel branches according to the ML rule:

$$\mathbf{b}^{O_{l_{\text{base}}}}(i) = \arg \min_{0 \le l_b \le K} \| \mathbf{y}_{sr_l}(i) - \mathbf{H}_{sr_l} \mathbf{b}^{O_{l_b}}(i) \|^2 \tag{3.22}$$

2. Re-examine the detected symbol for user k $(k = 1, 2, ..., K)$ by fixing the detected results of all other unexamined users in $\mathbf{b}^{O_{l_{\text{base}}}}(i)$.

3. Replace the k-th user's detection result $\hat{b}_k$ in $\mathbf{b}^{O_{l_{\text{base}}}}(i)$ by its corresponding detected values from all other K branches $\mathbf{b}^{O_{l_b}}(i)$, $(l_b \neq l_{\text{base}}, \mathbf{O} = \mathbf{O}_{l_0})$ with the same index, the combination of updated detections with the minimum Euclidean distance is selected through the ML rule and the improved estimate of user k is saved and kept.

4. The same process is then repeated with the next user in $\mathbf{b}^{O_{l_{\text{base}}}}(i)$ until all users in $\mathbf{b}^{O_{l_{\text{base}}}}(i)$ are examined.

The proposed modified ML selection technique is shown in Algorithm 2.

Algorithm 2 The modified ML selection process

$\mathbf{b}^{\text{opt}} = [\,]$ % define an empty vector initially
for k = 1 **to** K
  for n = 1 **to** K
    $\mathbf{b}_{\text{temp}}^{\mathbf{O}_{l_n}} = [\mathbf{b}^{\text{opt}}, \mathbf{b}^{\mathbf{O}_{l_n}}[k], \mathbf{b}^{\mathbf{O}_{l_{\text{base}}}}[k+1], ..., \mathbf{b}^{\mathbf{O}_{l_{\text{base}}}}[K]]$
  end
  Apply ML rule to choose the best combination
  % save the corresponding estimate for user k from the selected
    branch $\mathbf{O}_{l_{\text{selected}}}$ that provides the best combination
  $\mathbf{b}^{\text{opt}} = [\mathbf{b}^{\text{opt}}, \mathbf{b}^{\mathbf{O}_{l_{\text{selected}}}}[k]]$ % $\mathbf{O}_{l_{\text{selected}}}$ is the current selected branch
end

3.4 Proposed GL-PIC Multiuser Detection

In this section, we present a GL-PIC detector that can be applied at both the relays and destination in the uplink of a cooperative system. The GL-PIC detector uses the RAKE receiver as the front-end, so that the matrix inversion brought by the MMSE filter can be avoided. Specifically, the proposed GL-PIC algorithm determines the reliability of the detected symbol by comparing the Euclidean distance between the symbols of users of interest and the potential nearest constellation point with a chosen threshold. After checking the reliability of the symbol estimates, the n_q most unreliable users are re-examined in a greedy-like approach, which saves computational complexity by avoiding redundant processing with reliable users. The soft estimates of the RAKE receiver for each user are obtained by

$$u_k(i) = \mathbf{w}_{s_k r_l}^H \mathbf{y}_{sr_l}(i), \tag{3.23}$$

As shown in Fig. 3.2, for the k-th user, the reliability of its soft estimates is determined by the Euclidean distance between $u_k(i)$ and its nearest constellation points c. After the first round reliability check, n_a reliable users and n_b unreliable users are obtained ($n_a + n_b = K$).

Reliable decision:

If the soft estimates of n_a users satisfy the following condition

$$u_{\mathbf{t}_a(t)}(i) \notin \mathbf{C}_{\text{grey}}, \quad \text{for } t \in [1, 2, ..., n_a], \tag{3.24}$$

where $\mathbf{t}_a$ is a $1 \times n_a$ vector that contains n_a reliable estimates, $\mathbf{C}_{\text{grey}}$ is the grey area in Fig. 3.2 and the grey area would extend along both the vertical and horizontal directions. These soft estimates are then applied to a slicer $Q(\cdot)$ as described by

$$\hat{b}_{\mathbf{t}_a(t)}(i) = Q(u_{\mathbf{t}_a(t)}(i)), \text{ for } t \in [1, 2, ..., n_a], \tag{3.25}$$

where $\hat{b}_{\mathbf{t}_a(t)}(i)$ denotes the detected symbol for the $\mathbf{t}_a(t)$-th user.

Unreliable decision:

In case that n_b users are determined as unreliable, a $1 \times n_b$ vector $\mathbf{t}_b$ with n_b unreliable estimates included is produced, as given by

$$u_{\mathbf{t}_b(t)}(i) \in \mathbf{C}_{\text{grey}}, \quad \text{for } t \in [1, 2, ..., n_b], \tag{3.26}$$

we then sort these unreliable estimates in terms of their Euclidean distance in a descending order. Consequently, the first n_q users from the ordered set are deemed as the most unreliable ones as they experience the farthest distance to their reference constellation points. These n_q estimates are then examined in terms of all possible constellation values c^m (m denotes the index number and $m = 1, 2, ..., N_c$) from the $1 \times N_c$ constellation points set $\mathbf{C} \subseteq F$, where F is a subset of the complex field, and N_c is determined by the modulation type. Meanwhile, the remaining $n_p = n_b - n_q$ unreliable users are applied to the slicer $Q(\cdot)$ directly, as described by

$$\hat{b}_{\mathbf{t}_p(t)}(i) = Q(u_{\mathbf{t}_p(t)}(i)), \quad \text{for } t \in [1, 2, ..., n_p], \tag{3.27}$$

$$\hat{b}_{\mathbf{t}_q(t)}(i) = c^m, \quad \text{for } t \in [1, 2, ..., n_q], \tag{3.28}$$

where $\mathbf{t}_p \cap \mathbf{t}_q = \varnothing$ and $\mathbf{t}_p \cup \mathbf{t}_q = \mathbf{t}_b$.

Therefore, by listing all possible combinations of elements across the n_q most unreliable users, the following $K \times 1$ tentative candidate decision lists are generated

$$\mathbf{b}^j = [\mathbf{s}_a, \ \mathbf{s}_p, \ \mathbf{s}_q^j]^T, \ j \in [1, 2, ..., N_c^{n_q}], \tag{3.29}$$

where

$\mathbf{s}_a = [\hat{b}_{\mathbf{t}_a(1)}, \hat{b}_{\mathbf{t}_a(2)}, ..., \hat{b}_{\mathbf{t}_a(n_a)}]^T$ is a $n_a \times 1$ vector that contains the detected values for the n_a reliable users,

$\mathbf{s}_p = [\hat{b}_{\mathbf{t}_p(1)}, \hat{b}_{\mathbf{t}_p(2)}, ..., \hat{b}_{\mathbf{t}_p(n_p)}]^T$ is a $n_p \times 1$ vector that represents n_p unreliable users that are detected by the slicer $Q(\cdot)$ directly,

$\mathbf{s}_q^j = [c^m_{\mathbf{t}_q(1)}, c^m_{\mathbf{t}_q(2)}, ..., c^m_{\mathbf{t}_q(n_q)}]^T$ is a $n_q \times 1$ tentative candidate combination vector. Each entry of the vector is allocated a value from the constellation point set $\mathbf{C}$ and all possible $N_c^{n_q}$ combinations need to be considered and examined.

The trade-off between performance and complexity is highly related to the modulation type and the number (n_q) of users we choose from $\mathbf{t}_b$. Additionally, the threshold we set at the initial stage is also a key factor that could affect the quality of detection.

After the $N_c^{n_q}$ candidate lists are generated, the ML rule is used subsequently to choose the best candidate list as described by

$$\mathbf{b}^{\text{opt}} = \arg \min_{1 \leq j \leq N_c^{n_q}} \parallel \mathbf{y}_{sr_l}(i) - \mathbf{H}_{sr_l}\mathbf{b}^j(i) \parallel^2 . \tag{3.30}$$

Following that, $\mathbf{b}^{\text{opt}}$ is used as the input for a multi-iteration PIC process as described by

$$\hat{b}_k^i = Q\big(\mathbf{w}_{sr_l,k}^H \mathbf{y}_{sr_l} - \sum_{\substack{j=1 \\ j \neq k}}^{K} \mathbf{w}_{sr_l,k}^H \mathbf{H}_{sr_l,j} \hat{b}_j^{i-1}\big), i \geq 2 \tag{3.31}$$

where $\hat{b}_j^{\text{opt}} = \hat{b}_j^{(i-1)}$ denotes the detected symbol for user j that is used as the input $(i = 2)$ for the first PIC iteration, $\hat{b}_k^i$ denotes the detected value for user k at the i-th PIC iteration, $\mathbf{H}_{sr_l,j}$ stand for the channel matrices for the j-th user from the source to the l-th relay, $\mathbf{w}_{sr_l,k}^H$ represents the RAKE receiver for user k from the source to the l-th relay and $\hat{b}_j^{i-1}$ is the detected value for user j that comes from the $(i-1)$-th PIC iteration. Normally, the conventional PIC is performed in a multi-iteration way, where for each iteration, PIC simultaneously subtracts off the interference for each user produced by the remaining ones. The MAI generated by other users is reconstructed based on the tentative decisions from the previous iteration. Therefore, the accuracy of the first iteration would highly affect the PIC performance as error propagation occurs when incorrect information imports. In this case, with the help of the GL-PIC algorithm, the detection performance is improved. The key novelty is that GL-PIC employs more reliable estimates by exploiting prior knowledge of the constellation points.

The proposed GL-PIC algorithm is detailed in Algorithm 3.

Algorithm 3 The GL-PIC algorithm

$u_k(i) = \mathbf{w}_k^H \mathbf{y}_{sr_l}(i)$ % soft outputs of all candidates

for k=1:K

% Threshold comparison

if $u_{\mathbf{t}_a(t)}(i) \notin \mathbf{C}_{\text{grey}}$

$\hat{b}_{\mathbf{t}_a(t)}(i) = Q(u_{\mathbf{t}_a(t)}(i))$

else

n_b **unreliable users are prepared for reliability re-examination** % $u_{\mathbf{t}_b(t)}(i) \in \mathbf{C}_{\text{grey}}$

end

end

Sort unreliable estimates $\mathbf{t}_b$ in terms of the Euclidean distance

in a descending order

for t=1:n_q % for the first n_q most unreliable users

$\hat{b}_{\mathbf{t}_b(t)}(i) = c^m$

end

for t=n_q+1:length($\mathbf{t}_b$)

$\hat{b}_{\mathbf{t}_b(t)}(i) = Q(u_{\mathbf{t}_b(t)}(i))$

end

% Apply the ML rule to choose the best candidate list

$\mathbf{b}^{\text{opt}} = \arg\min_{1 \le j \le N_c^{n_q}} \parallel \mathbf{y}_{sr_l}(i) - \mathbf{H}_{sr_l}\mathbf{b}^j(i) \parallel^2$

% The three-iteration PIC process

% $\mathbf{b}^{\text{opt}}$ is used as the input

$\hat{b}_k^i = Q\big(\mathbf{w}_{sr_l,k}^H \mathbf{y}_{sr_l} - \sum_{\substack{j=1 \\ j \ne k}}^{K} \mathbf{w}_{sr_l,k}^H \mathbf{H}_{sr_l,j} \hat{b}_j^{i-1}\big)$

3.5 Proposed Greedy Multi-relay Selection Method

In this section, a greedy multi-relay selection method is introduced. For this problem, an exhaustive search of all possible subsets of relays is needed to attain the optimum relay combination for high-quality data transmission. However, the major problem that prevents us from applying an exhaustive search in practical communications is its very high computational complexity. With L relays involved in the re-transmission, an exponential complexity of $2^L - 1$ would be required. This fact motivates us to seek alternative methods. By eliminating the poorest relay-destination link stage by stage, the standard greedy algorithm can be used in the selection process, yet only a local optimum can be achieved. Unlike existing greedy techniques, the proposed greedy multi-relay selection method can go through a sufficient number of relay combinations and approach the best one based on previous decisions. In the proposed relay selection, the signal-to-interference-plus-noise ratio (SINR) is used as the criterion to determine the optimum relay set. The expression of the SINR for user q is given by

$$\mathrm{SINR_q} = \frac{E[|\mathbf{w}_q^H \mathbf{h}_q|^2]}{E[|\boldsymbol{\eta}|^2] + E[|\mathbf{n}|^2]}, \tag{3.32}$$

where $\mathbf{w}_q$ denotes the RAKE receiver for user q, $E[|\boldsymbol{\eta}|^2]$is the interference brought by all other users, and $\mathbf{n}$ is the noise vector that contains samples of zero mean complex Gaussian and variance $\sigma^2\mathbf{I}$. For the purpose of simplicity, the SINR for user q after applying the RAKE receiver is given by

$$\begin{aligned}\mathrm{SINR_q} =& \frac{\mathbf{w}_q^H \rho_{qq} \mathbf{w}_q}{\sum\limits_{\substack{k=1 \\ k\neq q}}^{K} \mathbf{w}_q^H \rho_{kq} \mathbf{w}_q + \sigma_N^2 \mathbf{w}_q^H \mathbf{w}_q} \\ =& \frac{|\mathbf{h}_q^H \mathbf{h}_q|^2}{\sum\limits_{\substack{k=1 \\ k\neq q}}^{K} |\mathbf{h}_q^H \mathbf{h}_k|^2 + \sigma_N^2 \mathbf{h}_q^H \mathbf{h}_q},\end{aligned} \tag{3.33}$$

where $\rho_{qq} = \mathbf{h}_q^H \mathbf{h}_q$ is the correlation coefficient of the desired user q, $\rho_{kq} = \mathbf{h}_q^H \mathbf{h}_k$ is the cross-correlation coefficient between the signatures of user q and user k (interference component), $\mathbf{h}_q$ is the channel vector for user q, it should be mentioned that in various relay combinations, the channel vector $\mathbf{h}_q$ for user q $(q = 1, 2, ..., K)$ is different as different relay-destination links are involved, σ_N^2 is the noise variance. This problem thus

can be cast as the following optimization:

$$\mathrm{SINR}_{\Omega_{\mathrm{best}}} = \max_{\Omega_{r(q)}} \{\min(\mathrm{SINR}_{\Omega_{\mathrm{r(q)}}}), \mathrm{q} = 1, ..., \mathrm{K}\}, \tag{3.34}$$

where q represents the index number for an arbitrary user, Ω_r denotes a possible combination set ($r \leq L(L+1)/2$) of any number of selected relays, $\mathrm{SINR}_{\Omega_{\mathrm{r(q)}}}$ represents the SINR for user q in set Ω_r, min $(\mathrm{SINR}_{\Omega_{\mathrm{r(q)}}}) = \mathrm{SINR}_{\Omega_{\mathrm{r}}}$ means that the SINR for relay set Ω_r is equal to the minimum SINR for a single user in set Ω_r. Ω_{best} is the best relay set that provides the highest SINR.

Clearly, we can also consider the SINR for different relay combinations after applying convention SIC, conventional PIC, linear MMSE or even the proposed detectors. However, RAKE receiver can bring the lowest complexity.

3.5.1 Standard Greedy Relay Selection Algorithm

The standard greedy relay selection method [65] works in stages by removing the single relay according to the channel path power, as given by

$$P_{h_{r_l d}} = \mathbf{h}_{r_l d}^H \mathbf{h}_{r_l d}, \tag{3.35}$$

where $\mathbf{h}_{r_l d}$ is the channel vector between the l-th relay and the destination. At the first stage, the initial SINR is determined when all L relays are involved in the transmission. Consequently, we cancel the worst relay-destination link and calculate the current SINR for the remaining $L-1$ relays, as compared with the previous SINR, if

$$\mathrm{SINR}_{\mathrm{cur}} > \mathrm{SINR}_{\mathrm{pre}}, \tag{3.36}$$

we update the previous SINR as

$$\mathrm{SINR}_{\mathrm{pre}} = \mathrm{SINR}_{\mathrm{cur}}, \tag{3.37}$$

and move to the third stage by removing the current poorest link and repeating the above process. The algorithm stops either when $\mathrm{SINR}_{\mathrm{cur}} < \mathrm{SINR}_{\mathrm{pre}}$ or when there is only one relay left. The selection is performed once at the beginning of each packet transmission.

3.5.2 Proposed Greedy Relay Selection Algorithm

In order to improve the performance of the standard algorithm, we propose a new greedy relay selection algorithm that is able to achieve a good balance between the performance and the complexity. The proposed method differs from the standard technique as we drop each of the relays in turns rather than drop them based on the channel condition at each stage. The algorithm can be summarized as:

1. Initially, a set Ω_A that includes all L relays is generated and its corresponding SINR is calculated, denoted by $\mathrm{SINR}_{\mathrm{pre}}$.

2. For the second stage, we calculate the SINR for L combination sets with each dropping one of the relays from Ω_A. After that, we choose the combination set with the highest SINR for this stage, recorded as $\mathrm{SINR}_{\mathrm{cur}}$.

3. Compare $\mathrm{SINR}_{\mathrm{cur}}$ with the previous stage $\mathrm{SINR}_{\mathrm{pre}}$, if (3.36) is true, we save this corresponding relay combination as Ω_{cur} at this stage. Meanwhile, we update the $\mathrm{SINR}_{\mathrm{pre}}$ as in (3.37).

4. After moving to the third stage, we drop relays in turn again from Ω_{cur} obtained in stage two. $L-1$ new combination sets are generated, we then select the set with the highest SINR and repeat the above process in the following stages until either $\mathrm{SINR}_{\mathrm{cur}} < \mathrm{SINR}_{\mathrm{pre}}$ or there is only one relay left.

This proposed greedy selection method considers the combination effect of the channel condition so that additional useful sets are examined. When compared with the standard greedy relay selection method, the previous stage decision is more accurate and the global optimum can be approached more closely. Furthermore, its complexity is less than
$L(L+1)/2$, which is much lower than the exhaustive search. Similarly, the whole process is performed only once before each packet and only needs to be repeated when the channels change.

Finally, it should also be noticed that relay selection can be also operated at the source-relay part as this is two phase process. However, in this thesis, we only consider the relay

selection that occurs during the relay–destination links for the purpose of simplicity.

The proposed greedy multi-relay selection algorithm is depicted in Algorithm 4.

Algorithm 4 The proposed greedy multi-relay selection algorithm

$\Omega_A = [1, 2, 3, ...L]\%$ Ω_A denotes the set when all relays are involved
$\mathrm{SINR}_{\Omega_\mathrm{A}} = \min(\mathrm{SINR}_{\Omega_{\mathrm{A(q)}}}), q = 1, 2, ...K$
$\mathrm{SINR}_{\mathrm{pre}} = \mathrm{SINR}_{\Omega_\mathrm{A}}$
for stage =1 **to** $L - 1$
  for r=1 **to** $L + 1$-stage
    $\Omega_r = \Omega_A - \Omega_{A(r)}\%$ drop each of the relays in turns
    $\mathrm{SINR}_{\Omega_\mathrm{r}} = \min(\mathrm{SINR}_{\Omega_{\mathrm{r(q)}}}), q = 1, 2, ..., K$
  end for
  $\mathrm{SINR}_{\mathrm{cur}} = \max(\mathrm{SINR}_{\Omega_\mathrm{r}})$
  $\Omega_{\mathrm{cur}} = \Omega_{\mathrm{SINR}_{\mathrm{cur}}}$
  if $\mathrm{SINR}_{\mathrm{cur}} > \mathrm{SINR}_{\mathrm{pre}}$ **and** $|\Omega_{\mathrm{cur}}| > 1$
    $\Omega_A = \Omega_{\mathrm{cur}}$
    $\mathrm{SINR}_{\mathrm{pre}} = \mathrm{SINR}_{\mathrm{cur}}$
  else
    break
  end if
end for

3.6 Analysis of the Proposed Algorithms

In this section, we analyze the computational complexity required by the proposed and existing interference cancellation algorithms and the proposed greedy relay selection method.

Table 3.1: Computational complexity of existing and proposed MUD algorithms

Algorithms	**Computational Complexity (Flops)**
Matched filter	$M(4L_p^2 + 4KL_p - 2L_p + 6K) - 2K$
Conventional SIC	$M(4L_p^2 + 4KL_p - 2L_p + 18K - 12) - 4K + 2$
Conventional PIC	$M(4L_p^2 + 4KL_p - 2L_p + 10K + 4K^2) - 4K$
Linear MMSE receiver	$8M^3 + M^2(16K - 8) + M(4L_p^2 + 4KL_p - 2L_p + 4K + 4) - 2K$
Proposed GL-SIC	$M(4L_p^2 + 4KL_p - 2L_p + 6K) - 2K + N_c^n(20MK - 8Mn + 4M - 2K + 2n - 2)$
Proposed GL-PIC	$M(4L_p^2 + 4KL_p - 2L_p + 10K + 4K^2) - 4K + N_c^{n_q}(8MK + 8M - 2)$
Standard Likelihood (ML) detector	$M(4L_p^2 + 4KL_p - 2L_p - 2K) + N_c^K(8MK + 8M - 2)$

3.6.1 Computational Complexity

We first compare the computational complexity of the proposed (GL-SIC and GL-PIC) and other existing interference cancellation algorithms in terms of the required floating point operations (flops). The resulting complexity is calculated as a function of the following parameters:

- Total number of users K.
- The number of multipath channel components L_p.
- The number of constellation points N_c that correspond to the modulation type.
- The parameter M which corresponds to the length of the receive filters, where $M = N + L_p - 1$ and N is the spreading gain.

Specifically, in the GL-SIC algorithm, n refers to the number of users we considered per each stage, and in the GL-PIC algorithm, n_q represents the number of unreliable users that need to be re-examined in the second processing stage. The required flops are considered both in the case of real and complex matrix operations. It is worth noting that, in real arithmetic, a multiplication followed by an addition requires 2 flops while for the complex numbers, 8 flops are required when an addition is executed after a multiplication. As a result, it can be approximated that the complexity of a complex matrix multiplication is 4 times of its real counterpart.

Table. 3.1 illustrates a comparison of the computational complexity for various existing detection methods and our proposed algorithms. The Y-axis is presented in log-scale form in order to make the figures more visible. It is worth noting that the GL-SIC algorithm has variable complexity according to different circumstances as an unpredictable number of unreliable users may appear in any of the stages. As a result, the corresponding worst-case scenario is evaluated when all n users are considered as unreliable at the first stage.

For each case shown in Table. 3.1, the upper bound of the complexity is given by the standard ML detector, where it explores all possible combinations of the detected

results and chooses the one with the minimum Euclidean distance. However, when a large number of users need to be considered, an exponential complexity growth would limit its application in practical utilization. In contrast, with careful control of the number of unreliable users n and n_q being re-examined in both proposed algorithms, a substantial complexity saving is achieved. Additionally, our proposed greedy list-based algorithms offer a clear complexity advantage over the linear MMSE receiver as they adopt the RAKE receiver as the front end, so that the cubic complexity can be avoided. Another feature to highlight is that although our proposed algorithms have a complexity slightly higher than the matched filter, the conventional SIC and the conventional PIC, they exhibit significant performance gains over existing techniques.

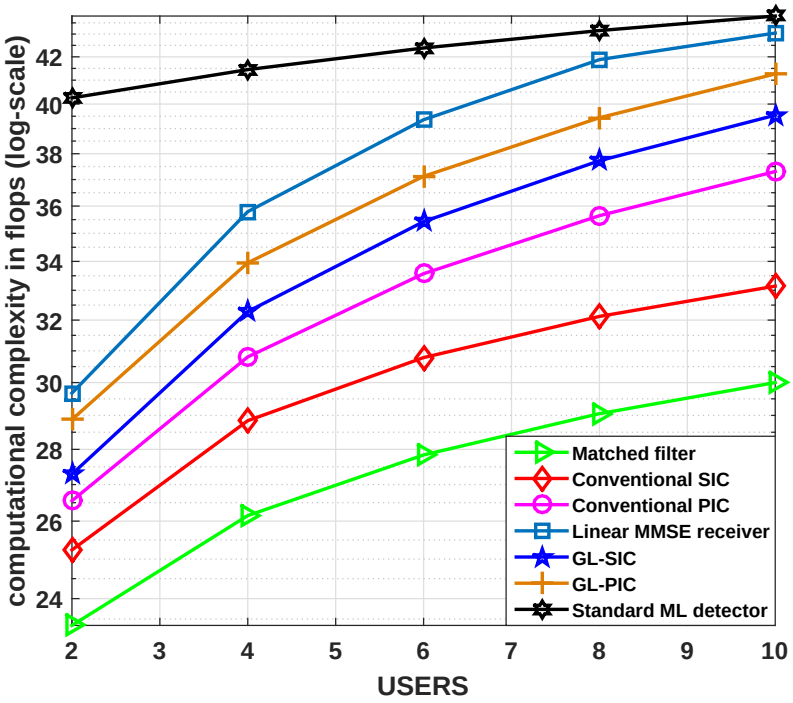

Figure 3.3: Computational complexity in flops for various MUD detectors

In order to further investigate the computational complexity for various MUD techniques, we fix the number of users $K = 10$, the number of multipaths in the channel $L_p = 3$ and assume the BPSK modulation is adopted. The required number of flops (log-scale) of the proposed and existing MUD algorithms are simulated in Fig. 3.3, where in the GL-SIC algorithm, $n = 2$ users are considered jointly at each stage and in the GL-PIC algorithm, $n_q = 3$ unreliable users need to be re-examined in the second processing stage. With the increase of the number of users, the standard ML detector

experienced the highest complexity when compared with other MUD schemes, which, from another point of view, demonstrates that the improvement in its performance is achieved at the expense of a large increase in computational complexity. A similar complexity trend for the linear MMSE receiver illustrated in Fig. 3.3 shows a relatively lower complexity than the standard ML detector, however, its complexity still substantially exceeds that of the remaining strategies as a cubic cost is brought. Another important point observed in Fig. 3.3 is that our proposed algorithms offer a moderately higher cost than the matched filter, the conventional SIC and the conventional PIC, whereas they provide a considerable performance advantage over these schemes, resulting in an attractive trade-off between complexity and performance.

3.6.2 Greedy Relay Selection Analysis

The proposed greedy multi-relay selection method is a stepwise backward selection algorithm, where we optimize the selection based on the SINR criterion at each stage. We begin the process when all relays participate in the transmission and then subtract off the contributions brought by each of the relays from set of selected relays of the previous stage. The relay combinations generated at each stage are presented as follows:

$$\begin{aligned}
&\text{Stage } 1: \ \{\Omega_1^1\},\\
&\text{Stage } 2: \ \{\Omega_1^2, \Omega_2^2, \Omega_3^2, ..., \Omega_L^2\},\\
&\qquad\qquad \vdots\\
&\text{Stage s}: \ \{\Omega_1^s, \Omega_2^s, \Omega_3^s, ..., \Omega_{L+2-s}^s\},\\
&\qquad\qquad \vdots\\
&\text{Stage } L-1: \ \{\Omega_1^{L-1}, \Omega_2^{L-1}, \Omega_3^{L-1}\},\\
&\text{Stage } L: \ \{\Omega_1^L, \Omega_2^L\},
\end{aligned}$$

where Ω_i^s denotes the i-th relay combination at the s-th stage. Clearly, the maximum number of relay combinations that we have to consider for all L stages is $1 + 2 + 3 + ... + L = (1 + L)L/2$, since this algorithm stops either when $\mathrm{SINR}_{\mathrm{cur}} < \mathrm{SINR}_{\mathrm{pre}}$ or when there is only one relay left, the associated complexity for the proposed greedy relay selection strategy is less than $(1 + L)L/2$.

Compared with the exhaustive search, which is considered as the optimum relay

selection method, the number of relay combinations examined at each stage is given by

$$\begin{aligned}
&\text{Stage } 1: \ \{\Omega_1^1\},\\
&\text{Stage } 2: \ \{\Omega_1^2, \Omega_2^2, \Omega_3^2, ..., \Omega_L^2\},\\
&\qquad\qquad \vdots\\
&\text{Stage s}: \ \{\Omega_1^s, \Omega_2^s, \Omega_3^s, ..., \Omega^s_{\frac{L(L-1)...(L-s+2)}{(s-1)!}}\},\\
&\qquad\qquad \vdots\\
&\text{Stage } L-1: \ \{\Omega_1^{L-1}, \Omega_2^{L-1}, \Omega_3^{L-1}, ..., \Omega^{L-1}_{\frac{L(L-1)}{2}}\},\\
&\text{Stage } L: \ \{\Omega_1^L, \Omega_2^L\, \Omega_3^L, ..., \Omega_L^L\}.
\end{aligned}$$

The total number of relay combinations can then be calculated as $C_L^L + C_L^{L-1} + C_L^{L-2} + ... + C_L^2 + C_L^1 = 2^L - 1$, where each term $C_m^n = \frac{m(m-1)...(m-n+1)}{n!}$ represents the number of combinations that we choose, i.e., n elements from m elements $(m \geq n)$. The proposed greedy algorithm provides a much lower cost with a moderate to large number of relays when compared with the exhaustive search as an exponential complexity is avoided.

In fact, the idea behind the proposed algorithm is to choose relay combinations in a greedy fashion. At each stage, we select the set of relays with the highest SINR and the previous stage result always affects the following stage set of relays candidates. Then we subtract off the contribution brought by each of the remaining relays and iterate on the residual. After several stages, the algorithm is able to identify the optimum relay set. To this end, we propose the following proposition.

Proposition: the proposed greedy algorithm achieves an SINR that is bounded as follows:

$$\text{SINR}_{\Omega\text{standard}} \leq \text{SINR}_{\Omega\text{proposed}} \leq \text{SINR}_{\Omega\text{exhaustive}}$$

Proof:

From the proposed greedy algorithm, the set containing the selected relay at the s-th stage is given by

$$\begin{aligned}
\Omega^s_{\text{proposed}} &= \{m, n, ..., p\}\\
&= \max\{\Omega^{s-1}_{\text{proposed}} \setminus \Omega^{s-1}_{\text{proposed}}(i), i \in [1, L+2-s]\},
\end{aligned}$$

where $\Omega^s \setminus \Omega^s(i)$ denotes a complementary set where we drop the i-th relay from the relay set Ω^s. m, n and p represent the relay m, the relay n and the relay p, respectively.

We first prove the lower bound for an arbitrary stage s by induction, other stages can be obtained accordingly. Assuming both algorithms achieve the same set at stage s, we have

$$\Omega^s_{\text{standard}} = \{m, n, ..., p\},$$
$$\Omega^s_{\text{proposed}} = \{m, n, ..., p\},$$

which leads to the equality $\text{SINR}_{\Omega^s_{\text{standard}}} = \text{SINR}_{\Omega^s_{\text{proposed}}}$, if we then proceed with the proposed greedy algorithm and choose a different set which provides a higher SINR, we have

$$\Omega^s_{\text{standard}} = \{m, n, ..., p\},$$
$$\Omega^s_{\text{proposed}} = \{m, n, ..., q\},$$

with the only different relay being $p \neq q$, and assuming that q provides a higher SINR than p, we prove the inequality that $\text{SINR}^{\text{s}}_{\Omega\text{standard}} \leq \text{SINR}^{\text{s}}_{\Omega\text{proposed}}$.

We then investigate the upper bound by comparing the proposed algorithm and the exhaustive search at an arbitrary stage s, other stages can be obtained accordingly. At an arbitrary stage s, since $\Omega^s_{\text{proposed}}$ is a candidate subset of the exhaustive search, we have

$$\Omega^s_{\text{exhaustive}} = \max\{\Omega^s_{\text{exhautive(i)}}, i \in [1, C_L^{L+1-s}]\},$$
$$\Omega^s_{\text{proposed}} \in \{\Omega^s_{\text{exhautive(i)}}, i \in [1, C_L^{L+1-s}]\},$$

where $\Omega^s_{\text{exhaustive(i)}}$ represents the i-th relay combination selected at the s-th stage of the exhaustive greedy relay selection method.

Assuming both strategies select the same relay combination at stage s, we have

$$\Omega^s_{\text{proposed}} = \{m, n, ..., p\},$$
$$\Omega^s_{\text{exhaustive}} = \{m, n, ..., p\},$$

this situation again leads to the equality that $\text{SINR}_{\Omega^s_{\text{proposed}}} = \text{SINR}_{\Omega^s_{\text{exhaustive}}}$. In contrast, if the exhaustive search picks another relay set belongs to $\{\Omega^s_{\text{exhautive(i)}}, i \in [1, C_L^{L+1-s}]\}$ that provides a higher SINR, clearly, $\Omega^s_{\text{proposed}} \neq \Omega^s_{\text{exhaustive}}$, we can then obtain the inequality that $\text{SINR}_{\Omega^s_{\text{proposed}}} \leq \text{SINR}_{\Omega^s_{\text{exhaustive}}}$.

3.7 Proposed Cross-layer Design

In this section, we present and analyze a cross-layer design strategy that combines the proposed MUD techniques with the proposed greedy multi-relay selection algorithm for the uplink of the cooperative DS-CDMA networks. This approach jointly considers the performance optimization across different layers of the network, since inappropriate data detection and estimation that are executed at the lower physical layer can spread incorrect information to the data and link layer where relay selection strategy performs, causing the loss of useful information and degradation of the overall system performance. In this case, when improved data detection is obtained at the physical layer, together with an effective relay selection, a better system performance can be achieved.

As stated in previous sections, the system operates in two phases, where for the first phase, the proposed MUD techniques are applied and processed at each of the relays with a DF protocol, after the detection process, the proposed greedy multi-relay selection algorithm is then performed to seek the optimum relay combination. In the second phase, the chosen relays take part in the transmission in order to forward the information to the destination. After all the data are received at the destination, the proposed MUD algorithms are applied to recover the transmitted data.

Given the received data $\mathbf{y}_{sd}$ and $\mathbf{y}_{sr_l}$ at the destination and each of the relays, we wish to optimize the overall system performance in terms of the bit error rate (BER), through the selection of the received signals $\mathbf{y}_{rd}$ at the destination from all relays, the accuracy of the detected symbols $\hat{b}_{r_l d,k}$ at each of the relays and the detected results $\hat{b}_k$ at the destination, subject to practical system constraints (K, L, L_p, $\mathbf{H}_{sd}$, $\mathbf{H}_{sr_l}$, $\mathbf{H}_{r_l d}$). The proposed cross-layer design can be cast into the following optimization problem:

$$(\hat{\mathbf{b}}, \Omega^{\text{opt}}) = \arg \min_{(\mathbf{b},\Omega_s)} \left\| \begin{bmatrix} \mathbf{y}_{sd} \\ \sum\limits_{l\in\Omega^s} \mathbf{H}_{r_l d}\hat{\mathbf{b}}_{r_l d} \end{bmatrix} - \begin{bmatrix} \mathbf{H}_{sd}\mathbf{b}^j \\ \sum\limits_{l\in\Omega^s} \mathbf{H}_{r_l d}\mathbf{b}^j \end{bmatrix} \right\|^2$$

$$\begin{aligned} &\text{subject to} \\ &\qquad 1).\ 1 \le j \le N_c^{n_q} \text{or } N_c^n, \\ &\qquad 2).\ \Omega^{\text{opt}} = \Omega^s \text{ when } \text{SINR}_{\Omega^s} < \text{SINR}_{\Omega^{s-1}}, \\ &\qquad 3).\ \text{SINR}_{\Omega^s} = \max\{\ \min\ (\text{SINR}_{\Omega^s_{i(k)}})\}, \\ &\qquad 4).\ k = 1, 2, ..., K, \\ &\qquad 5).\ s \le L, \\ &\qquad 6).\ i = 1, 2, ..., L + 2 - s \text{ when } s \in [2, L], \\ &\qquad 7).\ i = 1 \text{ when } s = 1, \end{aligned} \tag{3.38}$$

where $\mathbf{b}^j$ stands for the j-th candidate list generated after applying the GL-SIC/GL-PIC algorithms at the destination, s denotes stage index in the relay selection process, Ω^s represents the selected relay combination at the stage s, $\text{SINR}_{\Omega^s_{i(k)}}$ is the SINR for the k-th user in the i-th relay combination at stage s and Ω^{opt} is the optimum relay combination obtained through the proposed greedy relay selection method. The cross-layer optimization in (3.38) is a non-convex optimization problem due to the discrete nature of the joint detection and relay selection problems. We propose to solve it in two stages using the proposed greedy detection and relay selection algorithms.

During the first phase, the received vector $\mathbf{y}_{sr_l}$ passes through the proposed GL-SIC/GL-PIC algorithms at the relay l, lists of candidate combinations $\mathbf{b}^j_{r_l d}$ are generated in the lower physical layer and the corresponding detected result $\hat{b}_{r_l d,k}$ is then obtained via the following ML selection

$$\hat{\mathbf{b}}_{r_l d} = \arg \min_{\mathbf{b}_{r_l d}} \parallel \mathbf{y}_{sr_l} - \mathbf{H}_{sr_l}\mathbf{b}^j_{r_l d} \parallel^2,\ 1 \le j \le N_c^{n_q} \text{or } N_c^n. \tag{3.39}$$

This interference cancellation operation affects the following process in two different ways.

- The accuracy of $\hat{b}_{r_l d,k}$ directly controls the re-generated signals $\mathbf{y}_{rd}$ received at the destination via the physical layer as can be verified from (3.4), hence, it further affects the decisions $\hat{b}_k$ made at the end as (3.5) computes.

- Improper detection of $\hat{b}_{r_l d,k}$ can cause the error propagation spreads in the second phase.

Consequently, in the second phase, the proposed greedy relay selection strategy is performed at the data and link layer, the selection takes into account the physical layer characteristics as appropriate detection result coming from the lower physical layer can prevent error propagation spreading into the upper data and link layer.

In order to describe this process mathematically, we first define the SINR for the i-th relay combination at an arbitrary stage s as

$$\mathrm{SINR}_{\Omega_i^s} = \min \ \{\mathrm{SINR}_{\Omega_{i(k)}^s}\}, k = 1, 2, ..., K. \tag{3.40}$$

This algorithm operates in stages, and the SINR for the selected relay combination at each stage is given by

$$\begin{aligned}
\mathrm{SINR}_{\Omega^1} =& \mathrm{SINR}_{\Omega_A}, \Omega^1 = \Omega_A = [1, 2, 3, ..., L], \\
\mathrm{SINR}_{\Omega^2} =& \max \{\mathrm{SINR}_{\Omega_i^2}\}, \Omega_i^2 = \Omega^1 \setminus \Omega^1(i), i = 1, ..., L, \\
\mathrm{SINR}_{\Omega^3} =& \max \{\mathrm{SINR}_{\Omega_i^3}\}, \Omega_i^3 = \Omega^2 \setminus \Omega^2(i), i = 1, ..., L-1, \\
& \vdots \\
\mathrm{SINR}_{\Omega^L} =& \max \{\mathrm{SINR}_{\Omega_i^L}\}, \Omega_i^L = \Omega^{L-1} \setminus \Omega^{L-1}(i), i = 1, 2.
\end{aligned}$$

The selection stops when $\mathrm{SINR}_{\Omega^s} < \mathrm{SINR}_{\Omega^{s-1}}$ is achieved, and the optimum relay combination is then computed as $\Omega^{\mathrm{opt}} = \Omega^s$. After that, the selected relays continue to forward the re-generated signals to the destination in the second phase. At the destination, after we receive both the signals from the direct links and the selected relays, we then apply the GL-SIC/GL-PIC algorithms again to obtain lists of candidates combinations $\mathbf{b}^j$, and the ML algorithm is adopted afterwards to choose the optimum detection list as given by

$$\begin{aligned}
\hat{\mathbf{b}} &= \arg\min_{\mathbf{b}} \left\| \begin{bmatrix} \mathbf{y}_{sd} \\ \sum\limits_{l \in \Omega^{\mathrm{opt}}} \mathbf{y}_{r_l d} \end{bmatrix} - \begin{bmatrix} \mathbf{H}_{sd} \\ \sum\limits_{l \in \Omega^{\mathrm{opt}}} \mathbf{H}_{r_l d} \end{bmatrix} \mathbf{b}^j \right\|^2 \\
&= \arg\min_{\mathbf{b}} \left\| \begin{bmatrix} \mathbf{y}_{sd} \\ \sum\limits_{l \in \Omega^{\mathrm{opt}}} \mathbf{H}_{r_l d} \hat{\mathbf{b}}_{r_l d} \end{bmatrix} - \begin{bmatrix} \mathbf{H}_{sd} \mathbf{b}^j \\ \sum\limits_{l \in \Omega^{\mathrm{opt}}} \mathbf{H}_{r_l d} \mathbf{b}^j \end{bmatrix} \right\|^2,
\end{aligned} \tag{3.41}$$

$$\text{subject to}$$

$$1 \leq j \leq N_c^{n_q} \text{or } N_c^n.$$

The proposed cross-layer design is detailed in Algorithm 5.

Algorithm 5 The cross-layer design

Phase I

%received signals from the source-destination link

$\mathbf{y}_{sd} = \mathbf{H}_{sd}\mathbf{b}_k$

%received signals from the source to the l-th relay

$\mathbf{y}_{sr_l} = \mathbf{H}_{sr_l}\mathbf{b}_k$

% Interference cancellation process at each of the relays

Apply the GL-SIC/GL-PIC algorithms

at each of the relays to obtain $\mathbf{b}^j_{r_ld}$

% Apply the ML rule to select $\hat{\mathbf{b}}_{r_ld}$ from $\mathbf{b}^j_{r_ld}$

$\hat{\mathbf{b}}_{r_ld} = \arg\min \parallel \mathbf{y}_{sr_l} - \mathbf{H}_{sr_l}\mathbf{b}^j_{r_ld} \parallel^2, 1 \leq j \leq N_c^{n_q}$or N_c^n

Phase II

Apply the greedy multi-relay selection method

$\mathrm{SINR}_{\Omega^s_i} = \min \{\mathrm{SINR}_{\Omega^s_{i(k)}}\}, k = 1, 2, ..., K$

$\mathrm{SINR}_{\Omega^s} = \max \{\mathrm{SINR}_{\Omega^s_i}\}, \Omega^s_i = \Omega^{s-1} \setminus \Omega^{s-1}(i),$

$i = 1, 2, ..., L + 2 - s$

$\Omega^{\mathrm{opt}} = \Omega^s$ when $\mathrm{SINR}_{\Omega^s} < \mathrm{SINR}_{\Omega^{s-1}}$

%received signals from the selected relays to the destination

$\mathbf{y}_{rd} = \sum_{l \in \Omega^{\mathrm{opt}}} \mathbf{H}_{r_ld}\hat{\mathbf{b}}_{r_ld}$

Apply the GL-SIC/GL-PIC algorithms

at the destination to obtain $\mathbf{b}^j$

% Apply the ML rule to select $\hat{\mathbf{b}}_k$ from $\mathbf{b}^j (1 \leq j \leq N_c^{n_q}$or $N_c^n)$

$$\hat{\mathbf{b}} = \arg\min \left\| \begin{bmatrix} \mathbf{y}_{sd} \\ \sum_{l \in \Omega^{\mathrm{opt}}} \mathbf{H}_{r_ld}\hat{\mathbf{b}}_{r_ld} \end{bmatrix} - \begin{bmatrix} \mathbf{H}_{sd}\mathbf{b}^j \\ \sum_{l \in \Omega^{\mathrm{opt}}} \mathbf{H}_{r_ld}\mathbf{b}^j \end{bmatrix} \right\|^2.$$

3.8 Simulations

In this section, a simulation study of the proposed multiuser detectors and the low cost greedy multi-relay selection method is carried out. The DS-CDMA network uses

randomly generated spreading codes of length $N = 32$ and $N = 16$, it also employs $L_p = 3$ independent paths with the power profile $[0\text{dB}, -3\text{dB}, -6\text{dB}]$ for the transmission link. The channel is frequency selective and the corresponding channel coefficients are taken as complex Gaussian variables and normalized to ensure the average power is unity over the packet. We assume perfectly known channels at the receiver. Equal power allocation is employed during the transmission. The grey area in the GL-SIC and GL-PIC algorithm is determined by the threshold where $d_{th} = 0.25$. We consider packets with 1000 BPSK symbols and average the curves over 1000 trials. For the purpose of simplicity, $n = 2$ users are considered in the GL-SIC scheme at each stage and for the GL-PIC strategy, a three-iteration PIC process is adopted. The signal-to-noise ratio (SNR) is defined as $\text{SNR} = \sigma_b^2/\sigma^2$, where σ_b^2 corresponds to the signal power and σ^2 is the noise power. The following simulations are compared and analyzed in both non-cooperative and cooperative scenarios.

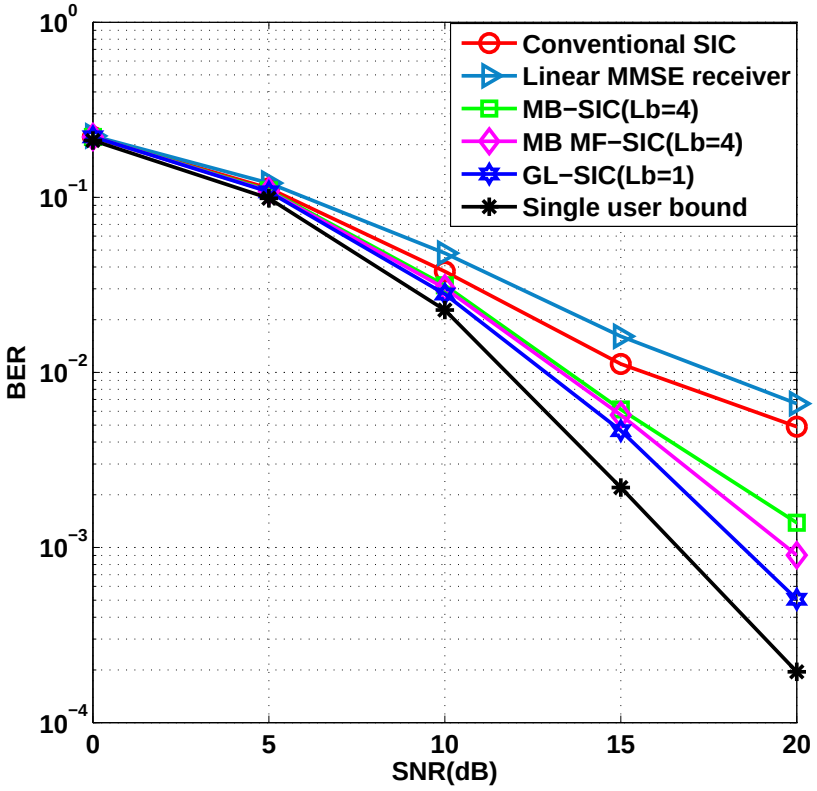

Figure 3.4: GL-SIC comparison in non-cooperative system with 20 users

The first example shown in Fig. 3.4 illustrates the performance comparison between the proposed GL-SIC interference suppression technique and other multiuser detection

methods. The proposed GL-SIC algorithm uses the spreading codes with length $N = 32$ and the overall system is equipped with 20 users that only takes into account the source to the destination link. The conventional SIC detector is the standard SIC with RAKE receivers employed at each stage and the Multi-branch Multi-feedback SIC (MB MF-SIC) detection algorithm proposed in [63] is presented here for comparison purposes. We also produce simulation results for the multi-branch SIC (MB-SIC) detector where four parallel branches with different detection orders are employed. Specifically, the detection order for the first branch is obtained through a power decreasing level, while the detection orders for the remaining three are attained by cyclically shifting the order index from the previous branch to right by one position. Similarly, RAKE receivers are adopted at each cancellation stage. Simulation results reveal that our proposed single branch GL-SIC significantly outperforms the linear MMSE receiver, the conventional SIC and exceeds the performance of MB-SIC with $L_b = 4$ and MB MF-SIC with $L_b = 4$ for the same BER performance.

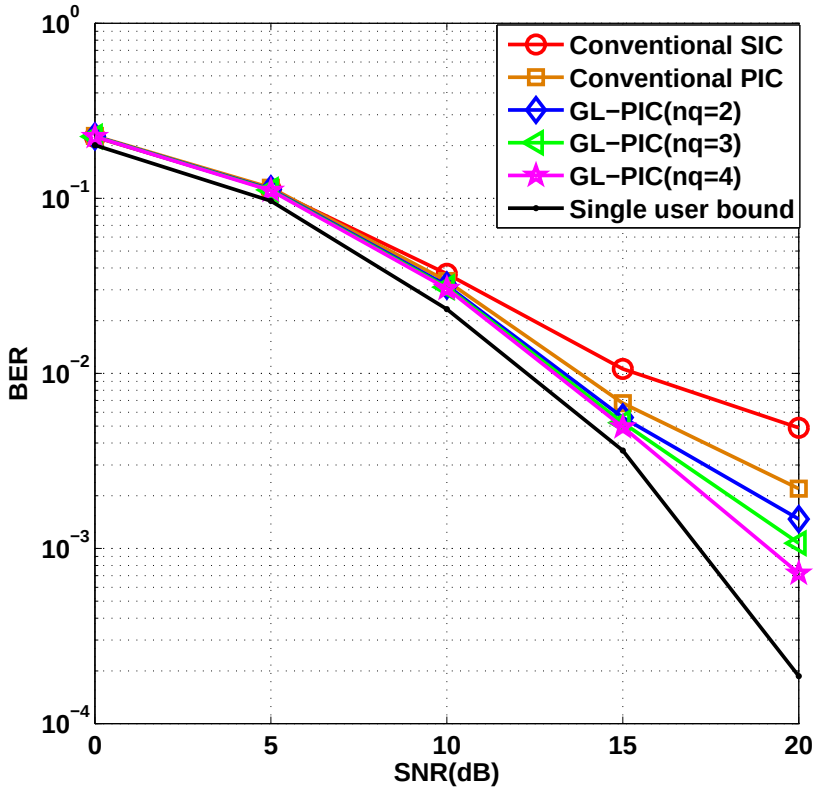

Figure 3.5: GL-PIC comparison in non-cooperative system with 20 users

In the second example, the BER performance of the analyzed detection schemes is then

examined for the proposed GL-PIC detector employed in the direct transmission, $N = 32$ and the user number is 20. As depicted in Fig. 3.5, the results compare the BER versus SNR performance between the conventional detectors and the GL-PIC techniques with different number of unreliable users being re-examined, the figure advises that the GL-PIC algorithm performs better than the conventional SIC detector and the conventional PIC detectors, both with RAKE receivers employed at each cancellation stage. Moreover, with the additional number of unreliable users being re-examined, extra performance gains can be obtained. However, in this non-cooperative system, the performance improvement is slight and the detection capability is not that good when compared with the GL-SIC scheme.

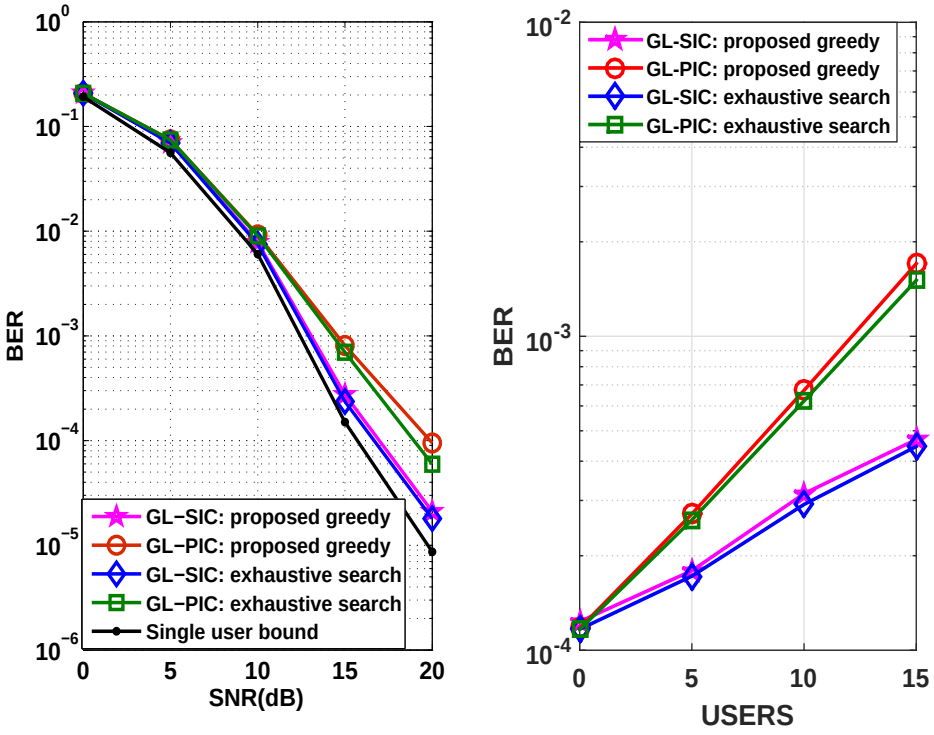

Figure 3.6: a) BER versus SNR for uplink cooperative system (left subplot) b) BER versus number of users for uplink cooperative system (right subplot)

The next scenario illustrated in Fig. 3.6(a) shows the BER versus SNR plot for the cross-layer design using the proposed detectors and the greedy relay selection method, where we apply the GL-SIC/GL-PIC algorithms at both the relays and the destination in an uplink cooperative scenario with 10 users, 6 relays and spreading gain $N = 16$. The performance bounds for an exhaustive search of different detectors are presented here for comparison purposes, where it examines all possible relay combinations and

picks the one with the highest SINR. From the results, it can be seen that with the relay selection, the GL-SIC $(L_b = 1)$ detector performs better than the GL-PIC detector in high SNR region. Furthermore, the BER performance curves of our proposed relay selection algorithm approach almost the same level of the exhaustive search, whilst keeping the complexity reasonably low for practical utilization.

In contrast, the algorithms are then assessed in terms of BER versus number of users in Fig. 3.6(b) with a fixed SNR=15dB. Similarly, we apply both the GL-SIC and the GL-PIC detectors at both the relays and destination. The results indicate that the overall system performance degrades as the number of users increases. In particular, this figure also suggests that our proposed greedy relay selection method has a big advantage for situations without a high load (limited number of users) and can approach the exhaustive search very closely with a relatively lower complexity. Additionally, the BER performance curves of GL-SIC detector is better than the GL-PIC detector especially for a large number of users.

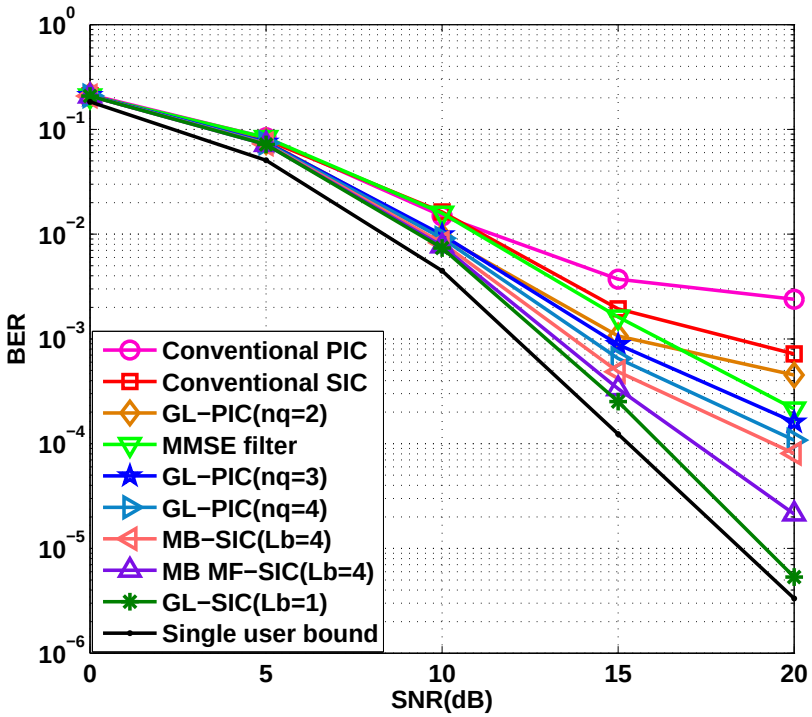

Figure 3.7: BER versus SNR for uplink cooperative system with different filters employed at the relays and the destination

In order to further verify the performance for the proposed cross-layer design, we compare the effect of different detectors with 10 users and 6 relays when this new greedy multi-relay selection algorithm is applied in the system. The results depicted in Fig. 3.7 with spreading gain $N = 16$ indicate that the GL-SIC $(L_b = 1)$ approach allows a more effective reduction of BER and achieves the best performance that is quite close to the single user scenario, followed by the MB MF-SIC $(L_b = 4)$ detector, the MB-SIC $(L_b = 4)$ detector, the GL-PIC detector, the linear MMSE receiver, the conventional SIC detector and the conventional PIC detector. Additionally, it is worth noting that some extra performance gains are attained for the GL-PIC approach as more n_q unreliable users are selected and re-examined.

3.9 Conclusions

In this chapter, the GL-SIC and GL-PIC interference cancellation algorithms, which can approach the ML performance at a much lower cost than competing techniques have been presented. Following by that, a greedy multi-relay selection algorithm that outperforms existing greedy algorithms and obtains a performance close to an exhaustive search have also been proposed. A novel cross-layer design strategy that incorporates GL-SIC or GL-PIC, and a greedy multi-relay selection algorithm for the uplink of cooperative DS-CDMA systems has been also presented. This approach effectively reduces the error propagation generated at the relays, avoiding the poorest relay-destination link while requiring a low complexity. Simulation results demonstrate that the performance of the proposed cross-layer design is superior to existing techniques and can approach an interference-free scenario.

Chapter 4

Buffer-Aided Distributed Space-Time Coding Schemes and Algorithms for Cooperative DS-CDMA Systems

Contents

4.1 Introduction

The ever-increasing demand for performance and reliability in wireless communications has encouraged the development of numerous innovative techniques. Among them,

cooperative diversity is one of the key techniques that has been considered in recent years [4, 66–68] as an effective tool to improving transmission performance and system reliability. Several cooperative schemes have been proposed [12, 47, 48], and among the most effective ones are Amplify-and-Forward (AF), Decode-and-Forward (DF) [12] and various distributed space-time coding (DSTC) techniques [14–18]. For an AF protocol, relays cooperate and amplify the received signals with a given transmit power. With the DF protocol, relays decode the received signals and then forward the re-encoded message to the destination. DSTC schemes exploit spatial and temporal transmit diversity by using a set of distributed antennas. With DSTC, multiple redundant copies of data are sent to the receiver to improve the quality and reliability of data transmission. Applying DSTC at the relays provides multiple processed signal copies to compensate for the fading and noise, helping to achieve the attainable diversity and coding gains so that the interference can be more effectively mitigated. As a result, better performance can be achieved when appropriate signal processing and relay selection strategies are applied.

In cooperative relaying systems, different strategies that employ multiple relays have been recently introduced in [52, 53, 56, 69–71]. The aim of relay selection is to find the optimum relay so that the signal can be transmitted and received with increased reliability. Recently, a new cooperative scheme with relays equipped with buffers has been introduced and analyzed in [72–75]. The main purpose is to select the best link according to a given criterion. In [72], a brief introduction of the buffer-aided relaying protocols for different networks is described and some practical challenges are discussed. A further study of the throughput and diversity gain of the buffer-aided system has been subsequently introduced in [73]. In [74], a new selection technique that is able to achieve the full diversity gain by selecting the strongest available link in every time slot is detailed. In [75], a max-max relay selection (MMRS) scheme for half-duplex relays with buffers is proposed. In particular, relays with the optimum source-relay links and relay-destination links are chosen and controlled for transmission and reception, respectively.

In this chapter, we propose buffer-aided DSTC schemes and algorithms for cooperative direct-sequence code-division multiple access (DS-CDMA) systems. In the proposed buffer-aided DSTC schemes, a relay pair selection algorithm automatically

selects the optimum set of relays according to the signal-to-interference-plus noise ratio (SINR) criterion. Specifically, the proposed algorithms can be divided into two parts. Initially, a link combination associated with the optimum relay group is selected, which determines if the buffer is ready for transmission or reception. For the second part, DSTC is performed from the selected relay combination to the destination when the buffers are switched to the transmission mode. The direct transmission is conducted between the source and the relay combination when the buffers are in the reception mode. With dynamic buffers equipped at each of the relays, the proposed schemes take advantage of the high storage capacity where multiple blocks of data can be stored so that the most appropriate ones can be selected at a suitable time instant. The key advantage of introducing the dynamic buffers in the system is their ability to store multiple blocks of data according to a chosen criterion so that the most appropriate ones can be selected at a suitable time instant with the highest efficiency.

The contributions of this chapter are summarized as follows:

- A buffer-aided DSTC scheme that is able to store enough data packets in the corresponding buffer entries according to different criteria so that more appropriate symbols can be selected in a suitable time instant is proposed.
- A relay selection algorithm that chooses a relay pair rather than a single relay as the DSTC transmission needs the cooperation of a pair of antennas is developed. The proposed algorithm automatically selects the target relay pair in order to forward the data.
- A greedy relay pair selection technique is then introduced to reduce the high cost brought by the exhaustive search that is required when a large number of relays are involved in the transmission.
- A dynamic approach that allows the buffer size to be adjustable according to different situations is then introduced.
- An analysis of the computational complexity, the average delay and the greedy algorithm are also presented.

4.2 DSTC Cooperative DS-CDMA System Model

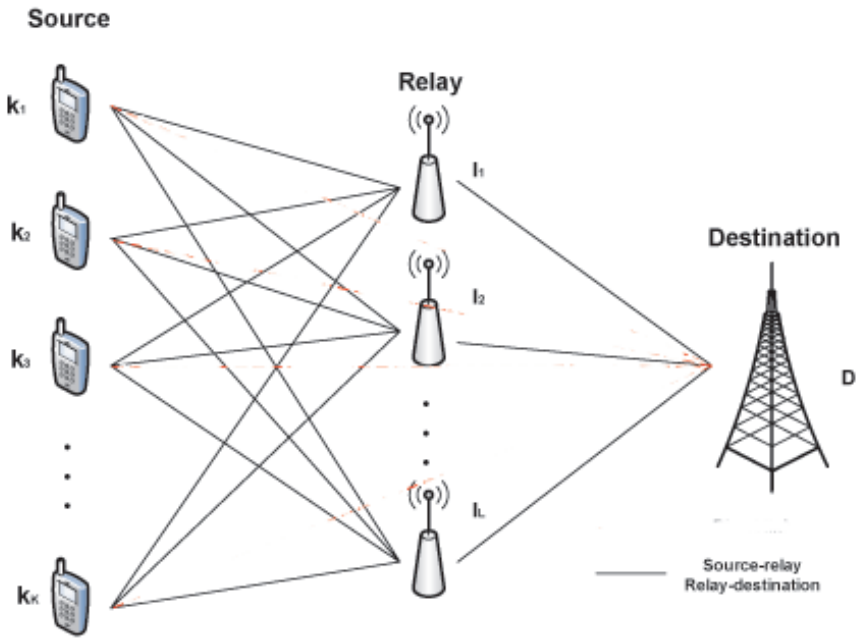

Figure 4.1: Uplink of a cooperative DS-CDMA system.

Consider the uplink of a DS-CDMA system with K users, L relays equipped with finite-size buffers capable of storing J packets and N chips per symbol that experience channels with flat fading. The system is equipped with a cooperative protocol at each relay and we assume that the transmit data are organized in packets comprising M symbols. The received signals are filtered by a filter matched to the chip pulse and sampled at chip rate to obtain sufficient statistics. As shown in Fig.4.1, the whole transmission is divided into two phases. In the first phase of our design, we randomly combine any two of the relays into a group, consequently, the sources transmit the data to the corresponding target relay pair over two consecutive time instants. The detected data for user k over two time slots, $\hat{b}_{r_m d,k}(2i-1)$ and $\hat{b}_{r_n d,k}(2i)$, are stored at relay m and relay n, respectively. After that, a DSTC scheme is employed at the following phase, where the corresponding 2×2 Alamouti [19, 26, 76] detected symbol matrix over relay m and relay n for user k among two consecutive time instants is given by

$$\mathbf{B}_k = \begin{bmatrix} \hat{b}_{r_m d,k}(2i-1) & -\hat{b}^*_{r_n d,k}(2i) \\ \hat{b}_{r_n d,k}(2i) & \hat{b}^*_{r_m d,k}(2i-1) \end{bmatrix}. \tag{4.1}$$

Consequently, the received signal for user k from relays m and n to the destination over

two consecutive time slots yields the $2N \times 1$ received vectors described by

$$\mathbf{y}_{r_{m,n}d,k}(2i-1) = \mathbf{h}^k_{r_m d}\hat{b}_{r_m d,k}(2i-1) + \mathbf{h}^k_{r_n d}\hat{b}_{r_n d,k}(2i) + \mathbf{n}(2i-1), \tag{4.2}$$

$$\mathbf{y}_{r_{m,n}d,k}(2i) = \mathbf{h}^k_{r_n d}\hat{b}^*_{r_m d,k}(2i-1) - \mathbf{h}^k_{r_m d}\hat{b}^*_{r_n d,k}(2i) + \mathbf{n}(2i), \tag{4.3}$$

where $\mathbf{h}^k_{r_l d} = a^k_{r_l d}\mathbf{s}_k h_{r_l d,k}$ denotes an $N \times 1$ effective signature vector for user k from the l-th relay to the destination with $m, n \in [1, 2, ..., L]$. The quantity $a^k_{r_l d}$ represents the k-th user's amplitude from the l-th relay to the destination, $\mathbf{s}_k = [s_k(1), s_k(2), ...s_k(N)]^T$ is the $N \times 1$ signature sequence for user k and $h_{r_l d,k}$ are the complex channel fading coefficients for user k from the l-th relay to the destination. The $N \times 1$ noise vectors $\mathbf{n}(2i-1)$ and $\mathbf{n}(2i)$ contain samples of zero mean complex Gaussian noise with variance $\sigma^2\mathbf{I}$, $\hat{b}_{r_m d,k}(2i-1)$ and $\hat{b}_{r_n d,k}(2i)$ are the decoded symbols at the output of relay m and relay n after using a cooperative protocol at time instants $(2i-1)$ and $(2i)$, respectively. Equivalently, (4.2) and (4.3) can be rewritten as

$$\mathbf{y}_{r_{m,n}d,k} = \mathbf{H}^k_{r_{m,n}d}\mathbf{b}_{r_{m,n}d,k} + \mathbf{n}_{r_{m,n}d}, \tag{4.4}$$

where $\mathbf{y}_{r_{m,n}d,k} = \left[\mathbf{y}^T_{r_{m,n}d,k}(2i-1), (\mathbf{y}^*_{r_{m,n}d,k}(2i))^T\right]^T$ represents the received signal from relay m and n over two time instants. The 2 N x 2 Alamouti matrix with the effective signatures for user k is given by

$$\mathbf{H}^k_{r_{m,n}d} = \begin{bmatrix} \mathbf{h}^k_{r_m d} & \mathbf{h}^k_{r_n d} \\ (\mathbf{h}^k_{r_n d})^* & -(\mathbf{h}^k_{r_m d})^* \end{bmatrix}, \tag{4.5}$$

where the 2×1 vector $\mathbf{b}_{r_{m,n}d,k} = \left[\hat{b}_{r_m d,k}(2i-1), \hat{b}_{r_n d,k}(2i)\right]^T$ is the processed vector when the DF protocol is employed at relays m and n at the corresponding time instant, and $\mathbf{n}_{r_{m,n}d} = \left[\mathbf{n}(2i-1)^T, (\mathbf{n}^*(2i))^T\right]^T$ is the noise vector that contains samples of zero mean complex Gaussian noise with variance $\sigma^2\mathbf{I}$.

At the destination side, various MUD decoding schemes can be employed. For the linear MUD detections, the detected symbols can be obtained as given by

$$\hat{\mathbf{b}}_{r_{m,n}d,k} = Q\big((\mathbf{w}^k_{r_{m,n}d})^H \mathbf{y}_{r_{m,n}d}\big) \tag{4.6}$$

where $\mathbf{w}^k_{r_{m,n}d}$ is the receive filter applied at the destination.

Similarly, the maximum likelihood (ML) detection method can also be applied at the destination after the following computation is obtained when Alamouti scheme is used

$$\begin{aligned}\tilde{b}_{r_m d,k}(2i-1) &= (\mathbf{h}^k_{r_m d})^H \mathbf{y}_{r_{m,n}d,k}(2i-1) + (\mathbf{h}^k_{r_n d})^T \mathbf{y}^*_{r_{m,n}d,k}(2i) \\ &= \Big((\mathbf{h}^k_{r_m d})^H \mathbf{h}^k_{r_m d} + (\mathbf{h}^k_{r_n d})^T (\mathbf{h}^k_{r_n d})^*\Big)\hat{b}_{r_m d,k}(2i-1) + \Big((\mathbf{h}^k_{r_m d})^H \mathbf{n}(2i-1) + (\mathbf{h}^k_{r_n d})^T \mathbf{n}^*(2i)\Big)\end{aligned}$$

$$\begin{aligned}\tilde{b}_{r_n d,k}(2i) &= (\mathbf{h}^k_{r_n d})^H \mathbf{y}_{r_{m,n}d,k}(2i-1) - (\mathbf{h}^k_{r_m d})^T \mathbf{y}^*_{r_{m,n}d,k}(2i) \\ &= \Big((\mathbf{h}^k_{r_n d})^H \mathbf{h}^k_{r_n d} + (\mathbf{h}^k_{r_m d})^T (\mathbf{h}^k_{r_m d})^*\Big)\hat{b}_{r_n d,k}(2i) + \Big((\mathbf{h}^k_{r_n d})^H \mathbf{n}(2i-1) - (\mathbf{h}^k_{r_m d})^T \mathbf{n}^*(2i)\Big)\end{aligned} \tag{4.7}$$

Consequently, after testing all possible symbols for ML decision, the most likely detection results are selected. This scheme groups the relays into different pairs and a more reliable transmission can be achieved if proper relay pair selection is performed.

4.3 Proposed Buffer-aided Cooperative DSTC Scheme

In this section, we present a buffer-aided cooperative DSTC scheme, where each relay is equipped with a buffer so that the processed data can be stored and the buffer can wait until the channel pair associated with the best performance is selected. Consequently, processed data are stored at the corresponding buffer entries and then re-encoded when the appropriate time interval comes. Specifically, the buffer with size J can store up to J packets of data and can either forward or wait for the best time instant to send data. This method effectively improves the quality of the transmission, guarantees that the most suitable signal is selected from the buffer entries and sent to the destination with a higher reliability.

The algorithm begins with a SINR calculation for all possible channel combinations. In the case of the Alamouti code, every two relays are combined into a group and all possible lists of corresponding channel pairs are considered. Thus, the corresponding SINR for an arbitrary relay pair is then calculated and recorded as follows:

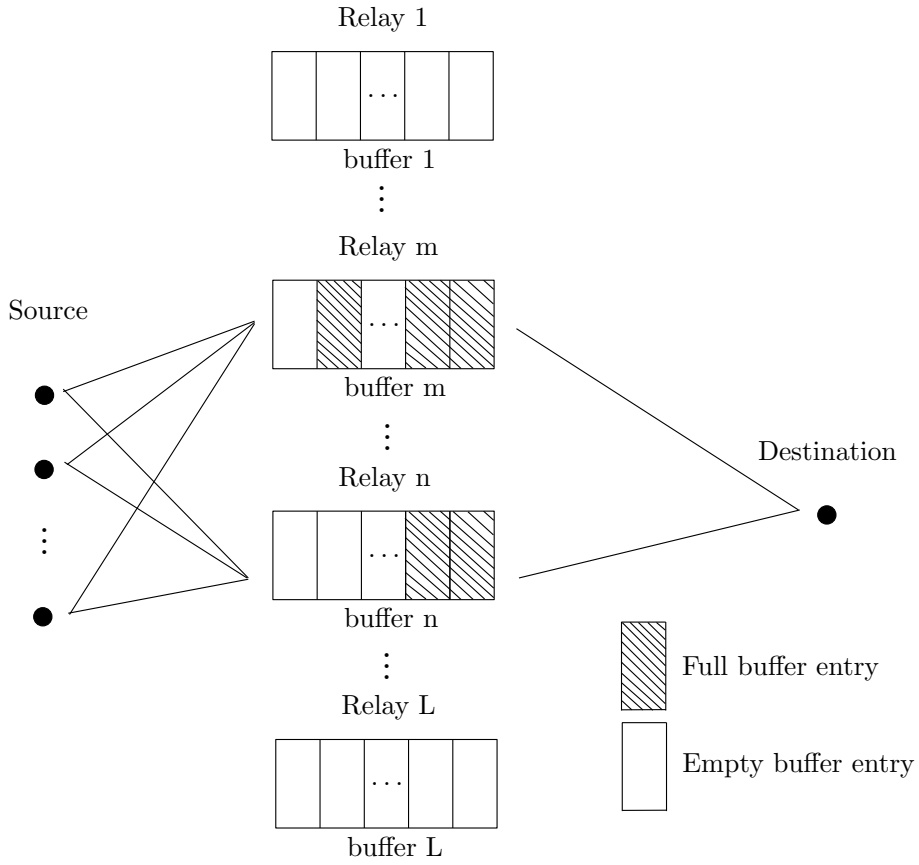

Figure 4.2: Proposed buffer-aided cooperative scheme.

$$\mathrm{SINR}_{sr_{m,n}} = \sum_{k=1}^{K} \frac{\mathbf{w}_{s_k r_m}^H \mathbf{h}_{s_k r_m} \mathbf{h}_{s_k r_m}^H \mathbf{w}_{s_k r_m} + \mathbf{w}_{s_k r_n}^H \mathbf{h}_{s_k r_n} \mathbf{h}_{s_k r_n}^H \mathbf{w}_{s_k r_n}}{\sum\limits_{\substack{j=1 \\ j \neq k}}^{K} \mathbf{w}_{s_k r_m}^H \mathbf{h}_{s_j r_m} \mathbf{h}_{s_j r_m}^H \mathbf{w}_{s_k r_m} + \sum\limits_{\substack{j=1 \\ j \neq k}}^{K} \mathbf{w}_{s_k r_n}^H \mathbf{h}_{s_j r_n} \mathbf{h}_{s_j r_n}^H \mathbf{w}_{s_k r_n} + \sigma^2 \mathbf{w}_{s_k r_m}^H \mathbf{w}_{s_k r_m} + \sigma^2 \mathbf{w}_{s_k r_n}^H \mathbf{w}_{s_k r_n}}, \tag{4.8}$$

$$\mathrm{SINR}_{r_{m,n}d} = \sum_{k=1}^{K} \frac{(\mathbf{w}_{r_m d}^k)^H \mathbf{h}_{r_m d}^k (\mathbf{h}_{r_m d}^k)^H \mathbf{w}_{r_m d}^k + (\mathbf{w}_{r_n d}^k)^H \mathbf{h}_{r_n d}^k (\mathbf{h}_{r_n d}^k)^H \mathbf{w}_{r_n d}^k}{\sum\limits_{\substack{j=1 \\ j \neq k}}^{K} (\mathbf{w}_{r_m d}^k)^H \mathbf{h}_{r_m d}^j (\mathbf{h}_{r_m d}^j)^H \mathbf{w}_{r_m d}^k + \sum\limits_{\substack{j=1 \\ j \neq k}}^{K} (\mathbf{w}_{r_n d}^k)^H \mathbf{h}_{r_n d}^j (\mathbf{h}_{r_n d}^j)^H \mathbf{w}_{r_n d}^k + \sigma^2 (\mathbf{w}_{r_m d}^k)^H \mathbf{w}_{r_m d}^k + \sigma^2 (\mathbf{w}_{r_n d}^k)^H \mathbf{w}_{r_n d}^k}. \tag{4.9}$$

In (4.8), $\mathrm{SINR}_{sr_{m,n}}$ denotes the SINR for the combined paths from all users to relay m and relay n, $\mathbf{w}_{s_k r_l}$ is the detector used at the relays. When the matched filter (MF) is adopted at the corresponding relay, $\mathbf{w}_{s_k r_l}$ is expressed as

$$\mathbf{w}_{s_k r_l} = \mathbf{h}_{s_k r_l}, \tag{4.10}$$

similarly, if the linear minimum mean-square error (MMSE) receiver [77] is employed at the relays, $\mathbf{w}_{s_k r_l}$ is equal to

$$\mathbf{w}_{s_k r_l} = \left(\sum_{k=1}^{K} \mathbf{h}_{s_k r_l} \mathbf{h}_{s_k r_l}^H + \sigma^2 \mathbf{I} \right)^{-1} \mathbf{h}_{s_k r_l}, \tag{4.11}$$

$\mathbf{h}_{s_k r_l} = a_{s_k r_l}\mathbf{s}_k h_{s_k r_l}$ is the effective signature vector from user k to the relay l. Similarly, in (4.9), $\mathrm{SINR}_{r_{m,n}d}$ represents the SINR for the combined paths from relay m and relay n to the destination. The receive filter $\mathbf{w}_{r_l d}^k$ is employed by the detector used at the destination. When the MF is adopted at the destination, $\mathbf{w}_{r_l d}^k$ is expressed as

$$\mathbf{w}_{r_l d}^k = \mathbf{h}_{r_l d}^k. \tag{4.12}$$

Similarly, if the linear MMSE receiver is employed at the relays, $\mathbf{w}_{r_l d}^k$ is equal to

$$\mathbf{w}_{r_l d}^k = \left(\sum_{k=1}^{K} \mathbf{h}_{r_l d}^k (\mathbf{h}_{r_l d}^k)^H + \sigma^2 \mathbf{I} \right)^{-1} \mathbf{h}_{r_l d}^k. \tag{4.13}$$

The above equations correspond to a cooperative system under the assumption that signals from all users are transmitted to the selected relays m and n. Both MF and MMSE receivers are considered here for the purpose of simplicity, it should be mentioned that other detectors [78] can also be used. We then sort all these SINR values in a decreasing order and select the one with the highest SINR as given by

$$\mathrm{SINR_{p,q}} = \arg \max_{m,n \in [1,2,\ldots,L]} \{\mathrm{SINR_{sr_{m,n}}}, \mathrm{SINR_{r_{m,n}d}}\}, \tag{4.14}$$

where $\mathrm{SINR_{p,q}}$ denotes the highest SINR associated with the relay p and relay q. After the highest SINR corresponding to the combined paths is selected, two different situations need to be considered as follows.

Source-relay link:

If the highest SINR belongs to the source-relay link, then the signal sent to the target relays p and q over two time instants is given by

$$\mathbf{y}_{sr_l}(2i-1) = \sum_{k=1}^{K} \mathbf{h}_{s_k r_l} b_k(2i-1) + \mathbf{n}(2i-1), l \in [p,q], \tag{4.15}$$

$$\mathbf{y}_{sr_l}(2i) = \sum_{k=1}^{K} \mathbf{h}_{s_k r_l} b_k(2i) + \mathbf{n}(2i), l \in [p,q]. \tag{4.16}$$

The received signal is then processed by the detectors as the DF protocol is adopted. Therefore, the decoded symbols that are stored and sent to the destination from the l-th relay are obtained as

$$\hat{b}_{r_l d,k}(2i-1) = Q(\mathbf{w}_{s_k r_l}^H \mathbf{y}_{sr_l}(2i-1)), \tag{4.17}$$

and

$$\hat{b}_{r_l d,k}(2i) = Q(\mathbf{w}_{s_k r_l}^H \mathbf{y}_{sr_l}(2i)), \tag{4.18}$$

where $Q(\cdot)$ denotes the slicer. After that, the buffers are switched to the reception mode, the decoded symbol is consequently stored in the corresponding buffer entries. Clearly, these operations are performed when the corresponding buffer entries are not full, otherwise, the second highest SINR is chosen as given by

$$\mathrm{SINR}_{\mathrm{p,q}}^{\mathrm{pre}} = \mathrm{SINR}_{\mathrm{p,q}} \tag{4.19}$$

$$\mathrm{SINR}_{\mathrm{u,v}} \in \max\{\mathrm{SINR}_{\mathrm{sr_{m,n}}}, \mathrm{SINR}_{\mathrm{r_{m,n}d}}\} \setminus \mathrm{SINR}_{\mathrm{p,q}}^{\mathrm{pre}}, \tag{4.20}$$

where $\mathrm{SINR}_{\mathrm{u,v}}$ denotes the second highest SINR associated with the updated relay pair $\Omega_{u,v}$. $\{\mathrm{SINR}_{\mathrm{sr_{m,n}}}, \mathrm{SINR}_{\mathrm{r_{m,n}d}}\} \setminus \mathrm{SINR}_{\mathrm{p,q}}^{\mathrm{pre}}$ denotes a complementary set where we drop the $\mathrm{SINR}_{\mathrm{p,q}}^{\mathrm{pre}}$ from the link SINR set $\{\mathrm{SINR}_{\mathrm{sr_{m,n}}}, \mathrm{SINR}_{\mathrm{r_{m,n}d}}\}$. Consequently, the above process repeats in the following time instants.

Relay-destination link:

If the highest SINR is selected from the relay-destination link, in the following two consecutive time instants, the buffers are switched to transmission mode and the decoded symbol for user k is re-encoded with the Alamouti matrix as in (4.1) so that DSTC is performed from the selected relays p and q to the destination as given by

$$\mathbf{y}_{r_{p,q}d,k}(2i-1) = \mathbf{h}_{r_p d}^k \hat{b}_{r_p d,k}(2i-1) + \mathbf{h}_{r_q d}^k \hat{b}_{r_q d,k}(2i) + \mathbf{n}(2i-1), \tag{4.21}$$

$$\mathbf{y}_{r_{p,q}d,k}(2i) = \mathbf{h}_{r_q d}^k \hat{b}_{r_p d,k}^*(2i-1) - \mathbf{h}_{r_p d}^k \hat{b}_{r_q d,k}^*(2i) + \mathbf{n}(2i). \tag{4.22}$$

The received signal is then processed by the detectors at the destination. Clearly, the above operation is conducted under the condition that the corresponding buffer entries are not empty, otherwise, the second highest SINR is chosen according to (4.19) and (4.20) and the above process is repeated.

It is worth noting that for the purpose of simplicity, the above technique employed fixed-size buffers at the relays so that the transmission delay can be controlled with accurate estimation. The key advantage of the proposed scheme is its ability to select the most appropriate symbols (experience the good channels) before they are forwarded to the next phase. In practice, the performance highly depends on the buffer size J, the number of users K and the accuracy of the detection at the relays.

The proposed buffer-aided cooperative DSTC scheme is detailed in Algorithm 6.

Algorithm 6 The proposed buffer-aided cooperative DSTC scheme

% List all possible relay pairs

% Select the combination with the highest SINR

$\mathrm{SINR_{p,q}} = \max\{\mathrm{SINR_{sr_{m,n}}}, \mathrm{SINR_{r_{m,n}d}}\}$

%Source-relay link

if $\mathrm{SINR_{p,q}} \in [\mathrm{SINR_{sr_{m,n}}}], m, n \in [1, L]$

if the buffers entries are not full %not all entries are occupied

$$\mathbf{y}_{sr_l}(2i-1) = \sum_{k=1}^{K} \mathbf{h}_{s_k r_l} b_k(2i-1) + \mathbf{n}_{sr_l}(2i-1), l \in [p, q],$$

$$\mathbf{y}_{sr_l}(2i) = \sum_{k=1}^{K} \mathbf{h}_{s_k r_l} b_k(2i) + \mathbf{n}_{sr_l}(2i), l \in [p, q].$$

%Apply the detectors at relay n and relay q to obtain

$\hat{b}_{r_l d,k}(2i-1)$ and $\hat{b}_{r_l d,k}(2i)$ and store them

in the corresponding buffer entries ($l \in [p, q]$)

break

else %choose the second highest SINR

$\mathrm{SINR^{pre}_{p,q}} = \mathrm{SINR_{p,q}}$

$\mathrm{SINR_{p,q}} \in \max\{\mathrm{SINR_{sr_{m,n}}}, \mathrm{SINR_{r_{m,n}d}}\} \setminus \mathrm{SINR^{pre}_{p,q}}$

end

else %Relay-destination link

$\mathrm{SINR_{p,q}} \in [\mathrm{SINR_{r_{m,n}d}}], m, n \in [1, L]$

if the buffers entries are not empty %There is at least one entry

$$\mathbf{y}_{r_{p,q}d,k}(2i-1) = \mathbf{h}^k_{r_p d} \hat{b}_{r_p d,k}(2i-1) + \mathbf{h}^k_{r_q d} \hat{b}_{r_q d,k}(2i) + \mathbf{n}(2i-1),$$

$$\mathbf{y}_{r_{p,q}d,k}(2i) = \mathbf{h}^k_{r_q d} \hat{b}^*_{r_p d,k}(2i-1) - \mathbf{h}^k_{r_p d} \hat{b}^*_{r_q d,k}(2i) + \mathbf{n}(2i).$$

%Apply the detectors/ML at the destination for detection

break

else%choose the second highest SINR

$\mathrm{SINR^{pre}_{p,q}} = \mathrm{SINR_{p,q}}$

$\mathrm{SINR_{p,q}} \in \max\{\mathrm{SINR_{sr_{m,n}}}, \mathrm{SINR_{r_{m,n}d}}\} \setminus \mathrm{SINR^{pre}_{p,q}}$

end

end

%Re-calculated the SINR for different link combinations and

repeat the above process

4.4 Greedy Relay Pair Selection Technique

In this section, a greedy relay pair selection algorithm is introduced. For this relay selection problem, the exhaustive search of all possible relay pairs is the optimum way to obtain the best performance. However, the major problem that prevents us from applying this method when a large number of relays involved in the transmission is its considerable computational complexity. When L relays ($L/2$ relay pairs if L is an even number) participate in the transmission, a cost of $L(L-1)$ link combinations is required as both source-relay links and relay-destination links need to be considered. Consequently, this fact motivates us to seek alternative approaches that can achieve a good balance between performance and complexity.

We propose a greedy relay pair selection algorithm that can approach the global optimum with a reduced computational complexity. The algorithm starts with a single relay selection where we examine the SINR for each of the relays with its associated links as given by

$$\mathrm{SINR}_{sr_p} = \sum_{k=1}^{K} \frac{\mathbf{w}_{s_k r_p}^H \mathbf{h}_{s_k r_p} (\mathbf{h}_{s_k r_p})^H \mathbf{w}_{s_k r_p}}{\sum\limits_{\substack{j=1 \\ j \neq k}}^{K} \mathbf{w}_{s_k r_p}^H \mathbf{h}_{s_j r_p} (\mathbf{h}_{s_j r_p})^H \mathbf{w}_{s_k r_p} + \sigma^2 \mathbf{w}_{s_k r_p}^H \mathbf{w}_{s_k r_p}}, \tag{4.23}$$

$$\mathrm{SINR}_{r_p d} = \sum_{k=1}^{K} \frac{(\mathbf{w}_{r_p d}^k)^H \mathbf{h}_{r_p d}^k (\mathbf{h}_{r_p d}^k)^H \mathbf{w}_{r_p d}^k}{\sum\limits_{\substack{j=1 \\ j \neq k}}^{K} (\mathbf{w}_{r_p d}^k)^H \mathbf{h}_{r_p d}^j (\mathbf{h}_{r_p d}^j)^H \mathbf{w}_{r_p d}^k + \sigma^2 (\mathbf{w}_{r_p d}^k)^H \mathbf{w}_{r_p d}^k}, \tag{4.24}$$

where SINR_{sr_p} and $\mathrm{SINR}_{r_p d}$ denote the SINR from the source to an arbitrary relay p and from relay p to the destination, respectively. We then select the link combination with the highest SINR and its associated relay q is recorded as the base relay and given by

$$\mathrm{SINR}_{\mathrm{q}}^{\mathrm{base}} = \arg \max_{p \in [1,2,\ldots,L]} \{\mathrm{SINR}_{\mathrm{sr_p}}, \mathrm{SINR}_{\mathrm{r_p d}}\}. \tag{4.25}$$

Consequently, all possible relay pairs involved with base relay q are listed as $\Omega_{p,q}$, where $p \in [1, L], p \neq q$. The SINR for these $(L-1)$ relay pairs are then calculated as in (4.8) and (4.9). After that, the optimum relay pair $\Omega_{n,q}$ is chosen according to (4.14) and the algorithm begins if the corresponding buffers are available for either transmission or reception.

Transmission mode:

When the buffers are switched to the transmission mode, a buffer space check is conducted firstly to ensure the corresponding buffers are not empty. We then have,

$$\Omega_n^{\text{buffer}} \neq \varnothing,\ n \in [1, 2, ..., L], \tag{4.26}$$

and

$$\Omega_q^{\text{buffer}} \neq \varnothing,\ q \in [1, 2, ..., L], \tag{4.27}$$

where Ω_n^{buffer} and Ω_q^{buffer} represents the buffer n and the buffer q associated with the relay pair $\Omega_{n,q}$. In this situation, the DSTC scheme is performed afterwards as in (4.21) and (4.22) through the selected relay pair. Conversely, empty buffer entries indicate that the selected relay pair is not capable of forwarding the data to the destination. In this case, we drop this relay pair, select another relay pair among the remaining $(L-2)$ candidate pairs with the highest SINR as given by

$$\text{SINR}_{\text{m,q}} = \arg \max_{\substack{p \neq n,q \\ p \in [1,2,...,L]}} \{\text{SINR}_{\text{p,q}}\}, \tag{4.28}$$

The algorithm then repeats with the new selected relay pair $\Omega_{m,q}$. Otherwise, if all possible relay pairs $\Omega_{p,q}$ ($p \neq n, q, p \in [1, L]$) are not available, we then reset the base relay associated with the second highest SINR as described by

$$\text{SINR}_{\text{q}}^{\text{pre}} = \text{SINR}_{\text{q}}^{\text{base}}, \tag{4.29}$$

$$\text{SINR}_{\text{q}}^{\text{base}} = \max\{\text{SINR}_{\text{sr}_\text{p}}, \text{SINR}_{\text{r}_\text{p}\text{d}}\} \setminus \text{SINR}_{\text{q}}^{\text{pre}}, \tag{4.30}$$

where $\{\text{SINR}_{\text{sr}_\text{p}}, \text{SINR}_{\text{r}_\text{p}\text{d}}\} \setminus \text{SINR}_{\text{q}}^{\text{pre}}$ denotes a complementary set where we drop the $\text{SINR}_{\text{q}}^{\text{pre}}$ from the link SINR set $\{\text{SINR}_{\text{sr}_\text{p}}, \text{SINR}_{\text{r}_\text{p}\text{d}}\}$. After this selection process, a new relay pair is chosen and the transmission procedure repeats as above according to the buffer status.

Reception mode:

When the buffers are switched to reception mode, similarly, a buffer space check is performed initially to ensure there is enough space for storing the processed data, namely,

$$\Omega_n^{\text{buffer}} \neq \text{U},\ n \in [1, 2, ..., L], \tag{4.31}$$

Algorithm 7 The proposed greedy relay pair selection algorithm for buffer-aided DSTC

%Choose a single relay with the highest SINR that

corresponds to a specific base relay q

$\mathrm{SINR}_{\mathrm{q}}^{\mathrm{base}} = \max\{\mathrm{SINR}_{\mathrm{sr_p}}, \mathrm{SINR}_{\mathrm{r_p d}}\}, p \in [1, L]$

For $\mathrm{p} = 1 : \mathrm{L}$ % all relay pairs associated with relay q

if $\mathrm{p} \neq \mathrm{q}$

$\Omega_{\mathrm{relaypair}} = [\mathrm{p}, \mathrm{q}]$

% when the links belong to the source-relay phase

$$\mathrm{SINR}_{sr_{p,q}} = \sum_{k=1}^{K} \frac{\mathbf{w}_{s_k r_p}^H \mathbf{h}_{s_k r_p} \mathbf{h}_{s_k r_p}^H \mathbf{w}_{s_k r_p} + \mathbf{w}_{s_k r_q}^H \mathbf{h}_{s_k r_q} \mathbf{h}_{s_k r_q}^H \mathbf{w}_{s_k r_q}}{\sum\limits_{\substack{j=1 \\ j \neq k}}^{K} \mathbf{w}_{s_k r_p}^H \mathbf{h}_{s_j r_p} \mathbf{h}_{s_j r_p}^H \mathbf{w}_{s_k r_p} + \sum\limits_{\substack{j=1 \\ j \neq k}}^{K} \mathbf{w}_{s_k r_q}^H \mathbf{h}_{s_j r_q} \mathbf{h}_{s_j r_q}^H \mathbf{w}_{s_k r_q} + \sigma^2 \mathbf{w}_{s_k r_p}^H \mathbf{w}_{s_k r_p} + \sigma^2 \mathbf{w}_{s_k r_q}^H \mathbf{w}_{s_k r_q}}$$

% when the links belong to the relay-destination phase

$$\mathrm{SINR}_{r_{p,q}d} = \sum_{k=1}^{K} \frac{(\mathbf{w}_{r_p d}^k)^H \mathbf{h}_{r_p d}^k (\mathbf{h}_{r_p d}^k)^H \mathbf{w}_{r_p d}^k + (\mathbf{w}_{r_q d}^k)^H \mathbf{h}_{r_q d}^k (\mathbf{h}_{r_q d}^k)^H \mathbf{w}_{r_q d}^k}{\sum\limits_{\substack{j=1 \\ j \neq k}}^{K} (\mathbf{w}_{r_p d}^k)^H \mathbf{h}_{r_p d}^j (\mathbf{h}_{r_p d}^j)^H \mathbf{w}_{r_p d}^k + \sum\limits_{\substack{j=1 \\ j \neq k}}^{K} (\mathbf{w}_{r_q d}^k)^H \mathbf{h}_{r_q d}^j (\mathbf{h}_{r_q d}^j)^H \mathbf{w}_{r_q d}^k + \sigma^2 (\mathbf{w}_{r_p d}^k)^H \mathbf{w}_{r_p d}^k + \sigma^2 (\mathbf{w}_{r_q d}^k)^H \mathbf{w}_{r_q d}^k}$$

% record each calculated relay pair SINR

end

end

$\mathrm{SINR}_{\mathrm{n,q}} = \max\{\mathrm{SINR}_{sr_{p,q}}\ ,\ \mathrm{SINR}_{r_{p,q}d}\}$

if%Reception mode

if the buffers entries are not full

$$\mathbf{y}_{sr_{n,q}}(2i-1) = \sum_{k=1}^{K} \mathbf{h}_{s_k r_{n,q}} b_k(2i-1) + \mathbf{n}(2i-1),$$

$$\mathbf{y}_{sr_{n,q}}(2i) = \sum_{k=1}^{K} \mathbf{h}_{s_k r_{n,q}} b_k(2i) + \mathbf{n}(2i).$$

%Apply the detectors at relay n and relay q to obtain

$\hat{b}_{r_{n,q}d,k}(2i-1)$ and $\hat{b}_{r_{n,q}d,k}(2i)$ and store them

in the corresponding buffer entries

else %choose another link with the second highest SINR

$\mathrm{SINR}_{\mathrm{q}}^{\mathrm{pre}} = \mathrm{SINR}_{\mathrm{q}}^{\mathrm{base}} \quad \mathrm{SINR}_{\mathrm{q}}^{\mathrm{base}} \in \max\{\mathrm{SINR}_{\mathrm{sr_p}}, \mathrm{SINR}_{\mathrm{r_p d}}\} \setminus \mathrm{SINR}_{\mathrm{q}}^{\mathrm{pre}}$

%Repeat the above greedy relay pair selection process

end

else%Transmission mode

if the buffers entries are not empty

$$\mathbf{y}_{r_{n,q}d,k}(2i-1) = \mathbf{h}_{r_n d}^k \hat{b}_{r_n d,k}(2i-1) + \mathbf{h}_{r_q d}^k \hat{b}_{r_q d,k}(2i) + \mathbf{n}(2i-1),$$

$$\mathbf{y}_{r_{n,q}d,k}(2i) = \mathbf{h}_{r_q d}^k \hat{b}_{r_n d,k}^*(2i-1) - \mathbf{h}_{r_n d}^k \hat{b}_{r_q d,k}^*(2i) + \mathbf{n}(2i).$$

%Apply the detectors/ML at the destination for detection

else%choose another link with the second highest SINR

$\mathrm{SINR}_{\mathrm{q}}^{\mathrm{pre}} = \mathrm{SINR}_{\mathrm{q}}^{\mathrm{base}}$; $\mathrm{SINR}_{\mathrm{q}}^{\mathrm{base}} \in \max\{\mathrm{SINR}_{\mathrm{sr_p}}, \mathrm{SINR}_{\mathrm{r_p d}}\} \setminus \mathrm{SINR}_{\mathrm{q}}^{\mathrm{pre}}$

%Repeat the above greedy relay pair selection process

end

end

%Repeat the above greedy relay pair selection process

and

$$\Omega_q^{\text{buffer}} \neq \mathrm{U},\ q \in [1, 2, ..., L], \tag{4.32}$$

where U represents a full buffer set. In this case, if the buffers are not full, then, the sources send the data to the selected relay pair $\Omega_{n,q}$ over two time instants according to (4.15) and (4.16). Otherwise, the algorithm reselects a new relay pair as in (4.28), (4.29) and (4.30).

The greedy relay pair selection algorithm is show in Algorithm 7.

4.5 Proposed Dynamic Buffer Scheme

The size J of the buffers also plays a key role in the performance of the system, which improves with the increase of the size as buffers with greater size allow more data packets to be stored. In this case, extra degrees of freedom in the system or choices for data transmission are available. Hence, in this section, we release the limitation on the size of the buffer to further explore the additional advantage brought by dynamic buffer design where the buffer size can vary according to different criteria such as the input SNR and the channel condition. When considering the input SNR, larger buffer space is required when the transmission is operated in low SNR region so that the most proper data can be selected among a greater number of candidates. On the other hand, in the high SNR region, a small buffer size is employed as most of the processed symbols are appropriate when compared with the situation in the low SNR region. In this work, we assume that the buffer size J is inversely proportional to the input SNR, namely, with the increase of the SNR, the buffer size decreases automatically.

The algorithm for calculating the buffer size J is detailed in Algorithm 8.

The buffer size can be determined by the current selected channel pair condition. In particular, we set a threshold γ that denotes the channel power, if the current selected channel power is under γ, the buffer size increases as more candidates need to be saved in order to select the best symbol, on the contrary, if the current selected channel pair power

Algorithm 8 The algorithm to calculate the buffer size J based on the input SNR

If $\mathrm{SNR}_{\mathrm{cur}} = \mathrm{SNR}_{\mathrm{pre}} + d_1$

then $J_{\mathrm{cur}} = J_{\mathrm{pre}} - d_2$,

where $\mathrm{SNR}_{\mathrm{cur}}$ and $\mathrm{SNR}_{\mathrm{pre}}$ represent the input SNR after and before increasing its value,

J_{cur} and J_{pre} denote the corresponding buffer size before and after decreasing its value,

d_1 and d_2 are the step sizes for the SNR and the buffer size, respectively.

exceeds γ, we decrease the buffer size as there is a high possibility that the transmission is not significantly affected.

The approach based on the channel power for varying the buffer can be summarized in Algorithm 9.

Algorithm 9 The algorithm for calculate buffer size J based on the channel power

If $\min \|h_{s_k r_l}\|^2 \leq \gamma$ **or** $\min \|h_{r_l d}\|^2 \leq \gamma,\ \ l \in [1, L]$

$J_{\mathrm{cur}} = J_{\mathrm{pre}} + d_3$

else

$J_{\mathrm{cur}} = J_{\mathrm{pre}} - d_3$

end

where d_3 represents the step size when adjusting the buffer size.

4.6 Analysis of the Proposed Algorithms

In this section, we analyse the computational complexity required by the proposed relay pair selection algorithm, the problem of the average delay brought by the proposed schemes and algorithms, followed by the discussion of the proposed greedy algorithm.

4.6.1 Computational Complexity

The proposed greedy relay pair selection method considers the combination effect of the channel condition so that the DSTC algorithm can be applied with a collection of relays. When compared with the exhaustive search that lists all possible subsets of relay pairs, less than $L(L-1)$ types of link combinations (associated with the corresponding $L(L-1)/2$ relay pairs) are examined as the proposed method explores both the source-relay links and relay-destination links. Specially, for the greedy relay selection strategy, the proposed scheme explores a moderate to large number of relay pairs at each stage, however, the algorithm stops when the corresponding buffer entries satisfy the current system requirement (transmission mode or reception mode), in this case, the maximum number of relay pair that we have to examine is $(L-1)+(L-2)+...+1 = L(L-1)/2$. On the other hand, when consider the exhaustive search, the total number of relay pairs that must be verified is $C_L^2 = L(L-1)/2$. It should be mentioned that when calculating the associated SINR, we have to double the number of calculation flops as we have to consider and compare both the SINR for source-relay links and relay-destination links. The detailed computational complexity is listed in Table 4.1. Clearly, when compare these two algorithms, the proposed greedy relay pair selection algorithm is an order of magnitude less costly when large number of relays employed in the system.

4.6.2 Average Delay Analysis

The improvement of the performance brought by the buffer-aided relays comes at the expense of the transmission delay. Hence, it is of great importance to investigate the

Table 4.1: Computational complexity required by the relay pair selection algorithms

Processing	Algorithm	Multiplications	Additions
Relay pair selection	Exhaustive Search	$48K^2NL^2 - 12KNL^2$ $-48K^2NL + 12KNL$ $-48K^2NL + 12KNL$	$40K^2NL^2 - 12KNL^2 - 16K^2L^2$ $+4KL^2 - 40K^2NL + 12KNL$ $+16K^2L - 4KL$
Relay pair selection	Greedy Search	$96K^2NL - 24KNL$ $-96K^2N + 24KN$ $-96K^2N + 24KN$	$80K^2NL - 24KNL - 32K^2L$ $+8KL - 80K^2N + 24KN$ $+32K^2 - 8K$

performance-delay trade-off of the proposed buffer-aided DSTC schemes [79]. In this subsection, we analyze the average delay of the proposed schemes and algorithms.

We assume that the source always has data to transmit and the delay is mostly caused by the buffers that are equipped at the relays. Let $T(i)$ and $Q(i)$ denote the delay of packets of M symbols transmitted by the source and the queue length in time instant i, respectively.

According to Little's law [80], the average delay $T = E[T(i)]$, which is also the average time that packets are stored in the corresponding buffer is given by

$$T = \frac{Q}{R_a} \quad \text{time slots}, \tag{4.33}$$

where $Q = E[Q(i)]$ represents the average queue length at the relay buffer, R_a (in packets/slot) is the average arrival rate into the queue.

In this analysis, we assume both the source and relay transmit at a constant instantaneous rate R ($e.g. R = 1 \ \text{packets/slot} = M \ \text{symbols/slot}$) when they are selected for transmission and the transmission is operated with one packets of M symbols per each time slot. We also for simplicity define the error probability for the source-relay link and relay-destination link as P_{sr} and P_{rd} ($P = P_{sr} = P_{rd}$), respectively. For a buffer with size J (up to J packets can be stored in the buffer), the average queue length is described by [79]

$$Q = \sum_{j=0}^{J} j P_{G_j} = J P_{G_J}, \tag{4.34}$$

where P_{G_j} represents the buffer state probability that has been explained in [79], $P_{G_J} =$

P_{full} denotes the probability when the buffer is full. Similarly, we then define $P_{G_0} = P_{\text{empty}}$ as the probability for empty buffer. Therefore, the average arrival rate into the buffer can be calculated as

$$R_a = (1 - P_{G_J})P + P_{G_0}P, \tag{4.35}$$

Similarly, the average departure rate from the buffer is given by

$$R_d = (1 - P_{G_0})P + P_{G_J}P. \tag{4.36}$$

Consequently, the above equations can be further derived as

$$T = \frac{Q}{R_a} = \frac{P_{G_J}}{(1 - P_{G_J})P + P_{G_0}P}J \ \text{ packets/slot} \tag{4.37}$$

Clearly, the above results demonstrate that the transmission delay is linear with the buffer size.

Apart from that, the DSTC scheme will introduce further delay. For the DSTC scheme, the relay pair need to wait an extra time slot for the second packets to arrive. Then, the relay pair can transmit the packets to the destination using DSTC scheme. In other word, the DSTC scheme takes two time slots to transmit two packets, as a result, it brings extra delay [81–83]. Meanwhile, the relay pair selection processing also brings delay. For both exhaustive and greedy selection, they need to calculate the best relay pair from the candidates pool. This processing need extra computation time until the best relay pair is selected.

4.6.3 Greedy Relay Selection Analysis

The proposed greedy relay pair selection method is a stepwise forward selection algorithm, where we optimize the selection based on the SINR criterion at each stage. We begin the process with a single link selection where we examine the SINR for each of the links and choose the link with the highest SINR, the associated relay is then selected and the candidate relay pair is generated by adding the remaining relays, respectively. The optimum relay pair is subsequently selected according to the SINR criterion. Since buffers are equipped at each relay, it is possible that the corresponding relay pair entries are not available for either transmission or reception. In this case, the

candidate relay pair from the first step with the second highest SINR is then chosen. Clearly, if all remaining candidate relay pairs are not selected due to the unavailability of the associated buffers, we reset the base relay and newly generated relay pairs are grouped in the second stage by adding other relays, respectively. Obviously, the number of all possible relay pair candidates at each stage is reduced gradually as the discarded relay pair from previous stages will not appear in the current stage. Hence, the relay pairs grouped at each step are presented as follows:

$$\begin{aligned}
&\text{Stage } 1: \ \{\Omega_1^1, \Omega_2^1, ..., \Omega_{L-1}^1\},\\
&\text{Stage } 2: \ \{\Omega_1^2, \Omega_2^2, ..., \Omega_{L-2}^2\},\\
&\qquad\vdots\\
&\text{Stage s}: \ \{\Omega_1^s, \Omega_2^s, ..., \Omega_{L-s}^s\},\\
&\qquad\vdots\\
&\text{Stage } \boldsymbol{L-1}: \ \{\Omega_1^1\},
\end{aligned}$$

where Ω_i^s denotes the i-th relay pair at the s-th stage. Clearly, the maximum number of relay pairs that we have to consider for all $L-1$ stages is $(L-1)+(L-2)+...+1 = L(L-1)/2$, since this algorithm stops when selected relay pair with its associated buffers are available, the associated complexity for the proposed greedy relay selection strategy is less than $L(L-1)/2$.

Compared with the exhaustive search, which is considered as the optimum relay selection method, the number of relay pairs examined for the processing is given by

$$\text{Stage } 1: \ \{\Omega_1^1, \Omega_2^1, ..., \Omega_{\frac{L(L-1)}{2}}^1\},$$

The total number of relay combinations can then be calculated as $C_L^2 = L(L-1)/2$, where each term $C_m^n = \frac{m(m-1)...(m-n+1)}{n!}$ represents the number of combinations that we choose, i.e., n elements from m elements$(m \geq n)$.

Because the number of relay pairs that we have to consider for the greedy algorithm is less than exhaustive search, the proposed greedy algorithm provides a much lower cost in terms of flops and running time when compared with the exhaustive search. In fact, the idea behind the proposed algorithm is to choose relay pairs in a greedy fashion. At each stage, we select the set of relays with the highest SINR. Then we consider the availability of the buffers, if the corresponding buffer entries do not satisfy the system

mode, we reselect the relay pair in the following stages. After several stages, the algorithm is able to identify the optimum (or a near optimum) relay set that can satisfy the current transmission. To this end, we state the following proposition.

Proposition: the proposed greedy algorithm achieves an SINR that is upper bounded as follows:

$$\mathrm{SINR}_{\Omega\mathrm{greedy}} \leq \mathrm{SINR}_{\Omega\mathrm{exhaustive}} \tag{4.38}$$

Proof:

We investigate the upper bound by comparing the proposed algorithm and the exhaustive search at the first stage. At stage 1, since $\Omega^s_{\mathrm{greedy}}$ is a candidate subset of the exhaustive search, we have

$$\Omega^1_{\mathrm{exhaustive}} = \max\{\Omega^1_{\mathrm{exhautive(i)}}, i \in [1, C^2_L]\}, \tag{4.39}$$

$$\Omega^s_{\mathrm{greedy}} \in \{\Omega^1_{\mathrm{exhautive(i)}}, i \in [1, C^2_L]\}, \tag{4.40}$$

where $\Omega^1_{\mathrm{exhaustive(i)}}$ represents the i-th relay pair selected at the 1st stage of the exhaustive relay selection method.

Assuming both strategies select the same relay pair and the greedy algorithm is conducted at stage s, we have

$$\begin{aligned}\Omega^s_{\mathrm{greedy}} &= \{p, q\},\\ \Omega^1_{\mathrm{exhaustive}} &= \{p, q\},\end{aligned}$$

this situation again leads to the equality that $\mathrm{SINR}_{\Omega^s_{\mathrm{greedy}}} = \mathrm{SINR}_{\Omega^1_{\mathrm{exhaustive}}}$. In contrast, if the exhaustive search chooses another relay set that belongs to $\{\Omega^1_{\mathrm{exhautive(i)}}, i \in [1, C^2_L]\}$ that provides a higher SINR, clearly, $\Omega^s_{\mathrm{greedy}} \neq \Omega^1_{\mathrm{exhaustive}}$, we can then obtain the inequality that $\mathrm{SINR}_{\Omega^s_{\mathrm{greedy}}} \leq \mathrm{SINR}_{\Omega^1_{\mathrm{exhaustive}}}$.

4.7 Simulations

In this section, a simulation study of the proposed buffer-aided DSTC techniques for cooperative systems is carried out. The DS-CDMA network uses randomly generated

spreading codes of length $N = 16$. The corresponding channel coefficients are modelled as complex Gaussian variables. We assume perfectly known channels at the receivers and we also present an example with channel estimation. Equal power allocation is employed. We consider packets with 1000 BPSK symbols and average the curves over 1000 trials. We set the step size $d = 2$ when evaluating the dynamic schemes. We consider fixed buffer–aided exhaustive/greedy (FBAE/FBAG) relay pair selection strategies (RPS) and dynamic buffer–aided exhaustive/greedy (DBAE/DBAG) RPS.

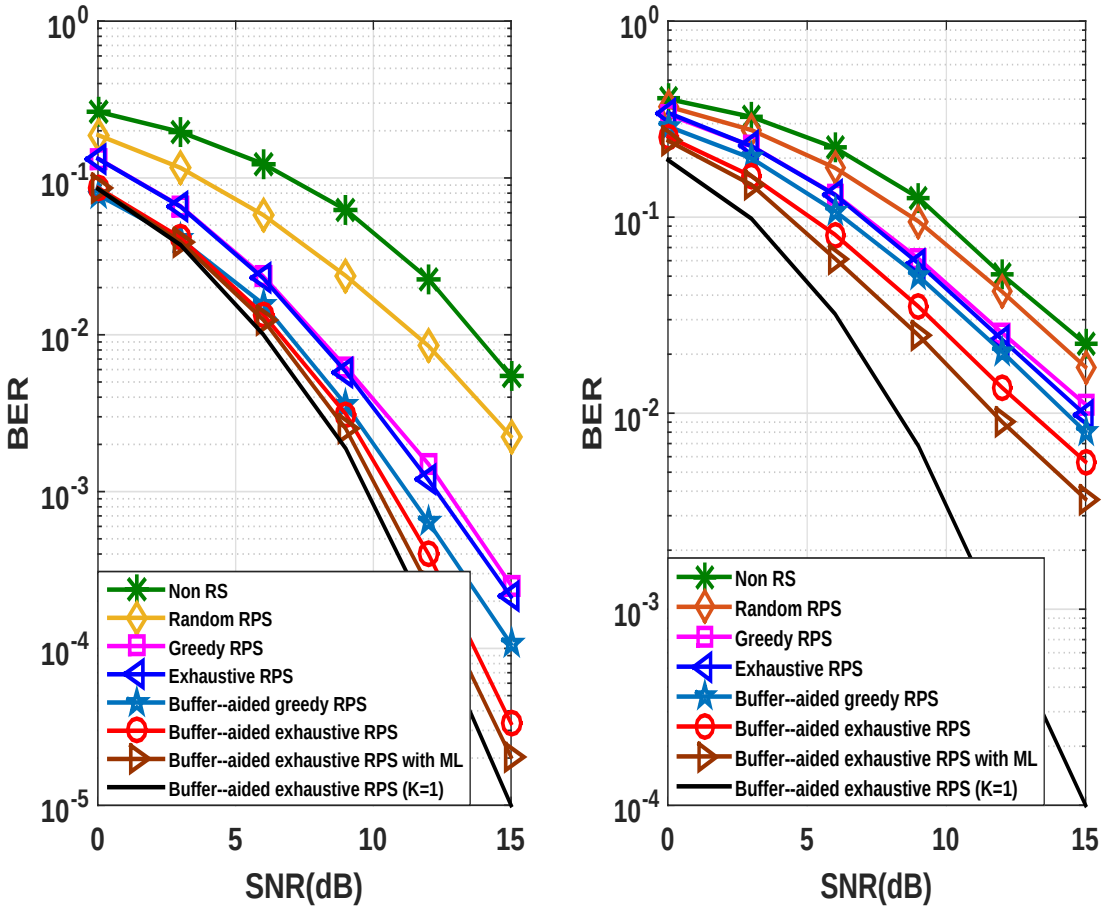

Figure 4.3: a) Performance comparison for buffer-aided scheme and non buffer-aided scheme in cooperative DS-CDMA system with perfect decoding at the relay, MF at the destination b) Performance comparison for buffer-aided scheme and non buffer-aided scheme in cooperative DS-CDMA system with MMSE at the relay, MF at the destination

In order to verify that the fixed buffer-aided relay pair DSTC cooperative scheme contributes to the performance gain, we compare the performance between the situations of the transmission with fixed size buffers and without buffers in Fig. 4.3. The first example shown in Fig. 4.3(a) illustrates the performance comparison between the

proposed buffer-aided DSTC transmission with different RPS and DSTC transmission with different RPS and no buffers. The system has 3 users, 6 relays, perfect decoding is assumed at each relay and the matched filter is adopted at the destination. Specifically, for the no relay selection (RS) DSTC technique, all relays participate in the DSTC transmission (every two consecutive relays are working in pairs). Similarly, for the non buffer-aided schemes, the RPS process only occurs during the second phase (relay-destination), where the random selection algorithm chooses an arbitrary relay pair, the proposed greedy algorithm chooses two relays associated with two optimum relay-destination links and the exhaustive relay pair scheme examines all possible relay pairs and selects the one with the highest SINR. In contrast, the proposed buffer-aided scheme automatically selects the relay pair over both source-relay links and relay-destination links. Moreover, with the help of the buffers, the most appropriate data are sent and better overall system performance can be achieved. As for different decoding methods, we have also tested the BER performance when the ML detector is applied at the destination and the result shows that ML detector behaves better than the simple MF. Apart from that, the performance for a single-user buffer-aided exhaustive RPS DSTC is presented here for comparison purposes. Consequently, the results reveal that our proposed buffer-aided strategies ($J = 6$) perform better than the ones without buffers. In particular, Fig. 4.3(a) also illustrates that our proposed buffer-aided schemes can approach the single-user bound very closely.

Another example depicted in Fig. 4.3(b) compares the proposed buffer-aided DSTC transmission with different RPS and non-buffer aided DSTC transmission with different RPS. In this scenario, where we apply the linear MMSE receiver at each of the relay and the MF at the destination in an uplink cooperative scenario with 3 users, 6 relays and buffer size $J = 6$. Similarly, the system gain brought by the use of ML detector at the destination and the performance bounds for a single-user buffer-aided exhaustive RPS DSTC are presented for comparison purposes. The results also indicate that our proposed buffer-aided strategies ($J = 6$) perform better than the one without buffers. Furthermore, the BER performance curves of our greedy RPS algorithm approaches the exhaustive RPS, while keeping the complexity reasonably low for practical use.

In the second example, we compare the proposed buffer-aided DSTC transmission with different RPS strategies and DSTC transmission with different RPS and no buffers

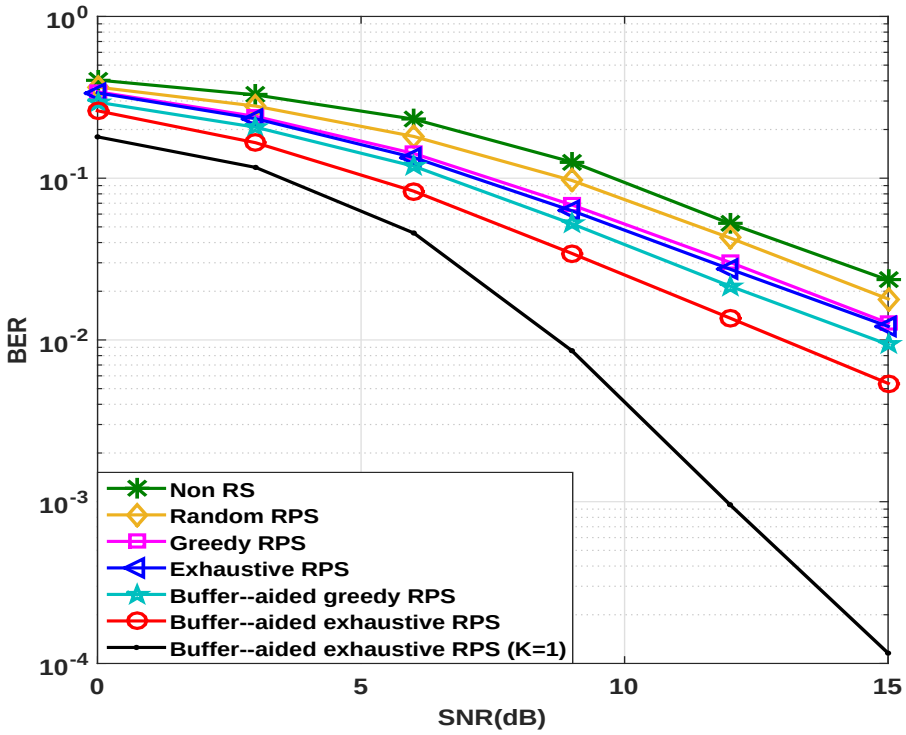

Figure 4.4: Performance comparison for buffer-aided scheme and non buffer-aided scheme in cooperative DS-CDMA system with MMSE at the relay, MF at the destination with channel estimation applied

with LS channel estimation (the length of pilot sequence is 1000). The results are shown in Fig. 4.4. In this scenario, where we apply the linear MMSE receiver at each of the relay and the MF at the destination in an uplink cooperative scenario with 3 users, 6 relays and buffer size $J = 6$. Clearly, it can been seen that, due to the introduction of channel estimation, the performance for all algorithms are slightly degraded when compared with the assumption of perfect CSI. However, our proposed buffer-aided strategies ($J = 6$) still perform better than the one without buffers.

The third example illustrates the performance comparison for the fixed buffer-aided design in Fig. 4.5(a) and dynamic buffer-aided design in Fig. 4.5(b) in a cooperative DSTC system with different RPS strategies. The overall network has 3 users, 6 relays, the linear MMSE receiver is applied at each relay and the MF is adopted at the destination. For dynamic algorithms, the buffer size J decreases when approaching higher SNR region. In both figures, the buffer-aided exhaustive RPS algorithm performs better than the greedy one. When we compare the two figures in Fig. 4.5, the dynamic

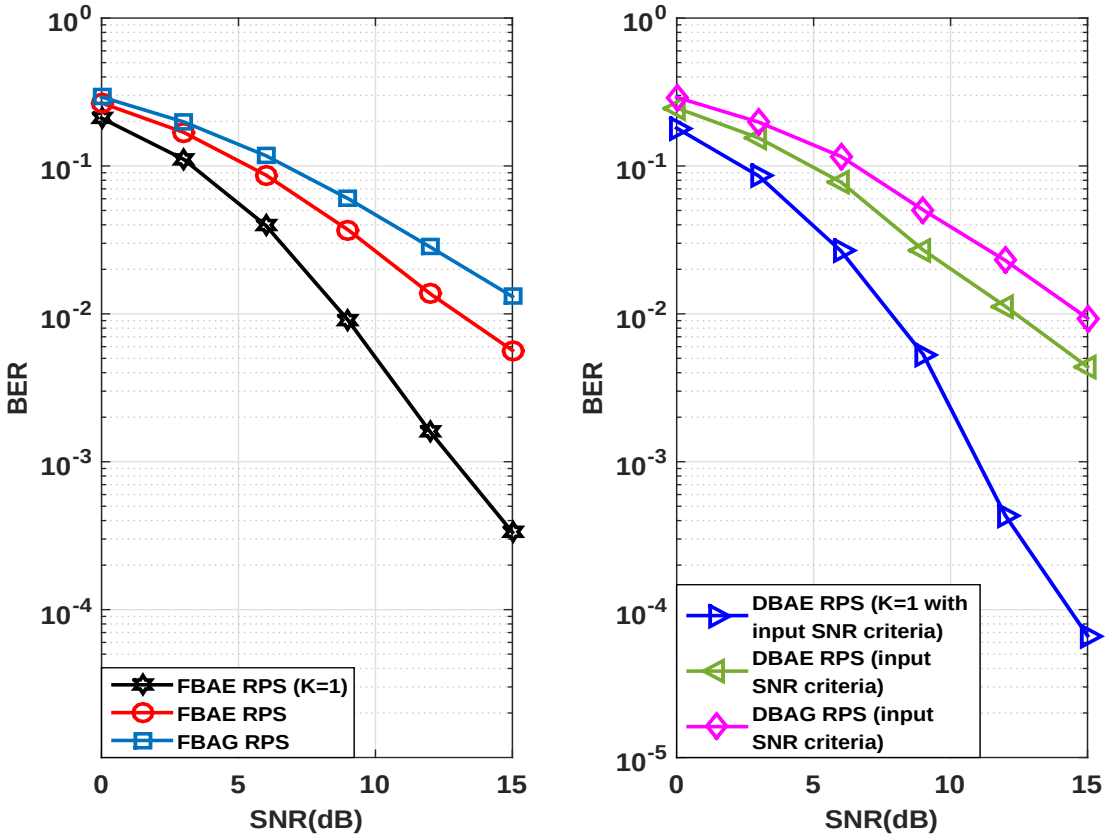

Figure 4.5: a) performance comparison for fixed buffer design (input SNR criterion) b) performance comparison for dynamic buffer design (input SNR criterion)

buffer techniques are more flexible than the fixed buffer ones as they explore the most suitable buffer size for the current transmission according to a given criterion. In this case, there is a greater possibility to select the most appropriate data when the transmission is operated in poor condition as more candidates are stored in the buffer space. On the other hand, the transmission delay can be avoided when the outer condition improves as most of the candidates are appropriate. Simulation results verify these points and indicate that the DBAE/DBAG RPS outperform the FBAE/FBAG ($J = 8$) RPS and the advantage increases when adopting the single user case. Furthermore, it can also be seen that the BER performance curves of the greedy relay pair selection algorithm approaches the exhaustive search, whilst keeping the complexity reasonably low for practical utilization.

The fourth example compares the FBAE/FBAG RPS scheme in Fig. 4.6(a) and the DBAE/DBAG RPS strategy in Fig. 4.6(b) in a DSTC cooperative system, where we

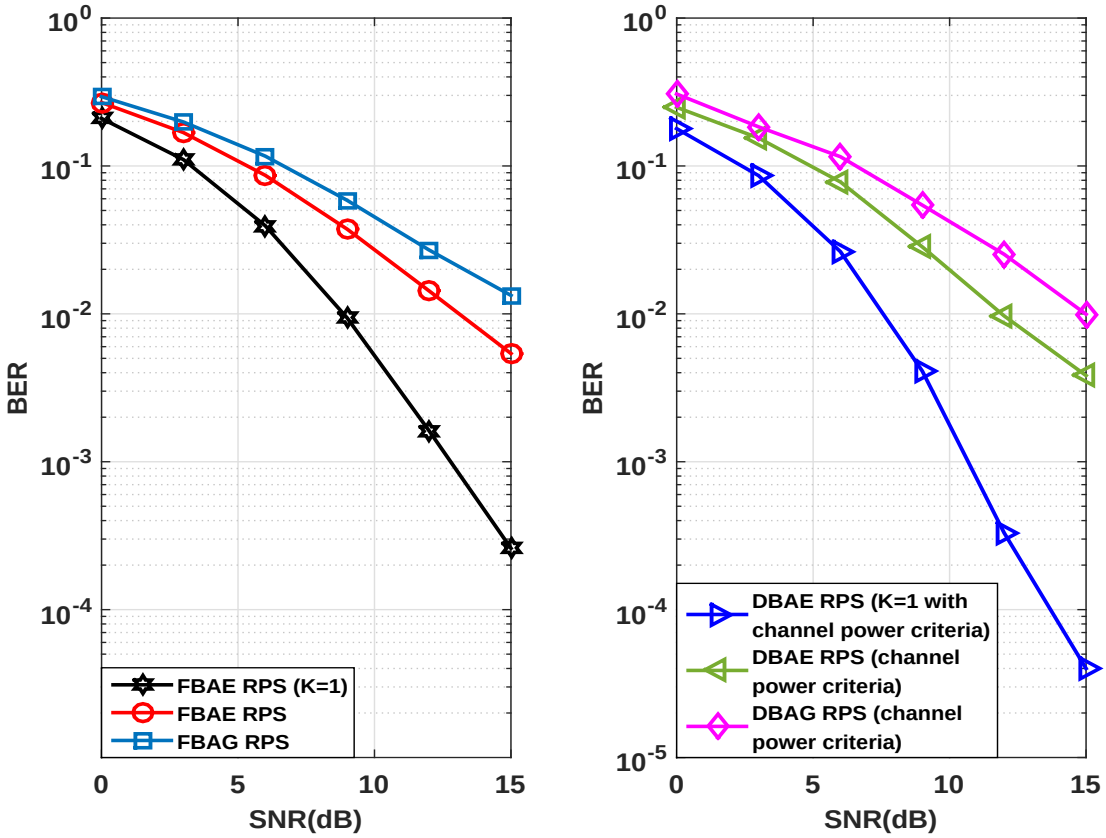

Figure 4.6: a) performance comparison for fixed buffer design (channel power criterion) b)performance comparison for dynamic buffer design (channel power criterion)

apply the linear MMSE receiver at each of the relay and the MF at the destination in an uplink cooperative scenario with 3 users, 6 relays and fixed buffer size $J = 8$. Similarly, the performance for a single-user buffer-aided exhaustive RPS DSTC is presented for comparison purposes. In both figures, the buffer-aided exhaustive search RPS algorithm performs better than the greedy one. The average dynamic buffer size J is highly dependant on the threshold γ and the step size d, clearly, with careful control on these parameters, better performance can be achieved. The simulation results also indicate that our proposed dynamic design perform better than the fixed buffer size ones when we apply the same relay selection method, as depicted in Fig. 4.6.

The algorithms are then assessed in terms of the BER versus buffer size J in Fig. 4.7 with a fixed SNR=15dB. In this scenario, we assume perfect decoding at the relays as accurate detection at relays would highly influence the following transmission and apply the MF at the destination. The results indicate that the overall BER degrades as the size

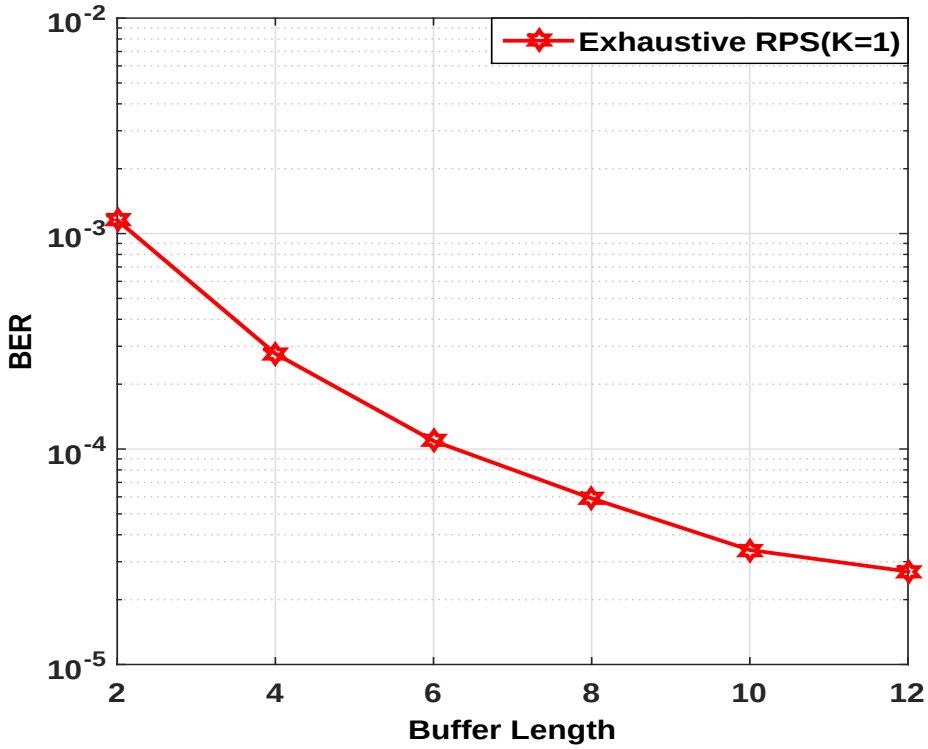

Figure 4.7: BER versus size of the buffers for uplink cooperative system

of the buffer increases. It also shows that with larger buffer sizes, the system experiences diminishing returns in performance. In this case, a good balance between the transmission delay and the buffer size can be obtained when the buffer size is carefully considered.

4.8 Conclusions

In this chapter, we have presented a dynamic buffer-aided DSTC scheme for cooperative DS-CDMA systems with different relay pair selection techniques. With the help of the dynamic buffers, this approach effectively improves the transmission performance and help to achieve a good balance between bit error rate (BER) and delay. We have developed algorithms for relay-pair selection based on an exhaustive search and on a greedy approach. A dynamic buffer design has also been devised to improve the performance of buffer-aided schemes. Simulation results show that the performance of the proposed scheme and algorithms can offer good gains as compared to previously reported techniques.

Chapter 5

Buffer-aided Network Coding Techniques for Cooperative DS-CDMA Systems

Contents

5.1 Introduction

Dealing with the interference that arises in wireless communications is one of the biggest challenges that has been investigated for a long time. In most of the studies, a large

number of approaches that are used for solving interference mitigation problem mainly focus on reducing or avoiding the interference. Unlike traditional strategies that treat interference as a nuisance to be avoided, physical-layer network coding (PNC) techniques take advantage of the superposition of electromagnetic (EM) waves and embrace the interference to improve throughput performance, namely, the coded symbols contains information of not only the user of interest but also the interfering users [20]. Especially, this technique has generated a number of fertile theoretical and application-oriented studies, and is foreseen to be successfully implemented in future wireless communication applications [22, 45, 46, 84, 85]. In wireless and cognitive radio networks, the physical superposition of the signals can be seen as a benefit instead of an interference and exploited for coding at the physical layer level [86]. The communication can be protected against attacks from malicious nodes [37], eavesdropping entities [87], and impairments such as noise and information losses [88] thanks to the property of the network of acting as a coding operator. In peer-to-peer networks, the distribution of a number of encoded versions of the source data avoids the well-known problem of the missing block at the end of the download [89].

Physical-layer network coding has significant advantages in wireless multi-hop networks. Multiple relay nodes are employed in the network to transmit data from sources to the destination [24]. It allows a node to exploit as far as possible all signals that are received simultaneously, rather than treating them as interference [24]. Additionally, instead of decoding each incoming data stream separately, a node detects and forwards the function of the incoming data streams [25]. There are several different network coding techniques, namely, the XOR mapping schemes and linear network coding designs
[20–23, 45, 46].

In cooperative relaying systems, various strategies that utilize relays have been investigated in [52, 53, 56, 69–71]. The main purpose of relay selection algorithms is to find the optimum link combinations so that the signal is sent under the most appropriate channel conditions. Moreover, in order to further increase the quality and reliability of the system transmission, the concept of buffer is introduced and used to equip relay nodes in cooperative relaying scenarios in [72–75].

In this chapter, we propose buffer-aided PNC techniques for cooperative direct-sequence code-division multiple access (DS-CDMA) systems. In the proposed buffer-aided PNC schemes, a relay pair selection algorithm is employed initially between the source-relay links and the relay-destination links. The relay pair with the highest SINR is selected and its associated link combinations are then used for data transmission. Additionally, each relay is equipped with a buffer for data storage so that the data associated with the best available propagation conditions can be selected . After that, various PNC schemes are adopted at each relay and the network coded symbols (NCS) are then sent to the destination. Specifically, we propose two novel linear network coding designs that are able to improve the system performance by introducing a linear network coding matrix $\mathbf{G}$ according to specific criteria.

The contributions of this chapter are summarized as follows:

- A buffer-aided PNC scheme that is able to store enough data packets in the corresponding buffer so that more appropriate symbols can be selected in a suitable time instant is proposed.
- A relay selection algorithm that chooses a relay pair rather than a single relay as the PNC transmission needs the cooperation of a pair of antennas is presented. The proposed algorithm automatically selects the target relay pair in order to forward the data. Moreover, we propose different designs of linear network coding techniques that help to further improve the system performance.
- A greedy relay pair selection technique is then introduced to reduce the high cost brought by the exhaustive search that is required when a large number of relays are involved in the transmission.
- An analysis of the computational complexity of the relay pair selection algorithms and novel linear network coding designs is also presented, along with a sum-rate analysis..

5.2 Cooperative DS-CDMA Network Coding System Model

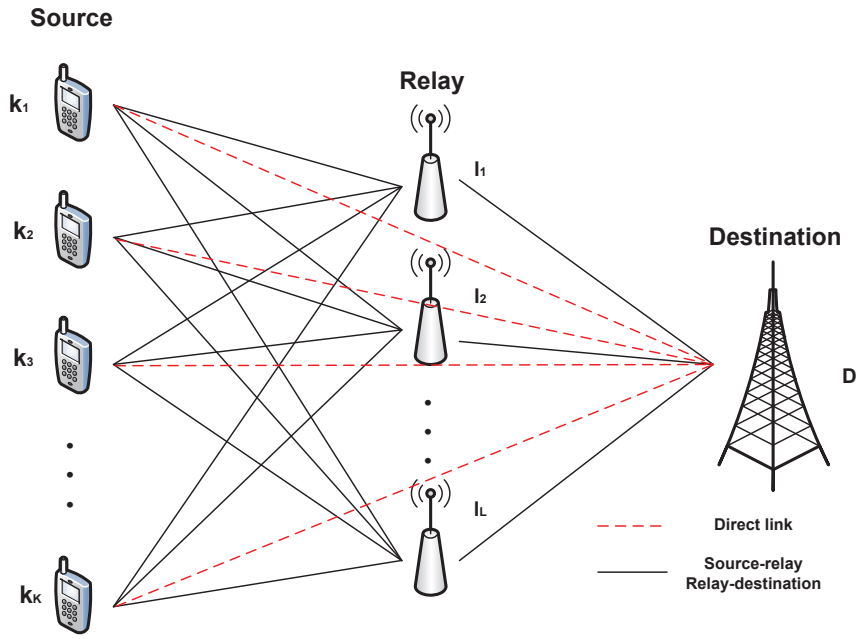

Figure 5.1: Uplink of a cooperative DS-CDMA system.

Consider the uplink of a synchronous DS-CDMA system with K users, L relays equipped with finite-size buffers capable of storing J packets and N chips per symbol that experiences channels with flat fading. The system is also equipped with a cooperative protocol at each relay and we assume that the transmit data are organized in packets comprising P symbols. The received signals are filtered by a filter matched to the chip pulse and sampled at chip rate to obtain sufficient statistics and organized into $N \times 1$ vectors $\mathbf{y}_{sr}$, $\mathbf{y}_{sd}$ and $\mathbf{y}_{rd}$, which represents the signals received from the sources to the relays, the sources to the destination and the relay to the destination, respectively. When considering the transmission process, every set of m users and every set of m relays are randomly assigned into a group. Therefore, for a specific pair of users and relays, the signal received from the remaining users to the target relays are seen as interference. As shown in Fig.5.1, the transmission is divided into two phases.

In the first phase, the signals received at the destination and the l-th relay can be

described as

$$\mathbf{y}_{sd} = \sum_{k=1}^{K} a_{sd}^{k} \mathbf{s}_k h_{sd,k} b_k + \mathbf{n}_{sd}, \tag{5.1}$$

$$\mathbf{y}_{sr_l} = \sum_{k=1}^{K} a_{sr_l}^{k} \mathbf{s}_k h_{sr_l,k} b_k + \mathbf{n}_{sr_l}, \tag{5.2}$$

where b_k correspond to the transmitted symbols ($b_k \in \{+1, -1\}$ if BPSK modulation is adopted and $b_k \in \{\pm 1/\sqrt{(2)} \pm j/\sqrt{(2)}\}$ when QPSK modulation is used). The quantities a_{sd}^{k} and $a_{sr_l}^{k}$ are the k-th user's amplitude from the source to the destination and from the source to relay l, respectively. Clearly, $a_{sd}^{k} = a_{sr_l}^{k}$. The vector $\mathbf{s}_k = [s_k(1), s_k(2), ...s_k(N)]^T$ is the signature sequence for user k. The quantities $h_{sd,k}$ and $h_{sr_l,k}$ represent the complex channel fading coefficient from user k to the destination and from user k to the l-th relay, respectively. The vectors $\mathbf{n}_{sd}$ and $\mathbf{n}_{sr_l}$ are the noise vectors that contain samples of zero mean complex Gaussian noise and variance $\sigma^2\mathbf{I}$.

After the detected symbols of interest are generated, a PNC scheme is then employed at each relay. When the bit-wise XOR operation (the modulo-2 sum in the binary field) is considered, the mathematical mapping from user symbol to BPSK (or another modulation) modulated symbol is then expressed as

$$b_k = 1 - 2c_k, \; c_k \in [0, 1]. \tag{5.3}$$

We then perform the above mapping from $\hat{b}_{r_l d,k}$, which represents the decoded symbol for user k at the output of relay l after using the DF protocol, to its corresponding user symbol as described by

$$\hat{b}_{r_l d,k} \rightarrow c_l^k. \tag{5.4}$$

Similarly, when linear network coding is adopted at the l-th relay, the corresponding mapping is obtained as given by

$$b_l = \sum_{k=1}^{K} g_{kl} \hat{b}_{r_l d,k}, \tag{5.5}$$

where g_{kl} stands for the coding coefficients for the link between the k-th user node and the l-th relay node.

In the following, we carefully review PNC schemes such as those that employ simple bit-wise XOR and existing linear network codes in each of the relays.

Bit-wise XOR mapping

When the signals are sent to the corresponding relays, the DF protocol is then performed and the corresponding detection is obtained

$$\hat{b}_{r_{\Omega(l)}d,\Upsilon(k)} = Q\Big((\mathbf{w}_{s_{\Upsilon(k)}r_{\Omega(l)}})^H \mathbf{y}_{sr_l}\Big), \tag{5.6}$$

where Υ is a $1 \times m$ user set and Ω is the corresponding $1 \times m$ relay set since we combine every m users and m relays into a sub transmission group. $\hat{b}_{r_{\Omega(l)}d,\Upsilon(k)}$ is the detected result for user $\Upsilon(k)$ at relay $\Omega(l)$, $\mathbf{w}_{s_{\Upsilon(k)}r_{\Omega(l)}}$ refers to the detector for user $\Upsilon(k)$ at relay $\Omega(l)$. After that, the detected result is mapped through (5.3) to obtain

$$c_{\Omega(l)}^{\Upsilon(k)} = (1 - \hat{b}_{r_{\Omega(l)}d,\Upsilon(k)})/2. \tag{5.7}$$

We then implement the bit-wise XOR operation at relay $\Omega(l)$ to form

$$c_{\Omega(l)} = c_{\Omega(l)}^{\Upsilon(1)} \oplus c_{\Omega(l)}^{\Upsilon(2)} \oplus ... \oplus c_{\Omega(l)}^{\Upsilon(m)}, \tag{5.8}$$

where $c_{\Omega(l)}$ denotes the network coded symbol (NCS) at relay $\Omega(l)$ and $\oplus$ is the bit-wise XOR operation. After that, in order to forward the encoded information to the destination, the following mapping operation is required

$$b_{\Omega(l)} = 1 - 2c_{\Omega(l)}. \tag{5.9}$$

Consequently, in the second phase the encoded symbols are stored and prepared to be sent to the destination, namely, the relay signal is transmitted from relay set Ω to the destination as described by

$$\mathbf{y}_{r_\Omega d} = \sum_{l=1}^{m} \mathbf{h}_{r_{\Omega(l)}d} b_{\Omega(l)} + \mathbf{n}_{r_\Omega d}, \tag{5.10}$$

where $\mathbf{h}_{r_{\Omega(l)}d} = a_{r_{\Omega(l)}d}^{\Upsilon} \mathbf{s}_\Upsilon h_{r_{\Omega(l)}d}$ denotes the $N \times 1$ channel vector from relay $\Omega(l)$ to the destination, $a_{r_{\Omega(l)}d}^{\Upsilon}$ is the amplitude for combined source (user set Υ) from the $\Omega(l)$-th relay to the destination, $h_{r_{\Omega(l)}d}$ is the complex channel fading coefficient from the $\Omega(l)$-th relay to the destination, $\mathbf{s}_\Upsilon$ is the $N \times 1$ spreading sequence assigned to the coded symbol $b_{\Omega(l)}$ and $\mathbf{n}_{r_\Omega d}$ is the $N \times 1$ zero mean complex Gaussian noise with variance $\sigma^2\mathbf{I}$.

At the destination, the detected symbol for user $\Upsilon(k)$ from the direct transmissions is obtained as

$$\hat{b}_{sd}^{\Upsilon(k)} = Q\Big((\mathbf{w}_{sd}^{\Upsilon(k)})^H \mathbf{y}_{sd}\Big), \tag{5.11}$$

where $\mathbf{w}_{sd}^{\Upsilon(k)}$ is the detector for user $\Upsilon(k)$ used at the destination. After that, according to (5.3), the corresponding user symbol $\hat{c}_{sd}^{\Upsilon(k)}$ is given by

$$\hat{c}_{sd}^{\Upsilon(k)} = (1 - \hat{b}_{sd}^{\Upsilon(k)})/2. \tag{5.12}$$

Similarly, the detected symbol for relay $\Omega(l)$ from the second phase transmission is given by

$$\hat{b}_{\Omega(l)} = Q\Big((\mathbf{w}_{r_{\Omega(l)}d})^H \mathbf{y}_{r_{\Omega}d}\Big), \tag{5.13}$$

where $\mathbf{w}_{r_{\Omega(l)}d}$ is the receive filter for the $\Omega(l)$-th relay-destination link. Consequently, its corresponding user symbol is obtained through (5.3) as given by

$$\hat{c}_{\Omega(l)} = (1 - \hat{b}_{\Omega(l)})/2. \tag{5.14}$$

Thus, the final detected symbol $\hat{c}^{\Upsilon(k)}$ when the XOR operation is adopted at the target relays is expressed as

$$\hat{c}^{\Upsilon(k)} = \hat{c}_{\Omega(l)} \oplus \hat{c}_{sd}^{\Upsilon(1)} \oplus ... \hat{c}_{sd}^{\Upsilon(k-1)} \oplus \hat{c}_{sd}^{\Upsilon(k+1)} ... \oplus \hat{c}_{sd}^{\Upsilon(m)}, \tag{5.15}$$

consequently, the final detected symbol for user $\Upsilon(k)$ is obtained according to the following mapping:

$$\hat{b}_{\Upsilon(k)} = 1 - 2\hat{c}^{\Upsilon(k)} \tag{5.16}$$

Linear network coding

Similarly, if a linear network coding technique is adopted at the relays, every relay group will be allocated a unique $m \times m$ coefficient matrix $\mathbf{G}$, where the structure of this matrix is given by

$$\mathbf{G} = \begin{bmatrix} g_{11} & g_{12} & \cdots & g_{1m} \\ g_{21} & g_{22} & \cdots & g_{2m} \\ & & \vdots & \\ g_{m1} & g_{m2} & \cdots & g_{mm} \end{bmatrix}. \tag{5.17}$$

Thus, the following linear combination can be obtained

$$b_{\Omega(l)} = \sum_{k=1}^{m} g_{kl}\, \hat{b}_{r_{\Omega(l)}d,\Upsilon(k)}, \tag{5.18}$$

where $\hat{b}_{r_{\Omega(l)}d,\Upsilon(k)}$ is the detected symbol for user $\Upsilon(k)$ at relay $\Omega(l)$. Therefore, the following transmission is operated according to (5.10) when a suitable time interval

comes. Equivalently, (5.10) can be rewritten as

$$\mathbf{y}_{r_\Omega d} = \mathbf{H}_{r_\Omega d}\mathbf{G}\mathbf{b}_\Omega + \mathbf{n}_{r_\Omega d} \tag{5.19}$$

where $\mathbf{H}_{r_\Omega d}$ is a $N \times m$ channel matrix, each $N \times 1$ column $\mathbf{h}_{r_{\Omega(l)}d}$ in this matrix represents the channel vector from the $\Omega(l)$-th relay to the destination, $\mathbf{b}_\Omega$ is a $m \times 1$ vector containing the detected symbols for all users from set Υ at any relay that belongs to Ω. The vector $\mathbf{n}_{r_\Omega d}$ is the $N \times 1$ noise vector.

Similarly, at the destination side, the detected symbol for users from set Υ after using the linear network coding operation at each of the relays is given by

$$\hat{b}_{\Omega(l)} = Q\Big(\mathbf{G}^{-1}(\mathbf{w}_{r_\Omega d})^H \mathbf{y}_{r_\Omega d}\Big). \tag{5.20}$$

Mathematically, the decoding process for linear network coding is expressed as given by

$$\begin{cases} \hat{b}_{\Omega(1)} &= g_{\Upsilon(1)\Omega(1)}\hat{b}_{\Upsilon(1)} + g_{\Upsilon(2)\Omega(1)}\hat{b}_{\Upsilon(2)} + ... + g_{\Upsilon(m)\Omega(1)}\hat{b}_{\Upsilon(m)} \\ \hat{b}_{\Omega(2)} &= g_{\Upsilon(1)\Omega(2)}\hat{b}_{\Upsilon(1)} + g_{\Upsilon(2)\Omega(2)}\hat{b}_{\Upsilon(2)} + ... + g_{\Upsilon(m)\Omega(2)}\hat{b}_{\Upsilon(m)} \\ & \cdots \ \cdots \\ \hat{b}_{\Omega(m)} &= g_{\Upsilon(1)\Omega(m)}\hat{b}_{\Upsilon(1)} + g_{\Upsilon(2)\Omega(m)}\hat{b}_{\Upsilon(2)} + ... + g_{\Upsilon(m)\Omega(m)}\hat{b}_{\Upsilon(m)} \end{cases} \tag{5.21}$$

Clearly, the m unknown detected results $\hat{b}_{\Upsilon(k)}, k = 1, 2, ...m$ for each user in user set Υ can easily be sorted out with the above m equations. However, in the given scenario, since we introduce the direct transmissions, there is another approach that can also be applied at the decoding process. Specifically, we can obtain the final detected symbol for the user $\hat{b}_{\Upsilon(k)}$ as given by

$$\hat{b}_{\Upsilon(k)} = \frac{\hat{b}_{\Omega(l)} - \big(g_{\Upsilon(1)\Omega(l)}\hat{b}_{sd}^{\Upsilon(1)} + ...g_{\Upsilon(k-1)\Omega(l)}\hat{b}_{sd}^{\Upsilon(k-1)} + g_{\Upsilon(k+1)\Omega(l)}\hat{b}_{sd}^{\Upsilon(k+1)} ... + g_{\Upsilon(m)\Omega(l)}\hat{b}_{sd}^{\Upsilon(m)}\big)}{g_{\Upsilon(k)\Omega(l)}}. \tag{5.22}$$

With the help of the direct transmissions, we can effectively reduce the bit error rate, in particular, there is a possibility that the detection for $\hat{b}_{\Omega(l)}, l \in \Omega$ is incorrect, which, could directly lead to a problem when solving the system of equations in (5.21), causing incorrect decisions for all users. However, this situation may not lead to significant performance degradation when applying (5.22) as we can select another detected symbol $\hat{b}_{\Omega(s)}, s \neq l$ as the minuend in (5.22) instead of the incorrect detected symbol $\hat{b}_{\Omega(l)}$.

5.3 Proposed Cooperative Linear Network Coding Schemes

In this section, we present two novel linear network code designs that are able to provide performance gains brought by the introduction of suitably designed matrix **G**. This idea is inspired and related to the work of [90] but applied in a completely different application. In the current cooperative PNC transmission scenario, the simplest way to construct the coefficient matrix **G** is to generate it randomly, however, this approach may not result in the optimum performance as it neither considers all other candidate matrices nor satisfies a certain criterion. Therefore, in order to obtain further performance advantages, we propose two different methods to construct the linear network coding matrix **G**.

Specifically, in our design, we limit the coefficients of the matrix **G** to the binary field. Naturally, this inspired us to seek for all possible candidate matrices as the computational complexity can be controlled within an acceptable level when the size of the matrix is carefully set up and constrained to be small.

Maximum Likelihood (ML) Design

When a linear network coding scheme is adopted at the relay, we introduce the $m \times m$ binary matrix **G**, where each element in the matrix of coefficients is multiplied by the corresponding user symbol to generate the network coded symbols (NCS). Clearly, the selection between all possible (2^{m^2}) binary matrices is required by the following maximum likelihood criterion:

$$\mathbf{G}^{\mathrm{ML}} = \arg\min \left[\left\| \begin{bmatrix} b_{\Omega(1)} \\ b_{\Omega(2)} \\ \vdots \\ b_{\Omega(m)} \end{bmatrix} - \mathbf{G}^{-1} \begin{bmatrix} \mathbf{w}_{r_{\Omega(1)}d}^{H} \mathbf{y}_{r_{\Omega(1)}d} \\ \mathbf{w}_{r_{\Omega(2)}d}^{H} \mathbf{y}_{r_{\Omega(2)}d} \\ \vdots \\ \mathbf{w}_{r_{\Omega(m)}d}^{H} \mathbf{y}_{r_{\Omega(m)}d} \end{bmatrix} \right\|^2 \right], 1 \leq j \leq 2^{m^2}, \tag{5.23}$$

where $\mathbf{w}_{r_l d}$ is the linear detector used at relay l, $\mathbf{y}_{r_l d}$ is the signal transmitted from relay l. Note that the above equation corresponds to a combinatorial problem where we must test all 2^{m^2} possible candidates to obtain the matrix $\mathbf{G}^{\mathrm{ML}}$ associated with the best performance according to this criterion. This is one of the disadvantages of this approach. Another disadvantage is that the decoding process for ML scheme did not consider the influence brought by the noise term as both the $\mathbf{G}^{-1}$ and the filter did not contain any decoding

information for the noise component.

As shown in (5.23), we generate an $m \times m$ matrix $\mathbf{G}^{\mathrm{ML}}$ at the relays to form the NCS. At the destination side, we employ the same matrix $\mathbf{G}^{\mathrm{ML}}$ that is able to match well with $\mathbf{G}^{\mathrm{ML}}$ that is applied at the relays in order to obtain accurate decoding results. The matrix $\mathbf{G}^{\mathrm{ML}}$ will be transmit from relay to destination after it has been generated only once and stored at the destination preparing for the decoding process. In summary, the principle of this approach is to obtain an $m \times m$ code matrix $\mathbf{G}^{\mathrm{ML}}$ for decoding at the destination to match with the same coefficient matrix that is applied at the relays for the purpose of encoding, thus, the minimum distance between the transmitted symbols and received detected symbols can be obtained.

Minimum Mean-Square Error (MMSE) Design

When we examine the decoding method in (5.23), clearly, it does not consider the influence brought by noise. In this case, although all possible binary matrices are tested and the optimum one is selected, the detected symbols at the destination might not reach the corresponding detected results at the relays. This fact motivates us to seek another efficient decoding method that can consider both interference and noise. In order to further exploit the minimum Euclidean distance and improve the transmission performance, we then introduce a candidate code matrix $\tilde{\mathbf{G}}$ at the destination to match the generated binary matrix $\mathbf{G}$ and perform the linear network coding operation. Consequently, the proposed MMSE linear network coding matrix $\mathbf{G}^{\mathrm{MMSE}}$ is obtained as follows:

$$\mathbf{G}^{\mathrm{MMSE}} = \arg\min_{\tilde{\mathbf{G}}} \; E\left[\left\| \begin{bmatrix} b_{\Omega(1)} \\ \vdots \\ b_{\Omega(m)} \end{bmatrix} - \tilde{\mathbf{G}} \begin{bmatrix} \mathbf{w}_{r_{\Omega(1)}d}^{H} \mathbf{y}_{r_{\Omega(1)}d} \\ \vdots \\ \mathbf{w}_{r_{\Omega(m)}d}^{H} \mathbf{y}_{r_{\Omega(m)}d} \end{bmatrix} \right\|^2\right], \tag{5.24}$$

Ideally, $b_{\Omega(1)}^{\Upsilon(k)} = b_{\Omega(2)}^{\Upsilon(k)} = ... = b_{\Omega(m)}^{\Upsilon(k)}, k \in [1, m]$. Let $\begin{bmatrix} b_{\Omega(1)} \\ \vdots \\ b_{\Omega(m)} \end{bmatrix}$=**a**, $\begin{bmatrix} \mathbf{w}_{r_{\Omega(1)}d}^{H} \mathbf{y}_{r_{\Omega(1)}d} \\ \vdots \\ \mathbf{w}_{r_{\Omega(m)}d}^{H} \mathbf{y}_{r_{\Omega(m)}d} \end{bmatrix}$=**b**, this problem can be cast into the following equation

$$\mathbf{G}^{\mathrm{MMSE}} = \arg \min_{\tilde{\mathbf{G}}} E[\left\| \mathbf{a} - \tilde{\mathbf{G}}\mathbf{b} \right\|^2], \tag{5.25}$$

by taking the gradient with respect to $\tilde{\mathbf{G}}$ and equating to zero, we can obtain the following

equations:

$$E[-\mathbf{b}\mathbf{a}^H + \mathbf{b}\mathbf{b}^H\tilde{\mathbf{G}}^H] = 0, \tag{5.26}$$

consequently, we have

$$\begin{aligned} &E[\mathbf{b}\mathbf{b}^H\tilde{\mathbf{G}}^H] = E[\mathbf{b}\mathbf{a}^H], \\ &E[(\mathbf{b}\mathbf{b}^H\tilde{\mathbf{G}}^H)^H] = E[(\mathbf{b}\mathbf{a}^H)^H], \\ &E[\tilde{\mathbf{G}}\mathbf{b}\mathbf{b}^H] = E[\mathbf{a}\mathbf{b}^H], \end{aligned} \tag{5.27}$$

and the MMSE matrix is given by

$$\begin{aligned} \mathbf{G}^{\mathrm{MMSE}} &= E[\mathbf{a}\mathbf{b}^H](E[\mathbf{b}\mathbf{b}^H])^{-1}, \\ &= \mathbf{P}_{ab}\mathbf{R}_b^{-1}, \end{aligned} \tag{5.28}$$

where the statistical quantities in the MMSE code matrix are the auto-correlation matrix $\mathbf{R}_b$ and the cross-correlation matrix $\mathbf{P}_{ab}$ whose structures are given by

$$\begin{aligned} \mathbf{R}_b = E[\mathbf{b}\mathbf{b}^H] &= E\left[\begin{bmatrix} \mathbf{w}^H_{r_{\Omega(1)}d}\mathbf{y}_{r_{\Omega(1)}d} \\ \vdots \\ \mathbf{w}^H_{r_{\Omega(m)}d}\mathbf{y}_{r_{\Omega(m)}d} \end{bmatrix}\begin{bmatrix} \mathbf{w}^H_{r_{\Omega(1)}d}\mathbf{y}_{r_{\Omega(1)}d} \\ \vdots \\ \mathbf{w}^H_{r_{\Omega(m)}d}\mathbf{y}_{r_{\Omega(m)}d} \end{bmatrix}^H\right] \\ &= \begin{bmatrix} \mathbf{w}^H_{r_{\Omega(1)}d} & 0 & \cdots & 0 \\ & \cdots & & \\ 0 & 0 & \cdots & \mathbf{w}^H_{r_{\Omega(m)}d} \end{bmatrix} E\left[\begin{bmatrix} \mathbf{y}_{r_{\Omega(1)}d} \\ \vdots \\ \mathbf{y}_{r_{\Omega(m)}d} \end{bmatrix}\begin{bmatrix} \mathbf{y}_{r_{\Omega(1)}d} \\ \vdots \\ \mathbf{y}_{r_{\Omega(m)}d} \end{bmatrix}^H\right] \begin{bmatrix} \mathbf{w}^H_{r_{\Omega(1)}d} & 0 & \cdots & 0 \\ & \cdots & & \\ 0 & 0 & \cdots & \mathbf{w}^H_{r_{\Omega(m)}d} \end{bmatrix}^H \\ &= \begin{bmatrix} \mathbf{w}^H_{r_{\Omega(1)}d} & 0 & \cdots & 0 \\ & \cdots & & \\ 0 & 0 & \cdots & \mathbf{w}^H_{r_{\Omega(m)}d} \end{bmatrix} \begin{bmatrix} \mathbf{h}_{r_{\Omega(1)}d}\mathbf{h}^H_{r_{\Omega(1)}d} + \sigma^2\mathbf{I} & \mathbf{0} & \cdots & \mathbf{0} \\ & \cdots & & \\ \mathbf{0} & \mathbf{0} & \cdots & \mathbf{h}_{r_{\Omega(m)}d}\mathbf{h}^H_{r_{\Omega(m)}d} + \sigma^2\mathbf{I} \end{bmatrix} \begin{bmatrix} \mathbf{w}^H_{r_{\Omega(1)}d} & 0 & \cdots & 0 \\ & \cdots & & \\ 0 & 0 & \cdots & \mathbf{w}^H_{r_{\Omega(m)}d} \end{bmatrix}^H \end{aligned} \tag{5.29}$$

$$\begin{aligned} \mathbf{P}_{ab} = E[\mathbf{a}\mathbf{b}^H] &= E\left[\begin{bmatrix} b_{\Omega(1)} \\ \vdots \\ b_{\Omega(m)} \end{bmatrix}\begin{bmatrix} \mathbf{y}_{r_{\Omega(1)}d} \\ \vdots \\ \mathbf{y}_{r_{\Omega(m)}d} \end{bmatrix}^H \begin{bmatrix} \mathbf{w}_{r_{\Omega(1)}d} & 0 & \cdots & 0 \\ & \cdots & & \\ 0 & 0 & \cdots & \mathbf{w}_{r_{\Omega(m)}d} \end{bmatrix}\right] \\ &= E\left[\begin{bmatrix} b_{\Omega(1)}\mathbf{y}^H_{r_{\Omega(1)}d}\mathbf{w}_{r_{\Omega(1)}d} & b_{\Omega(1)}\mathbf{y}^H_{r_{\Omega(2)}d}\mathbf{w}_{r_{\Omega(2)}d} & \cdots & b_{\Omega(1)}\mathbf{y}^H_{r_{\Omega(m)}d}\mathbf{w}_{r_{\Omega(m)}d} \\ & \vdots & & \\ b_{\Omega(m)}\mathbf{y}^H_{r_{\Omega(1)}d}\mathbf{w}_{r_{\Omega(1)}d} & b_{\Omega(m)}\mathbf{y}^H_{r_{\Omega(2)}d}\mathbf{w}_{r_{\Omega(2)}d} & \cdots & b_{\Omega(m)}\mathbf{y}^H_{r_{\Omega(m)}d}\mathbf{w}_{r_{\Omega(m)}d} \end{bmatrix}\right] \end{aligned}$$

$$
\begin{aligned}
=E\Bigg[\Bigg[&\begin{bmatrix} b_{\Omega(1)}(b^*_{\Omega(1)}\mathbf{h}^H_{r_{\Omega(1)}d}+\mathbf{n}^H_{rd})\mathbf{w}_{r_{\Omega(1)}d} & b_{\Omega(1)}(b^*_{\Omega(2)}\mathbf{h}^H_{r_{\Omega(2)}d}+\mathbf{n}^H_{rd})\mathbf{w}_{r_{\Omega(2)}d} & \cdots \\ & \vdots & \\ b_{\Omega(m)}(b^*_{\Omega(1)}\mathbf{h}^H_{r_{\Omega(1)}d}+\mathbf{n}^H_{rd})\mathbf{w}_{r_{\Omega(1)}d} & b_{\Omega(m)}(b^*_{\Omega(2)}\mathbf{h}^H_{r_{\Omega(2)}d}+\mathbf{n}^H_{rd})\mathbf{w}_{r_{\Omega(2)}d} & \cdots \end{bmatrix} \\
&\begin{matrix} \cdots & b_{\Omega(1)}(b^*_{\Omega(m)}\mathbf{h}^H_{r_{\Omega(m)}d}+\mathbf{n}^H_{rd})\mathbf{w}_{r_{\Omega(m)}d} \\ \\ \cdots & b_{\Omega(m)}(b^*_{\Omega(m)}\mathbf{h}^H_{r_{\Omega(m)}d}+\mathbf{n}^H_{rd})\mathbf{w}_{r_{\Omega(m)}d} \end{matrix}\Bigg]\Bigg] \\
=E\Bigg[\Bigg[&\begin{bmatrix} b_{\Omega(1)}b^*_{\Omega(1)}\mathbf{h}^H_{r_{\Omega(1)}d}\mathbf{w}_{r_{\Omega(1)}d} & b_{\Omega(1)}b^*_{\Omega(2)}\mathbf{h}^H_{r_{\Omega(2)}d}\mathbf{w}_{r_{\Omega(2)}d} & \cdots \\ & \vdots & \\ b_{\Omega(m)}b^*_{\Omega(1)}\mathbf{h}^H_{r_{\Omega(1)}d}\mathbf{w}_{r_{\Omega(1)}d} & b_{\Omega(m)}b^*_{\Omega(2)}\mathbf{h}^H_{r_{\Omega(2)}d}\mathbf{w}_{r_{\Omega(2)}d} & \cdots \end{bmatrix} \\
&\begin{matrix} \cdots & b_{\Omega(1)}b^*_{\Omega(m)}\mathbf{h}^H_{r_{\Omega(m)}d}\mathbf{w}_{r_{\Omega(m)}d} \\ & \vdots \\ \cdots & b_{\Omega(m)}b^*_{\Omega(m)}\mathbf{h}^H_{r_{\Omega(m)}d}\mathbf{w}_{r_{\Omega(m)}d} \end{matrix}\Bigg]\Bigg] \\
=E\Bigg[\Bigg[&\begin{bmatrix} \big(\sum_{i=1}^{m}\sum_{j=1}^{m} g_{i1}g^*_{j1}b^{\Upsilon(i)}_{\Omega(1)}(b^{\Upsilon(j)}_{\Omega(1)})^*\big)\mathbf{h}^H_{r_{\Omega(1)}d}\mathbf{w}_{r_{\Omega(1)}d} & \cdots \\ & \vdots \\ \big(\sum_{i=1}^{m}\sum_{j=1}^{m} g_{im}g^*_{j1}b^{\Upsilon(i)}_{\Omega(m)}(b^{\Upsilon(j)}_{\Omega(1)})^*\big)\mathbf{h}^H_{r_{\Omega(1)}d}\mathbf{w}_{r_{\Omega(1)}d} & \cdots \end{bmatrix} \\
&\begin{matrix} \cdots & \big(\sum_{i=1}^{m}\sum_{j=1}^{m} g_{i1}g^*_{jm}b^{\Upsilon(i)}_{\Omega(1)}(b^{\Upsilon(j)}_{\Omega(m)})^*\big)\mathbf{h}^H_{r_{\Omega(m)}d}\mathbf{w}_{r_{\Omega(m)}d} \\ \\ \cdots & \big(\sum_{i=1}^{m}\sum_{j=1}^{m} g_{im}g^*_{jm}b^{\Upsilon(i)}_{\Omega(m)}(b^{\Upsilon(j)}_{\Omega(m)})^*\big)\mathbf{h}^H_{r_{\Omega(m)}d}\mathbf{w}_{r_{\Omega(m)}d} \end{matrix}\Bigg]\Bigg] \\
=E\Bigg[\Bigg[&\begin{bmatrix} \big(\sum_{i=1}^{m}\sum_{j=1}^{m} g_{i1}g_{j1}b^{\Upsilon(i)}_{\Omega(1)}b^{\Upsilon(j)}_{\Omega(1)}\big)\mathbf{h}^H_{r_{\Omega(1)}d}\mathbf{w}_{r_{\Omega(1)}d} & \cdots \\ & \vdots \\ \big(\sum_{i=1}^{m}\sum_{j=1}^{m} g_{im}g_{j1}b^{\Upsilon(i)}_{\Omega(m)}b^{\Upsilon(j)}_{\Omega(1)}\big)\mathbf{h}^H_{r_{\Omega(1)}d}\mathbf{w}_{r_{\Omega(1)}d} & \cdots \end{bmatrix} \\
&\begin{matrix} \cdots & \big(\sum_{i=1}^{m}\sum_{j=1}^{m} g_{i1}g_{jm}b^{\Upsilon(i)}_{\Omega(1)}b^{\Upsilon(j)}_{\Omega(m)}\big)\mathbf{h}^H_{r_{\Omega(m)}d}\mathbf{w}_{r_{\Omega(m)}d} \\ & \vdots \\ \cdots & \big(\sum_{i=1}^{m}\sum_{j=1}^{m} g_{im}g_{jm}b^{\Upsilon(i)}_{\Omega(m)}b^{\Upsilon(j)}_{\Omega(m)}\big)\mathbf{h}^H_{r_{\Omega(m)}d}\mathbf{w}_{r_{\Omega(m)}d} \end{matrix}\Bigg]\Bigg] \\
=E\Bigg[&\begin{bmatrix} \sum_{i=1}^{m}\sum_{j=1}^{m} g_{i1}g_{j1}b^{\Upsilon(i)}_{\Omega(1)}b^{\Upsilon(j)}_{\Omega(1)} & \cdots & 0 \\ & \vdots & \\ \sum_{i=1}^{m}\sum_{j=1}^{m} g_{im}g_{j1}b^{\Upsilon(i)}_{\Omega(m)}b^{\Upsilon(j)}_{\Omega(1)} & \cdots & 0 \end{bmatrix}\mathbf{h}^H_{r_{\Omega(1)}d}\mathbf{w}_{r_{\Omega(1)}d}+\cdots
\end{aligned}
$$

$$
\begin{aligned}
&+\left[\begin{array}{ccc} 0 & \cdots & \sum_{i=1}^{m}\sum_{j=1}^{m} g_{i1}g_{jm}b_{\Omega(1)}^{\Upsilon(i)}b_{\Omega(m)}^{\Upsilon(j)} \\ & & \vdots \\ 0 & \cdots & \sum_{i=1}^{m}\sum_{j=1}^{m} g_{im}g_{jm}b_{\Omega(m)}^{\Upsilon(i)}b_{\Omega(m)}^{\Upsilon(j)} \end{array}\right]\mathbf{h}_{r_{\Omega(m)}d}^{H}\mathbf{w}_{r_{\Omega(m)}d}\Bigg] \\
=&E\Bigg[\left[\begin{array}{ccc} \sum_{i=1}^{m} g_{i1}g_{i1}b_{\Omega(1)}^{\Upsilon(i)}b_{\Omega(1)}^{\Upsilon(i)} & \cdots & 0 \\ & \vdots & \\ \sum_{i=1}^{m} g_{im}g_{i1}b_{\Omega(m)}^{\Upsilon(i)}b_{\Omega(1)}^{\Upsilon(i)} & \cdots & 0 \end{array}\right]\mathbf{h}_{r_{\Omega(1)}d}^{H}\mathbf{w}_{r_{\Omega(1)}d}+\cdots \\
&+\left[\begin{array}{ccc} 0 & \cdots & \sum_{i=1}^{m} g_{i1}g_{im}b_{\Omega(1)}^{\Upsilon(i)}b_{\Omega(m)}^{\Upsilon(i)} \\ & \vdots & \\ 0 & \cdots & \sum_{i=1}^{m} g_{im}g_{im}b_{\Omega(m)}^{\Upsilon(i)}b_{\Omega(m)}^{\Upsilon(i)} \end{array}\right]\mathbf{h}_{r_{\Omega(m)}d}^{H}\mathbf{w}_{r_{\Omega(m)}d}\Bigg] \\
=&E\Bigg[\left[\begin{array}{ccc} \big(\sum_{i=1}^{m} g_{i1}g_{i1}b_{\Omega(1)}^{\Upsilon(i)}b_{\Omega(1)}^{\Upsilon(i)}\big)\mathbf{h}_{r_{\Omega(1)}d}^{H}\mathbf{w}_{r_{\Omega(1)}d} & \cdots & \big(\sum_{i=1}^{m} g_{i1}g_{im}b_{\Omega(1)}^{\Upsilon(i)}b_{\Omega(m)}^{\Upsilon(i)}\big)\mathbf{h}_{r_{\Omega(m)}d}^{H}\mathbf{w}_{r_{\Omega(m)}d} \\ & \vdots & \\ \big(\sum_{i=1}^{m} g_{im}g_{i1}b_{\Omega(m)}^{\Upsilon(i)}b_{\Omega(1)}^{\Upsilon(i)}\big)\mathbf{h}_{r_{\Omega(1)}d}^{H}\mathbf{w}_{r_{\Omega(1)}d} & \cdots & \big(\sum_{i=1}^{m} g_{im}g_{im}b_{\Omega(m)}^{\Upsilon(i)}b_{\Omega(m)}^{\Upsilon(i)}\big)\mathbf{h}_{r_{\Omega(m)}d}^{H}\mathbf{w}_{r_{\Omega(m)}d} \end{array}\right]\Bigg] \\
=&\left[\begin{array}{ccc} \big(\sum_{i=1}^{m} g_{i1}g_{i1}\sigma_i^2\big)\mathbf{h}_{r_{\Omega(1)}d}^{H}\mathbf{w}_{r_{\Omega(1)}d} & \cdots & \big(\sum_{i=1}^{m} g_{i1}g_{im}\sigma_i^2\big)\mathbf{h}_{r_{\Omega(m)}d}^{H}\mathbf{w}_{r_{\Omega(m)}d} \\ & \vdots & \\ \big(\sum_{i=1}^{m} g_{im}g_{i1}\sigma_i^2\big)\mathbf{h}_{r_{\Omega(1)}d}^{H}\mathbf{w}_{r_{\Omega(1)}d} & \cdots & \big(\sum_{i=1}^{m} g_{im}g_{im}\sigma_i^2\big)\mathbf{h}_{r_{\Omega(m)}d}^{H}\mathbf{w}_{r_{\Omega(m)}d} \end{array}\right], \qquad (5.30)
\end{aligned}
$$

where σ_i^2 is the variance of the transmitted symbol. Therefore, the optimum $\mathbf{G}^{\mathrm{MMSE}}$ is formed as

$$
\begin{aligned}
\mathbf{G}^{\mathrm{MMSE}} =& \left[\begin{array}{ccc} \big(\sum_{i=1}^{m} g_{i1}g_{i1}\sigma_i^2\big)\mathbf{h}_{r_{\Omega(1)}d}^{H}\mathbf{w}_{r_{\Omega(1)}d} & \cdots & \big(\sum_{i=1}^{m} g_{i1}g_{im}\sigma_i^2\big)\mathbf{h}_{r_{\Omega(m)}d}^{H}\mathbf{w}_{r_{\Omega(m)}d} \\ & \vdots & \\ \big(\sum_{i=1}^{m} g_{im}g_{i1}\sigma_i^2\big)\mathbf{h}_{r_{\Omega(1)}d}^{H}\mathbf{w}_{r_{\Omega(1)}d} & \cdots & \big(\sum_{i=1}^{m} g_{im}g_{im}\sigma_i^2\big)\mathbf{h}_{r_{\Omega(m)}d}^{H}\mathbf{w}_{r_{\Omega(m)}d} \end{array}\right] \\
&\Bigg(\left[\begin{array}{ccccc} \mathbf{w}_{r_{\Omega(1)}d}^{H} & 0 & & \cdots & 0 \\ & & \cdots & & \\ 0 & 0 & & \cdots & \mathbf{w}_{r_{\Omega(m)}d}^{H} \end{array}\right]\left[\begin{array}{ccccc} \mathbf{h}_{r_{\Omega(1)}d}\mathbf{h}_{r_{\Omega(1)}d}^{H}+\sigma^2\mathbf{I} & \mathbf{0} & & \cdots & \mathbf{0} \\ & & \cdots & & \\ \mathbf{0} & \mathbf{0} & & \cdots & \mathbf{h}_{r_{\Omega(m)}d}\mathbf{h}_{r_{\Omega(m)}d}^{H}+\sigma^2\mathbf{I} \end{array}\right] \\
&\left[\begin{array}{ccccc} \mathbf{w}_{r_{\Omega(1)}d}^{H} & 0 & & \cdots & 0 \\ & & \cdots & & \\ 0 & 0 & & \cdots & \mathbf{w}_{r_{\Omega(m)}d}^{H} \end{array}\right]^{H}\Bigg)^{-1} \qquad (5.31)
\end{aligned}
$$

Algorithm 10 The proposed cooperative PNC scheme $(m \times m)$

%Randomly group m users and m relays that belong to set Υ and Ω, respectively

Source-relay phase

$\mathbf{y}_{sr_l} = \sum_{k=1}^{K} a_{sr_l}^{k} \mathbf{s}_k h_{sr_l,k} b_k + \mathbf{n}_{sr_l}$

% Apply MUD to obtain $\hat{b}_{r_{\Omega(l)}d,\Upsilon(k)}$

%PNC schemes

%XOR mapping at relays

$\hat{b}_{r_{\Omega(l)}d,\Upsilon(k)} \rightarrow c_{\Omega(l)}^{\Upsilon(k)}, l \in [1,m], k \in [1,m]$

$c_{\Omega(l)} = c_{\Omega(l)}^{\Upsilon(1)} \oplus c_{\Omega(l)}^{\Upsilon(2)} \oplus ... \oplus c_{\Omega(l)}^{\Upsilon(m)}, l \in [1,m], k \in [1,m]$

$b_{\Omega(l)} = 1 - 2c_{\Omega(l)}$

%Linear network coding at relays

%Design of code matrix $\mathbf{G}^{\mathrm{ML}}$

$$\mathbf{G}^{\mathrm{ML}} = \arg\min_{1 \le j \le 2^{m^2}} \left\| \begin{bmatrix} b_{\Omega(1)} \\ b_{\Omega(2)} \\ \vdots \\ b_{\Omega(m)} \end{bmatrix} - \mathbf{G}^{-1} \begin{bmatrix} \mathbf{w}_{r_{\Omega(1)}d}^{H} \mathbf{y}_{r_{\Omega(1)}d} \\ \mathbf{w}_{r_{\Omega(2)}d}^{H} \mathbf{y}_{r_{\Omega(2)}d} \\ \vdots \\ \mathbf{w}_{r_{\Omega(m)}d}^{H} \mathbf{y}_{r_{\Omega(m)}d} \end{bmatrix} \right\|^2$$

%Design of code matrix $\mathbf{G}^{\mathrm{MMSE}}$

$$\mathbf{G}^{\mathrm{MMSE}} = \arg\ \min_{\tilde{\mathbf{G}}}\ E\left\| \begin{bmatrix} b_{\Omega(1)} \\ b_{\Omega(2)} \\ \vdots \\ b_{\Omega(m)} \end{bmatrix} - \tilde{\mathbf{G}} \begin{bmatrix} \mathbf{w}_{r_{\Omega(1)}d}^{H} \mathbf{y}_{r_{\Omega(1)}d} \\ \mathbf{w}_{r_{\Omega(2)}d}^{H} \mathbf{y}_{r_{\Omega(2)}d} \\ \vdots \\ \mathbf{w}_{r_{\Omega(m)}d}^{H} \mathbf{y}_{r_{\Omega(m)}d} \end{bmatrix} \right\|^2$$

$b_{\Omega(l)} = \sum_{k=1}^{m} g_{kl}\, \hat{b}_{r_{\Omega(l)}d}^{\Upsilon(k)}$

Relay-destination phase

$\mathbf{y}_{r_\Omega d} = \sum_{l=1}^{m} \mathbf{h}_{r_{\Omega(l)}d} b_{\Omega(l)} + \mathbf{n}_{rd}$

%Apply MUD to obtain $\hat{b}_{\Omega(l)}$

Source-destination phase

$\mathbf{y}_{sd} = \sum_{k=1}^{K} a_{sd}^{k} \mathbf{s}_k h_{sd,k} b_k + \mathbf{n}_{sd}$

%Apply MUD to obtain $\hat{b}_{sd}^{\Upsilon(k)}$

%Decoding at the destination

%If XOR is adopted at relays

$\hat{c}_{\Omega(l)} = (1 - \hat{b}_{\Omega(l)})/2,\ \hat{c}_{sd}^{\Upsilon(k)} = (1 - \hat{b}_{sd}^{\Upsilon(k)})/2$

$\hat{c}^{\Upsilon(k)} = \hat{c}_{\Omega(l)} \oplus \hat{c}_{sd}^{\Upsilon(1)} \oplus ... \hat{c}_{sd}^{\Upsilon(k-1)} \oplus \hat{c}_{sd}^{\Upsilon(k+1)} ... \oplus \hat{c}_{sd}^{\Upsilon(m)}$

$\hat{b}_{\Upsilon(k)} = 1 - 2\hat{c}^{\Upsilon(k)}$

%If linear network coding is applied at relays

$$\hat{b}_{\Upsilon(k)} = \frac{\hat{b}_{\Omega(l)} - \left(g_{\Upsilon(1)\Omega(l)} \hat{b}_{sd}^{\Upsilon(1)} + ... g_{\Upsilon(k-1)\Omega(l)} \hat{b}_{sd}^{\Upsilon(k-1)} + g_{\Upsilon(k+1)\Omega(l)} \hat{b}_{sd}^{\Upsilon(k+1)} ... + g_{\Upsilon(m)\Omega(l)} \hat{b}_{sd}^{\Upsilon(m)} \right)}{g_{\Upsilon(k)\Omega(l)}}$$

The proposed cooperative PNC scheme ($m \times m$) is detailed in Algorithm 10.

5.4 Proposed Buffer-aided Cooperative PNC Scheme

In this section, we combine every m users and m relays (we focus here on the case for $m = 2$) into a group and present a buffer-aided PNC scheme, where each relay is equipped with a buffer so that the processed data can be stored and wait until the most appropriate link pair associated with the best performance for the second phase transmission is selected. Consequently, encoded data are stored at the corresponding buffer entries and are then forwarded to the destination when the appropriate time interval comes. Additionally, the destination is also equipped with a buffer so that the detected symbols from the direct transmissions can be stored. After that, the final detected symbols are consequently obtained through the PNC decoding and mapping operations at the appropriate time instant. Specifically, the size J of the buffer can be set as adjustable according to a given criterion so that the best encoded data can be selected among a large number of candidates and a shorter delay can be achieved. This design effectively increases the reliability of the transmission, reduces the bit error rate and guarantees that the most proper data are transmitted after processing at the relays.

Transmission between a selected user-relay pair ($m = 2$)

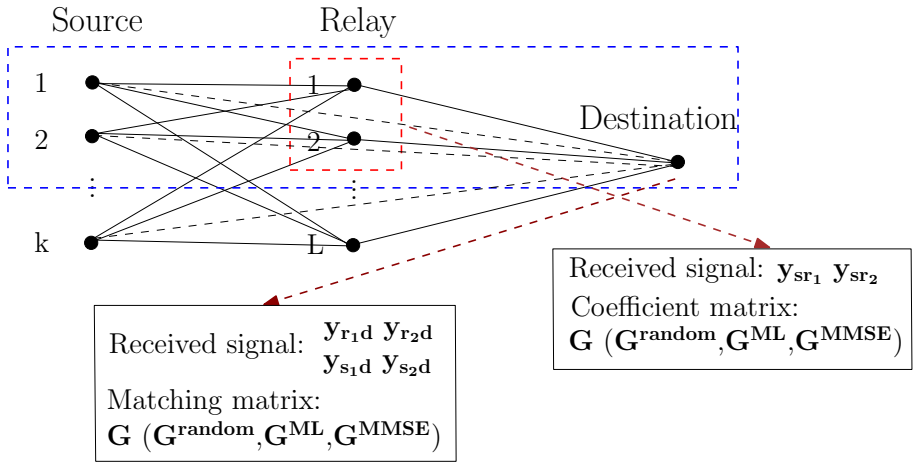

Figure 5.2: Transmission between a selected user-relay pair

In order to illustrate the transmission process with PNC schemes more precisely, we

detail the transmission between a selected user-relay pair in the proposed buffer-aided cooperative PNC scheme as shown by Fig. 5.2. At the corresponding target relays, the received signal is sent for detection and the coefficient matrix (if linear network coding technique is selected) is stored and multiplied by the corresponding detected symbols (encoding process). At the destination, the encoded signal is received and the corresponding matching matrix is applied for the purpose of decoding.

Specifically, this algorithm starts with a selection using all possible link combinations associated with all relay pairs from both source-relay and relay-destination phases. Since the bit-wise XOR operation and a linear network coding technique can be adopted, every ($m = 2$) relays are combined into a group and paired with ($m = 2$) users. Note that arbitrary numbers of users and relays can also be considered but for the sake of simplicity, we only consider $m = 2$ relays and users. Thus, since all possible link combinations are considered, their corresponding SINR are then calculated and recorded as follows:

$$\mathrm{SINR}_{sr_\Omega} = \sum_{k=1}^{K} \frac{\sum_{l=1}^{m} \mathbf{w}_{s_k r_{\Omega(l)}}^H \mathbf{h}_{s_k r_{\Omega(l)}} \mathbf{h}_{s_k r_{\Omega(l)}}^H \mathbf{w}_{s_k r_{\Omega(l)}}}{\sum_{l=1}^{m} \sum_{\substack{j=1 \\ j\neq k}}^{K} \mathbf{w}_{s_k r_{\Omega(l)}}^H \mathbf{h}_{s_j r_{\Omega(l)}} \mathbf{h}_{s_j r_{\Omega(l)}}^H \mathbf{w}_{s_k r_{\Omega(l)}} + \sum_{l=1}^{m} \sigma^2 \mathbf{w}_{s_k r_{\Omega(l)}}^H \mathbf{w}_{s_k r_{\Omega(l)}}}, \tag{5.32}$$

$$\mathrm{SINR}_{r_\Omega d} = \sum_{k=1}^{K} \frac{\sum_{l=1}^{m} (\mathbf{w}_{r_{\Omega(l)}d}^k)^H \mathbf{h}_{r_{\Omega(l)}d}^k (\mathbf{h}_{r_{\Omega(l)}d}^k)^H \mathbf{w}_{r_{\Omega(l)}d}^k}{\sum_{l=1}^{m} \sum_{\substack{j=1 \\ j\neq k}}^{K} (\mathbf{w}_{r_{\Omega(l)}d}^k)^H \mathbf{h}_{r_{\Omega(l)}d}^j (\mathbf{h}_{r_{\Omega(l)}d}^j)^H \mathbf{w}_{r_{\Omega(l)}d}^k + \sum_{l=1}^{m} \sigma^2 (\mathbf{w}_{r_{\Omega(l)}d}^k)^H \mathbf{w}_{r_{\Omega(l)}d}^k}, \tag{5.33}$$

where $\mathbf{h}_{s_k r_{\Omega(l)}} = a_{s_k r_{\Omega(l)}} \mathbf{s}_k h_{s_k r_{\Omega(l)}}$ is the effective signature vector from user k to the relay $\Omega(l)$, $\mathbf{h}_{r_{\Omega(l)}d}^k = a_{r_{\Omega(l)}d}^k \mathbf{s}_k h_{r_{\Omega(l)}d}^k$ is the effective signature vector for user k from the relay $\Omega(l)$ to the destination. In Eq. (5.32), $\mathrm{SINR}_{sr_\Omega}$ denotes the SINR for the combined paths from all users to relay set Ω, $\mathbf{w}_{s_k r_{\Omega(l)}}$ is the detector used at the relay $\Omega(l)$. When the MF is adopted at the corresponding relay, $\mathbf{w}_{s_k r_{\Omega(l)}}$ is expressed as

$$\mathbf{w}_{s_k r_{\Omega(l)}} = \mathbf{h}_{s_k r_{\Omega(l)}}. \tag{5.34}$$

Similarly, if the linear minimum mean-square error (MMSE) receiver [77] is employed at the relays, $\mathbf{w}_{s_k r_{\Omega(l)}}$ is equal to

$$\mathbf{w}_{s_k r_{\Omega(l)}} = \left(\sum_{k=1}^{K} \mathbf{h}_{s_k r_{\Omega(l)}} \mathbf{h}_{s_k r_{\Omega(l)}}^H + \sigma^2 \mathbf{I} \right)^{-1} \mathbf{h}_{s_k r_{\Omega(l)}}, \tag{5.35}$$

In (5.33), $\mathrm{SINR}_{r_\Omega d}$ represents the SINR for the combined paths from relay set Ω to the destination. The receive filter $\mathbf{w}^k_{r_{\Omega(l)}d}$ is employed by the detector used at the destination. When the MF is adopted at the destination, $\mathbf{w}^k_{r_{\Omega(l)}d}$ is expressed as

$$\mathbf{w}^k_{r_{\Omega(l)}d} = \mathbf{h}^k_{r_{\Omega(l)}d}. \tag{5.36}$$

In an analog way, if the linear MMSE receiver is employed at the relays, $\mathbf{w}^k_{r_{\Omega(l)}d}$ is

$$\mathbf{w}^k_{r_{\Omega(l)}d} = \left(\sum_{k=1}^{K} \mathbf{h}^k_{r_{\Omega(l)}d} (\mathbf{h}^k_{r_{\Omega(l)}d})^H + \sigma^2 \mathbf{I} \right)^{-1} \mathbf{h}^k_{r_{\Omega(l)}d}. \tag{5.37}$$

Both MF and MMSE receivers are considered here due to their reasonably low complexity and it should be mentioned that other detectors [78] including the ML detector can also be used.

After the calculation, we sort all these results according to a decreasing power level and choose the relay pair ($m = 2$) with the highest SINR as given by

$$\mathrm{SINR_{i,j}} = \arg \max_{\Omega \in [1,2,\ldots,L]} \{\mathrm{SINR_{sr_\Omega}}, \mathrm{SINR_{r_\Omega d}}\}, \tag{5.38}$$

where $\mathrm{SINR_{i,j}}$ denotes the highest SINR associated with the relay i and relay j. After the relay pair ($m = 2$) with the highest SINR is selected, the signal is transmitted through the corresponding channels. In this case, two different situations of the buffer mode need to be considered as follows.

Transmission mode:
If the link combinations associated with the selected relay set belongs to relay-destination phase, the buffers are turned to the transmission mode. A buffer space check needs to be conducted first to ensure the corresponding buffer entries are not empty, namely:

$$\Phi_i^{\mathrm{buffer}} \neq \varnothing,\ i \in [1, 2, ..., L], \tag{5.39}$$

and

$$\Phi_j^{\mathrm{buffer}} \neq \varnothing,\ j \in [1, 2, ..., L], \tag{5.40}$$

where Φ_i^{buffer} and Φ_j^{buffer} denote the buffers equipped at relay i and relay j. If the corresponding buffer entries are not empty, we transmit the NCS according to (5.10) or (5.19). On the other hand, if the buffer condition does not satisfy the transmission

requirement, namely, the buffer entries are empty, the selected relay pair can not help to forward the information.

In this case, we drop the current relay pair i and j and choose another relay pair with the second highest SINR as given by

$$\mathrm{SINR}_{\mathrm{i,j}}^{\mathrm{pre}} = \mathrm{SINR}_{\mathrm{i,j}} \tag{5.41}$$

$$\mathrm{SINR}_{\mathrm{u,v}} \in \max\{\mathrm{SINR}_{\mathrm{sr}_\Omega}, \mathrm{SINR}_{\mathrm{r}_\Omega\mathrm{d}}\} \setminus \mathrm{SINR}_{\mathrm{i,j}}^{\mathrm{pre}}, \tag{5.42}$$

where $\mathrm{SINR}_{\mathrm{u,v}}$ denotes the second highest SINR associated with the updated relay pair u and v. $\{\mathrm{SINR}_{\mathrm{sr}_\Omega}, \mathrm{SINR}_{\mathrm{r}_\Omega\mathrm{d}}\} \setminus \mathrm{SINR}_{\mathrm{i,j}}^{\mathrm{pre}}$ represents a complementary set, where we drop the $\mathrm{SINR}_{\mathrm{i,j}}^{\mathrm{pre}}$ from the set of SINR links $\{\mathrm{SINR}_{\mathrm{sr}_\Omega}, \mathrm{SINR}_{\mathrm{r}_\Omega\mathrm{d}}\}$. Consequently, the above process repeats until the buffer condition achieves the transmission requirement.

Reception mode:
On the other hand, if the link combination associated with the highest relay pair SINR belongs to the source-relay phase, the buffers are switched to reception mode. Similarly, a buffer space examination is operated to ensure that the corresponding buffer entries are not full. We then have

$$\Phi_i^{\mathrm{buffer}} \neq \mathrm{U},\ i \in [1, 2, ..., L], \tag{5.43}$$

and

$$\Phi_j^{\mathrm{buffer}} \neq \mathrm{U},\ j \in [1, 2, ..., L], \tag{5.44}$$

where U represents a full buffer set. If the buffers are not full, then, the sources send the data to the selected relay pair i and j according to (5.2). Otherwise, the algorithm reselects a new relay pair as in (5.41) and (5.42). The re-selection process stops when the corresponding buffer entries are not full.

At the destination, a buffer with size J is also employed. Since the direct transmission occurs when the buffers at relays are under the reception mode, the detected results that are stored in the corresponding buffer entries coming from the direct links are then adopted to help with the PNC decoding process. It should be noticed that the buffer entries at the destination are empty in accordance with the buffer conditions at the relays.

Moreover, the size J of buffers also plays an important role in the behaviour of the system performance. Specifically, when we increase the buffer size, data associated with

Algorithm 11 The proposed buffer-aided cooperative PNC scheme

% List all possible link combinations with associated relay pairs

% Select the combination with the highest SINR

$\mathrm{SINR_{i,j}} = \max\{\mathrm{SINR_{sr_\Omega}}, \mathrm{SINR_{r_\Omega d}}\}$

%Reception mode

if $\mathrm{SINR_{i,j}} \in [\mathrm{SINR_{sr_\Omega}}]$

if the buffers entries are not full

$\mathbf{y}_{sd} = \sum_{k=1}^{K} a_{sd}^{k}\mathbf{s}_k h_{sd,k} b_k + \mathbf{n}_{sd}$; $\mathbf{y}_{sr_l} = \sum_{k=1}^{K} a_{sr_l}^{k}\mathbf{s}_k h_{sr_l,k} b_k + \mathbf{n}_{sr_l}$

%Apply MUD to obtain $\hat{b}_{r_{\Omega(l)}d,\Upsilon(k)}$

%XOR operation

$\hat{b}_{r_{\Omega(l)}d,\Upsilon(k)} \rightarrow c_{\Omega(l)}^{\Upsilon(k)}, l \in [1,2], k \in [1,2]$; $c_{\Omega(l)} = c_{\Omega(l)}^{\Upsilon(1)} \oplus c_{\Omega(l)}^{\Upsilon(2)}$,

$b_{\Omega(l)} = 1 - 2c_{\Omega(l)}$

%Linear network coding scheme

$b_{\Omega(l)} = \sum_{k=1}^{2} g_{kl}\, \hat{b}_{r_{\Omega(l)}d,\Upsilon(k)}$

break

else %choose the second highest SINR

$\mathrm{SINR_{i,j}^{pre}} = \mathrm{SINR_{i,j}}$; $\mathrm{SINR_{i,j}} \in \max\{\mathrm{SINR_{sr_\Omega}}, \mathrm{SINR_{r_\Omega d}}\} \setminus \mathrm{SINR_{i,j}^{pre}}$

end

else %Transmission mode

$\mathrm{SINR_{i,j}} \in [\mathrm{SINR_{r_\Omega d}}]$

if the buffers entries are not empty

%If XOR operation is adopted at relays

$\mathbf{y}_{r_\Omega d} = \sum_{l=1}^{m} \mathbf{h}_{r_{\Omega(l)}d} b_{\Omega(l)} + \mathbf{n}_{r_\Omega d}, l = 1,2$

%Operations at the destination

$\hat{b}_{\Omega(l)} = Q((\mathbf{w}_{r_{\Omega(l)}d})^H \mathbf{y}_{r_\Omega d}), l = 1,2$; $\hat{b}_{sd}^{\Upsilon(k)} = Q((\mathbf{w}_{sd}^{\Upsilon(k)})^H \mathbf{y}_{sd}), k = 1,2$

$\hat{c}_{\Omega(l)} = (1 - \hat{b}_{\Omega(l)})/2, l = 1,2$; $\hat{c}_{sd}^{\Upsilon(k)} = (1 - \hat{b}_{sd}^{\Upsilon(k)})/2, k = 1,2$

$\hat{c}^{\Upsilon(k)} = \hat{c}_{\Omega} \oplus \hat{c}_{sd}^{\Upsilon(s)}, s \cup k = \{1,2\}, s \neq k$

$\hat{b}^{\Upsilon(k)} = 1 - 2\hat{c}^{\Upsilon(k)}, k = 1,2$

%If linear network coding is adopted at relays

$\mathbf{y}_{r_\Omega d} = \mathbf{H}_{r_\Omega d}\mathbf{G}\mathbf{b}_\Omega + \mathbf{n}_{r_\Omega d}$

%Operations at the destination

$\hat{b}_{\Omega(l)} = Q(\tilde{\mathbf{G}}(\mathbf{w}_{r_{\Omega(l)}d})^H \mathbf{y}_{r_\Omega d}), l = 1,2$

$\hat{b}_{sd}^{\Upsilon(k)} = Q((\mathbf{w}_{sd}^{\Upsilon(k)})^H \mathbf{y}_{sd}), k = 1,2$; $\hat{b}_{\Upsilon(k)} = \frac{\hat{b}_{\Omega(l)} - \left(g_{\Upsilon(s)\Omega(l)}\hat{b}_{sd}^{\Upsilon(s)}\right)}{g_{\Upsilon(k)\Omega(l)}}, s \cup k = \{1,2\}, s \neq k$

break

else%choose the second highest SINR

$\mathrm{SINR_{i,j}^{pre}} = \mathrm{SINR_{i,j}}$; $\mathrm{SINR_{i,j}} \in \max\{\mathrm{SINR_{sr_\Omega}}, \mathrm{SINR_{r_\Omega d}}\} \setminus \mathrm{SINR_{i,j}^{pre}}$

end

end

%Re-calculated the SINR for different link combinations and

repeat the above process

better channel conditions can be selected as a relatively larger candidate pool is generated. Therefore, extra degrees of freedom in the system are also available. Conversely, a shorter delay can be obtained when we reduce the buffer size. In practice, the performance highly depends on the buffer size J, the number of users K and the accuracy of the detection process at the relays.

The proposed buffer-aided cooperative PNC scheme is detailed in Algorithm 11

5.5 Greedy Relay Pair Selection Technique

In this section, we introduce a greedy relay pair selection technique that can approach the performance of the exhaustive relay pair search with a reasonably lower computational cost. Traditionally, the exhaustive search examines all possible link combinations between both the source-relay phase and the relay-destination phase so that the optimum relay pair with the highest SINR can be obtained. In particular, with L relays ($L/2$ relay pairs if L is an even number) equipped in the cooperative system, a cost of $2C_L^2 = L(L-1)$ link combinations need to be considered. Clearly, a considerable computational complexity can not be avoided when large number of relays are participated in the transmission. Motivated by this fact, we then propose the following greedy relay pair selection technique that can achieve a good balance between the system performance and the computational complexity.

This algorithm starts with single relay selection where we evaluate the SINR for each of the relays with its associated link combinations between both the source-relay phase and relay-destination phase as given by

$$\mathrm{SINR}_{sr_p} = \sum_{k=1}^{K} \frac{\mathbf{w}_{s_k r_p}^H \mathbf{h}_{s_k r_p} \mathbf{h}_{s_k r_p}^H \mathbf{w}_{s_k r_p}}{\sum\limits_{\substack{j=1 \\ j\neq k}}^{K} \mathbf{w}_{s_k r_p}^H \mathbf{h}_{s_j r_p} \mathbf{h}_{s_j r_p}^H \mathbf{w}_{s_k r_p} + \sigma^2 \mathbf{w}_{s_k r_p}^H \mathbf{w}_{s_k r_p}}, \tag{5.45}$$

$$\mathrm{SINR}_{r_p d} = \sum_{k=1}^{K} \frac{(\mathbf{w}_{r_p d}^k)^H \mathbf{h}_{r_p d}^k (\mathbf{h}_{r_p d}^k)^H \mathbf{w}_{r_p d}^k}{\sum\limits_{\substack{j=1 \\ j\neq k}}^{K} (\mathbf{w}_{r_p d}^k)^H \mathbf{h}_{r_p d}^j (\mathbf{h}_{r_p d}^j)^H \mathbf{w}_{r_p d}^k + \sigma^2 (\mathbf{w}_{r_p d}^k)^H \mathbf{w}_{r_p d}^k}, \tag{5.46}$$

where SINR_{sr_p} and SINR_{r_pd} denote the SINR from the source to an arbitrary relay p and from relay p to the destination, respectively.$\mathbf{w}_{s_k r_p}$ and $\mathbf{w}_{r_p d}^{k}$ are the receiver filters for user k from the source to relay p and from the relay p to the destination, respectively.

We then select the link combination with the highest SINR and its associated relay q is recorded as the base relay and given by

$$\mathrm{SINR}_{\mathrm{q}}^{\mathrm{base}} = \arg \max_{p\in[1,2,...,L]} \{\mathrm{SINR}_{\mathrm{sr_p}}, \mathrm{SINR}_{\mathrm{r_pd}}\}. \tag{5.47}$$

After that, all possible $L-1$ candidate relay pair (contains relay q) are listed as $\Omega_{p,q}$, where $p \in [1, L], p \neq q$. We then calculate the SINR for these $L-1$ relay pairs ($2(L-1)$ link combinations) according to (5.32) and (5.33). Consequently, the optimum relay pair $\Omega_{n,q}$ with the highest SINR is selected through (5.38). Finally, the signal is sent according to the corresponding current buffer state.

Transmission mode:
When the buffer state is under the transmission mode, a buffer space check is required firstly to guarantee that the corresponding buffer entries are not empty. Thus We have,

$$\Omega_n^{\mathrm{buffer}} \neq \varnothing,\ n \in [1, 2, ..., L], \tag{5.48}$$

and

$$\Omega_q^{\mathrm{buffer}} \neq \varnothing,\ q \in [1, 2, ..., L], \tag{5.49}$$

where $\Omega_n^{\mathrm{buffer}}$ and $\Omega_q^{\mathrm{buffer}}$ represents the buffer n and the buffer q associated with the relay pair $\Omega_{n,q}$. In this case, the NCS is sent via the selected relay buffer entries to the destination according to either (5.10) or (5.19). Conversely, if the buffer space check is not successful, which, indicates that current empty buffer entries are not capable of forwarding the NCS from the selected relays to the destination, thus, we have to replace the current relay pair by the one that has the highest SINR among the remaining $L-2$ candidates pool as given by

$$\mathrm{SINR}_{\mathrm{m,q}} = \arg \max_{\substack{p\neq n,q \\ p\in[1,2,...,L]}} \{\mathrm{SINR}_{\mathrm{p,q}}\}, \tag{5.50}$$

The algorithm then repeats with the newly generated relay pair $\Omega_{m,q}$. However, if all remaining candidate relay pair $\Omega_{p,q}$ ($p \neq q, p \in [1, L]$) are not available, we have to update the base relay as given by

$$\mathrm{SINR}_{\mathrm{q}}^{\mathrm{pre}} = \mathrm{SINR}_{\mathrm{q}}^{\mathrm{base}}, \tag{5.51}$$

Algorithm 12 The proposed greedy relay pair selection algorithm for buffer-aided PNC

%Choose a single relay with the highest SINR that

corresponds to a specific base relay q

$\mathrm{SINR}_{\mathrm{q}}^{\mathrm{base}} = \max\{\mathrm{SINR}_{\mathrm{sr_p}}, \mathrm{SINR}_{\mathrm{r_p d}}\}, p \in [1, L]$

For $\mathrm{p} = 1 : \mathrm{L}$ % all relay pairs associated with relay q

if $\mathrm{p} \neq \mathrm{q}$

$\Omega_{\mathrm{relaypair}} = [\mathrm{p}, \mathrm{q}]$

% when the links belong to the source-relay phase

$$\mathrm{SINR}_{sr_{p,q}} = \sum_{k=1}^{K} \frac{\mathbf{w}_{s_k r_p}^H \mathbf{h}_{s_k r_p} \mathbf{h}_{s_k r_p}^H \mathbf{w}_{s_k r_p} + \mathbf{w}_{s_k r_q}^H \mathbf{h}_{s_k r_q} \mathbf{h}_{s_k r_q}^H \mathbf{w}_{s_k r_q}}{\sum\limits_{\substack{j=1 \\ j \neq k}}^{K} \mathbf{w}_{s_k r_p}^H \mathbf{h}_{s_j r_p} \mathbf{h}_{s_j r_p}^H \mathbf{w}_{s_k r_p} + \sum\limits_{\substack{j=1 \\ j \neq k}}^{K} \mathbf{w}_{s_k r_q}^H \mathbf{h}_{s_j r_q} \mathbf{h}_{s_j r_q}^H \mathbf{w}_{s_k r_q} + \sigma^2 \mathbf{w}_{s_k r_p}^H \mathbf{w}_{s_k r_p} + \sigma^2 \mathbf{w}_{s_k r_q}^H \mathbf{w}_{s_k r_q}}$$

% when the links belong to the relay-destination phase

$$\mathrm{SINR}_{r_{p,q}d} = \sum_{k=1}^{K} \frac{(\mathbf{w}_{r_p d}^k)^H \mathbf{h}_{r_p d}^k (\mathbf{h}_{r_p d}^k)^H \mathbf{w}_{r_p d}^k + (\mathbf{w}_{r_q d}^k)^H \mathbf{h}_{r_q d}^k (\mathbf{h}_{r_q d}^k)^H \mathbf{w}_{r_q d}^k}{\sum\limits_{\substack{j=1 \\ j \neq k}}^{K} (\mathbf{w}_{r_p d}^k)^H \mathbf{h}_{r_p d}^j (\mathbf{h}_{r_p d}^j)^H \mathbf{w}_{r_p d}^k + \sum\limits_{\substack{j=1 \\ j \neq k}}^{K} (\mathbf{w}_{r_q d}^k)^H \mathbf{h}_{r_q d}^j (\mathbf{h}_{r_q d}^j)^H \mathbf{w}_{r_q d}^k + \sigma^2 (\mathbf{w}_{r_p d}^k)^H \mathbf{w}_{r_p d}^k + \sigma^2 (\mathbf{w}_{r_q d}^k)^H \mathbf{w}_{r_q d}^k}$$

% record and calculated the SINR for all relay pairs

end

end

$\mathrm{SINR}_{\mathrm{n,q}} = \max\{\mathrm{SINR}_{sr_{p,q}}, \mathrm{SINR}_{r_{p,q}d}\}$

if%Reception mode

if the buffers entries are not full

$\mathbf{y}_{sd} = \sum_{k=1}^{K} a_{sd}^k \mathbf{s}_k h_{sd,k} b_k + \mathbf{n}_{sd}$; $\mathbf{y}_{sr_l} = \sum_{k=1}^{K} a_{sr_l}^k \mathbf{s}_k h_{sr_l,k} b_k + \mathbf{n}_{sr_l}$ $(l = n, q)$

%Apply the detectors at relay n and relay q for detection

and store the detected symbols in the corresponding buffer entries

else %choose another relay with the second highest SINR

$\mathrm{SINR}_{\mathrm{q}}^{\mathrm{pre}} = \mathrm{SINR}_{\mathrm{q}}^{\mathrm{base}}$; $\mathrm{SINR}_{\mathrm{q}}^{\mathrm{base}} \in \max\{\mathrm{SINR}_{\mathrm{sr_p}}, \mathrm{SINR}_{\mathrm{r_p d}}\} \setminus \mathrm{SINR}_{\mathrm{q}}^{\mathrm{pre}}$

%Repeat the above greedy relay pair selection process

end

else%Transmission mode

if the buffers entries are not empty

% XOR mapping applied at selected relays

$\mathbf{y}_{r_\Omega d} = \sum_{l=1}^{m} \mathbf{h}_{r_{\Omega(l)} d} b_{\Omega(l)} + \mathbf{n}_{r_\Omega d}$

%Linear network coding applied at selected relays

$\mathbf{y}_{r_\Omega d} = \mathbf{H}_{r_\Omega d} \mathbf{G} \mathbf{b}_\Omega + \mathbf{n}_{r_\Omega d}$

%Apply the detectors at the destination for detection and decoding

else%choose another link with the second highest SINR

$\mathrm{SINR}_{\mathrm{q}}^{\mathrm{pre}} = \mathrm{SINR}_{\mathrm{q}}^{\mathrm{base}}$; $\mathrm{SINR}_{\mathrm{q}}^{\mathrm{base}} \in \max\{\mathrm{SINR}_{\mathrm{sr_p}}, \mathrm{SINR}_{\mathrm{r_p d}}\} \setminus \mathrm{SINR}_{\mathrm{q}}^{\mathrm{pre}}$

%Repeat the above greedy relay pair selection process

end

end

%Repeat the above greedy relay pair selection process

$$\mathrm{SINR}_{\mathrm{q}}^{\mathrm{base}} = \max\{\mathrm{SINR}_{\mathrm{sr_p}}, \mathrm{SINR}_{\mathrm{r_pd}}\} \setminus \mathrm{SINR}_{\mathrm{q}}^{\mathrm{pre}}, \tag{5.52}$$

where $\{\mathrm{SINR}_{\mathrm{sr_p}}, \mathrm{SINR}_{\mathrm{r_pd}}\} \setminus \mathrm{SINR}_{\mathrm{q}}^{\mathrm{pre}}$ denotes a complementary set where we drop the $\mathrm{SINR}_{\mathrm{q}}^{\mathrm{pre}}$ from the link SINR set $\{\mathrm{SINR}_{\mathrm{sr_p}}, \mathrm{SINR}_{\mathrm{r_pd}}\}$. After this selection process, we repeat the above process and a new relay pair is chosen consequently. The corresponding transmission procedure then repeats according to the buffer status.

Reception mode:

When the buffer state is switched to the reception mode, similarly, a buffer space check needs to be performed initially to ensure the corresponding buffer entries are not full so that the storage of data is still available, namely, we have,

$$\Omega_n^{\mathrm{buffer}} \neq \mathrm{U},\ n \in [1, 2, ..., L], \tag{5.53}$$

and

$$\Omega_q^{\mathrm{buffer}} \neq \mathrm{U},\ q \in [1, 2, ..., L], \tag{5.54}$$

where U represents a full buffer set. In this case, if the buffers are not full, the sources then send the data to the selected relay pair $\Omega_{n,q}$ according to (5.2). Otherwise, the algorithm stops and then re-select a new relay pair according to (5.50), (5.51) and (5.52).

The greedy relay pair selection algorithm is show in Algorithm 12.

5.6 Analysis of the Proposed Algorithms

In this section, we analyse the computational complexity required by the proposed relay pair selection algorithm together with the novel linear network coding designs.

5.6.1 Computational Complexity

In the proposed schemes, there are several design parts that cause the computational complexity, namely, the proposed relay pair selection algorithms and the various linear network coding processing at relays.

Table 5.1: Computational complexity required by relay pair selection and linear network coding schemes

Processing	Algorithm	Flops
Relay pair selection	Exhaustive Search	$88K^2NL^2 - 24KNL^2 - 88K^2NL + 24KNL$ $-16K^2L^2 + 4KL^2 + 16K^2L - 4KL$
Relay pair selection	Greedy Search	$176K^2NL - 48KNL - 176K^2N + 48KN$ $-32K^2L + 8KL + 32K^2 - 8K$
Linear network coding	With $\mathbf{G}^{\mathrm{opt}}$	$2^{m^2}(8m^3 + 8Nm + 7m)$
Linear network coding	With $\mathbf{G}^{\mathrm{MMSE}}$	$21m^3 + 8m^2N - m^2 + 2m + 6mN^2$

For the relay sets selection algorithms, we calculate the combination SINR for every relay set and use the SINR as the selection criterion. We adopt both the exhaustive search and greedy relay selection approach for the purpose of comparison. Specifically, when L relays participate in the transmission, $L/2$ relay sets are generated as we combine every two relays into a group, thus, the total number of relay pairs that we have to examine when an exhaustive search is conducted is $C_L^2 = L(L-1)/2$. On the other hand, for the proposed greedy relay pair selection algorithm, it explores a moderate to large number of relay pairs per each stage, since this selection stops once the corresponding buffer entries satisfy the current system requirement (transmission mode or reception mode), a maximum number of relay pairs of $(L-1)+(L-2)+...+1 = L(L-1)/2$ is required. It should be noticed that when calculating the associated SINR, the calculation flops need to be doubled as the selection is performed in both source-relay links and relay-destination links. These results are summarized in Table 5.1.

Applying the proposed linear network coding techniques at each relay also introduces extra computational complexity. For these techniques, the process for obtaining $\mathbf{G}^{\mathrm{ML}}$ and $\mathbf{G}^{\mathrm{MMSE}}$ occupies most of the calculation flops as detailed in Table 5.1.

Clearly, it can be seen from the table that the proposed greedy relay pair selection algorithm is an order of magnitude less costly when compared with the exhaustive search. Additionally, the size of the matrix $\mathbf{G}$ mainly determines the complexity when introducing $\mathbf{G}^{\mathrm{ML}}$ and $\mathbf{G}^{\mathrm{MMSE}}$ into the linear network coding techniques.

5.6.2 Sum Rate Analysis

The sum rate is an important parameter to evaluate the system performance and it is usually measured according to the source, channel relay and destination parameters of a given system. Thus, in the following, we analyzed the sum rate of the proposed buffer-aided cooperative PNC schemes and algorithms.

The buffer-aided cooperative DS-CDMA system with simple DF

We first investigate the sum rate of a cooperative DS-CDMA system that employs a buffer with size J at each of the relays and a simple DF protocol is considered. The sum rate of a given system is, however, upper bounded by the system capacity. In this context, the capacity of a buffer-aided cooperative DS-CDMA system with simple DF adopted is given by [12, 91]

$$C_{DF} = \max\ I_{DF}(\mathbf{b};\mathbf{y}) = \frac{1}{N+N(J+1)} \min\{I_{DF}^{sr},\ I_{DF}^{sd,rd}\}. \tag{5.55}$$

Conversely, the sum rate of the buffer-aided cooperative DS-CDMA system can be expressed as

$$R \leq C_{DF} = \frac{1}{N+N(J+1)} \min\{I_{DF}^{sr},\ I_{DF}^{sd,rd}\}. \tag{5.56}$$

For the mutual information between the source and selected relays ($m = 2$), we have [91]

$$\begin{aligned} I_{DF}^{sr} &= I_{DF}(\mathbf{b}_k^{sr};\mathbf{y}_{sr} \mid \mathbf{H}_{sr}) \\ &= E[\log\det(\sigma^2\mathbf{I}_{2N} + \mathbf{H}_{sr}\mathbf{Q}\mathbf{H}_{sr}^H)], \end{aligned} \tag{5.57}$$

where $\mathbf{H}_{sr}$ represents a $2N \times 2K$ channel matrix between the source and the selected relays $\Omega(l)$ and $\Omega(s)$ ($l \neq s$) as given by

$$\mathbf{H}_{sr} = \begin{bmatrix} \mathbf{H}_{sr_{\Omega(l)}} & \mathbf{0} \\ \mathbf{0} & \mathbf{H}_{sr_{\Omega(s)}} \end{bmatrix}. \tag{5.58}$$

The matrix $\mathbf{H}_{sr_{\Omega(l)}}$ denotes the $N \times K$ channel matrix between the sources and the relay $\Omega(l)$, $\mathbf{y}_{sr} = [\mathbf{y}_{sr_{\Omega(l)}}^T, \mathbf{y}_{sr_{\Omega(s)}}^T]^T$ is the $2N \times 1$ received signal vector with zero mean and covariance as given by

$$\begin{aligned} E[\mathbf{y}_{sr}\mathbf{y}_{sr}^H] &= E[(\mathbf{H}_{sr}\mathbf{b}_k + \mathbf{n}_{sr})(\mathbf{H}_{sr}\mathbf{b}_k + \mathbf{n}_{sr})^H] \\ &= E[\mathbf{H}_{sr}\mathbf{b}_k^{sr}(\mathbf{b}_k^{sr})^H(\mathbf{H}_{sr})^H + \mathbf{n}_{sr}(\mathbf{n}_{sr})^H] \\ &= \mathbf{H}_{sr}\mathbf{Q}(\mathbf{H}_{sr})^H + \sigma^2\mathbf{I}_{2N}. \end{aligned} \tag{5.59}$$

Thus, $\mathbf{Q} = E[\mathbf{b}_k^{sr}(\mathbf{b}_k^{sr})^H]$ is the covariance matrix of the transmitted symbols, $\mathbf{b}_k^{sr} = [(\mathbf{b}_k^{sr_{\Omega(l)}})^T, (\mathbf{b}_k^{sr_{\Omega(s)}})^T]^T$ is the $2K \times 1$ transmitted symbols ($\mathbf{b}_k^{sr_{\Omega(l)}} = \mathbf{b}_k^{sr_{\Omega(s)}}$).

Moreover, for the mutual information between the source (including the selected relays) and the destination, we have

$$\begin{aligned} I_{DF}^{sd,rd} &= I_{DF}(\mathbf{b}_k^{sd,rd}; \mathbf{y}_{sd,rd}) \\ &= E\Big[\log\,(1 + \sum_{k=1}^{K} \mathrm{SINR}_{sd}^k + \sum_{l=1}^{m}\sum_{k=1}^{K} \mathrm{SINR}_{r_{\Omega(l)}d}^k)\Big] \\ &= E\Big[\log\,(1 + \sum_{k=1}^{K} \frac{(\mathbf{w}_{sd,k})^H \mathbf{h}_{sd,k}(\mathbf{h}_{sd,k})^H \mathbf{w}_{sd,k}}{\sum\limits_{\substack{p=1 \\ p\neq k}}^{K} (\mathbf{w}_{sd,k})^H \mathbf{h}_{sd,p}(\mathbf{h}_{sd,p})^H \mathbf{w}_{sd,k} + \sigma^2 (\mathbf{w}_{sd,k})^H \mathbf{w}_{sd,k}} \\ &+ \sum_{l=1}^{m}\sum_{k=1}^{K} \frac{(\mathbf{w}_{r_{\Omega(l)}d}^k)^H \mathbf{h}_{r_{\Omega(l)}d}^k (\mathbf{h}_{r_{\Omega(l)}d}^k)^H \mathbf{w}_{r_{\Omega(l)}d}^k}{\sum\limits_{\substack{p=1 \\ p\neq k}}^{K} (\mathbf{w}_{r_{\Omega(l)}d}^k)^H \mathbf{h}_{r_{\Omega(l)}d}^p (\mathbf{h}_{r_{\Omega(l)}d}^p)^H \mathbf{w}_{r_{\Omega(l)}d}^k + \sigma^2 (\mathbf{w}_{r_{\Omega(l)}d}^k)^H \mathbf{w}_{r_{\Omega(l)}d}^k})\Big], \end{aligned} \tag{5.60}$$

where $\mathbf{b}_k^{sd,rd} = [(\mathbf{b}_k^{sd})^T, (\hat{\mathbf{b}}_k^{rd})^T]^T$ is the $2K \times 1$ vector for the input symbols and $\mathbf{y}_{sd,rd} = [\mathbf{y}_{sd}^T, \mathbf{y}_{rd}^T]^T$ is the $2N \times 1$ received signal vector. The last summation term $\sum\limits_{l=1}^{m}\sum\limits_{k=1}^{K} \mathrm{SINR}_{r_{\Omega(l)}d}^k$ represents the overall SINR for all users that come from the selected relay pair Ω to the destination.

Thus, the sum rate of the scenario under consideration is given by

$$\begin{aligned} R &\leq \frac{1}{N + N(J+1)} \min\,\{I_{DF}^{sr},\ \ I_{DF}^{sd,rd}\} \\ &= \frac{1}{N + N(J+1)} \min\,\{\ E[\log\det(\sigma^2 \mathbf{I}_{2N}\ +\ \mathbf{H}_{sr}\mathbf{Q}\mathbf{H}_{sr}^H)], \\ &E\Big[\log\,(1 + \sum_{k=1}^{K} \frac{(\mathbf{w}_{sd,k})^H \mathbf{h}_{sd,k}(\mathbf{h}_{sd,k})^H \mathbf{w}_{sd,k}}{\sum\limits_{\substack{p=1 \\ p\neq k}}^{K} (\mathbf{w}_{sd,k})^H \mathbf{h}_{sd,p}(\mathbf{h}_{sd,p})^H \mathbf{w}_{sd,k} + \sigma^2 (\mathbf{w}_{sd,k})^H \mathbf{w}_{sd,k}} \\ &+ \sum_{l=1}^{m}\sum_{k=1}^{K} \frac{(\mathbf{w}_{r_{\Omega(l)}d}^k)^H \mathbf{h}_{r_{\Omega(l)}d}^k (\mathbf{h}_{r_{\Omega(l)}d}^k)^H \mathbf{w}_{r_{\Omega(l)}d}^k}{\sum\limits_{\substack{p=1 \\ p\neq k}}^{K} (\mathbf{w}_{r_{\Omega(l)}d}^k)^H \mathbf{h}_{r_{\Omega(l)}d}^p (\mathbf{h}_{r_{\Omega(l)}d}^p)^H \mathbf{w}_{r_{\Omega(l)}d}^k + \sigma^2 (\mathbf{w}_{r_{\Omega(l)}d}^k)^H \mathbf{w}_{r_{\Omega(l)}d}^k})\Big]\}. \end{aligned} \tag{5.61}$$

Thus, when referring to a cooperative DS-CDMA system that has two transmission phases, employs a DF protocol without the employment of buffers ($J = 0$), the factor multiplying the minimum of the terms should be $1/2N$, while in a simple cooperative

system without buffers and without spreading sequences (N=1), the factor is equal to $1/2$.

The buffer-aided cooperative DS-CDMA system with PNC

In this section, since we develop a buffer-aided cooperative DS-CDMA system with PNC techniques employed during the relay-destination phase, we therefore investigate the corresponding sum rate in the following.

In particular, when XOR is applied at the selected relays, the SINR for the NCS from the $\Omega(l)$-th relay to the destination is given by

$$\mathrm{SINR}_{r_{\Omega(l)}d} = \frac{\mathbf{w}_{r_{\Omega(l)}d}^H \mathbf{h}_{r_{\Omega(l)}d} \mathbf{h}_{r_{\Omega(l)}d}^H \mathbf{w}_{r_{\Omega(l)}d}}{\sigma^2 \mathbf{w}_{r_{\Omega(l)}d}^H \mathbf{w}_{r_{\Omega(l)}d}} \tag{5.62}$$

Thus, the sum rate for the corresponding system is given by

$$\begin{aligned}
R &\leq \frac{1}{N+N(J+1)} \min\{I_{DF}^{sr},\ I_{DF}^{sd,rd}\} \\
&= \frac{1}{N+N(J+1)} \min\{\ E[\log\det(\sigma^2\mathbf{I}_{2N} + \mathbf{H}_{sr}\mathbf{Q}\mathbf{H}_{sr}^H)], \\
&E\Big[\log\big(1+\sum_{k=1}^{K}\mathrm{SINR}_{sd}^k + \sum_{l=1}^{m}\mathrm{SINR}_{r_{\Omega(l)}d}\big)\Big] \\
&= \frac{1}{N+N(J+1)} \min\{\ E[\log\det(\sigma^2\mathbf{I}_{2N} + \mathbf{H}_{sr}\mathbf{Q}\mathbf{H}_{sr}^H)], \\
&E\Big[\log\big(1+\sum_{k=1}^{K}\frac{(\mathbf{w}_{sd,k})^H\mathbf{h}_{sd,k}(\mathbf{h}_{sd,k})^H\mathbf{w}_{sd,k}}{\sum\limits_{\substack{p=1\\p\neq k}}^{K}(\mathbf{w}_{sd,k})^H\mathbf{h}_{sd,p}(\mathbf{h}_{sd,p})^H\mathbf{w}_{sd,k}+\sigma^2(\mathbf{w}_{sd,k})^H\mathbf{w}_{sd,k}} \\
&+\sum_{l=1}^{m}\frac{\mathbf{w}_{r_{\Omega(l)}d}^H\mathbf{h}_{r_{\Omega(l)}d}\mathbf{h}_{r_{\Omega(l)}d}^H\mathbf{w}_{r_{\Omega(l)}d}}{\sigma^2\mathbf{w}_{r_{\Omega(l)}d}^H\mathbf{w}_{r_{\Omega(l)}d}})\Big]\},
\end{aligned} \tag{5.63}$$

where the last summation term $\sum\limits_{l=1}^{m}\mathrm{SINR}_{r_{\Omega(l)}d}$ denotes the overall SINR for all NCS that received from the selected relay pair Ω to the destination. When linear network coding is applied at the destination, the NCS is the linear combination of the detected symbols at the output of relay $\Omega(l)$, consequently, the SINR for the corresponding NCS from the $\Omega(l)$-th relay to the destination is obtained as given by

$$\mathrm{SINR}_{r_{\Omega(l)}d} = \frac{\sum\limits_{k=1}^{K} g_{k\Omega(l)}^2 \mathbf{w}_{r_{\Omega(l)}d}^H \mathbf{h}_{r_{\Omega(l)}d} \mathbf{h}_{r_{\Omega(l)}d}^H \mathbf{w}_{r_{\Omega(l)}d}}{\sigma^2 \mathbf{w}_{r_{\Omega(l)}d}^H \mathbf{w}_{r_{\Omega(l)}d}} \tag{5.64}$$

Similarly, the sum rate for the cooperative system when linear network coding is employed at the relays is expressed as given by

$$\begin{aligned} R &\leq \frac{1}{N+N(J+1)} \min\{I_{DF}^{sr},\ I_{DF}^{sd,rd}\} \\ &= \frac{1}{N+N(J+1)} \min\{\ E[\log\det(\sigma^2\mathbf{I}_{2N}\ +\ \mathbf{H}_{sr}\mathbf{Q}\mathbf{H}_{sr}^H)], \\ &E\Big[\log\,(1+\sum_{k=1}^{K}\mathrm{SINR}_{sd}^{k}+\sum_{l=1}^{m}\mathrm{SINR}_{r_{\Omega(l)}d})\Big] \\ &= \frac{1}{N+N(J+1)} \min\{\ E[\log\det(\sigma^2\mathbf{I}_{2N}\ +\ \mathbf{H}_{sr}\mathbf{Q}\mathbf{H}_{sr}^H)], \\ &E\Big[\log\,(1+\sum_{k=1}^{K}\frac{(\mathbf{w}_{sd,k})^H\mathbf{h}_{sd,k}(\mathbf{h}_{sd,k})^H\mathbf{w}_{sd,k}}{\sum\limits_{\substack{p=1\\p\neq k}}^{K}(\mathbf{w}_{sd,k})^H\mathbf{h}_{sd,p}(\mathbf{h}_{sd,p})^H\mathbf{w}_{sd,k}+\sigma^2(\mathbf{w}_{sd,k})^H\mathbf{w}_{sd,k}} \\ &+\sum_{l=1}^{m}\frac{\sum\limits_{k=1}^{K}g_{k\Omega(l)}^2\mathbf{w}_{r_{\Omega(l)}d}^H\mathbf{h}_{r_{\Omega(l)}d}\mathbf{h}_{r_{\Omega(l)}d}^H\mathbf{w}_{r_{\Omega(l)}d}}{\sigma^2\mathbf{w}_{r_{\Omega(l)}d}^H\mathbf{w}_{r_{\Omega(l)}d}})\Big]\}. \end{aligned} \tag{5.65}$$

Similarly, the last summation term $\sum_{l=1}^{m}\mathrm{SINR}_{r_{\Omega(l)}d}$ is the overall SINR for all NCS that received from the selected relay pair Ω to the destination.

5.7 Simulations

In this section, a simulation study of the proposed buffer-aided PNC techniques for cooperative systems is carried out. The DS-CDMA network uses randomly generated spreading codes of length $N = 16$. The corresponding channel coefficients are modelled as complex Gaussian random variables.We assume perfectly known channels at the receivers and we also present an example with channel estimation. Equal power allocation is employed. We consider packets with 1000 QPSK (BPSK) symbols and average the curves over 1000 trials. Linear MMSE receiver is employed at both the relays and destination for detection purposes. We consider fixed buffer-aided exhaustive/greedy (FBAE/FBAG) relay pair selection strategies (RPS) and non buffer-aided exhaustive/greedy (NBAE/NBAG) RPS. For network coding techniques, we test both XOR mapping and linear network coding schemes with different designs of the matrix **G** that are used at both the relays and destination for the purpose of encoding and

decoding.

BER versus SNR performance

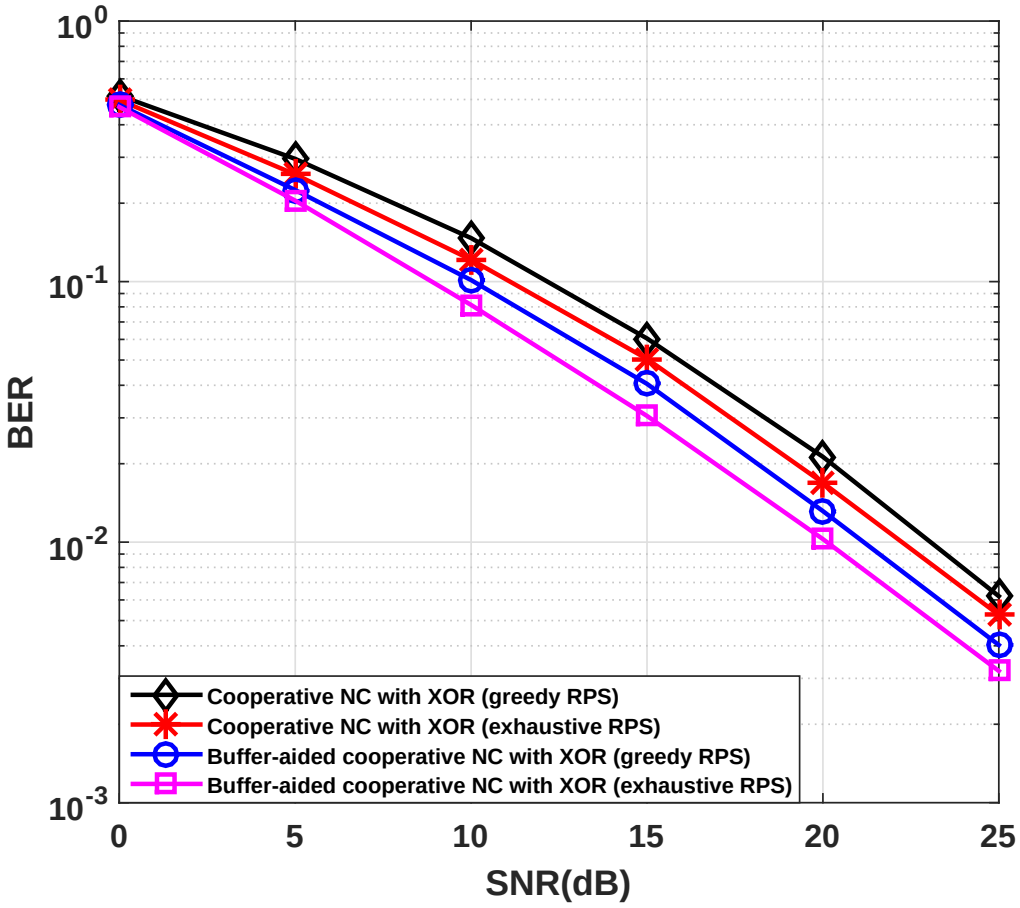

Figure 5.3: Performance comparison for buffer-aided and non buffer-aided cooperative transmissions with XOR and different RPS

In order to verify that the proposed buffer-aided cooperative PNC scheme with relay selection algorithms contributes to the performance gain, we compare the performance between the situations of the transmission with fixed size buffers ($J = 4$) and without buffers that employ different RPS in Fig. 5.3 and Fig. 5.4.

The first example shown in Fig. 5.3 illustrates the performance comparison between the proposed buffer-aided cooperative transmission with XOR mapping and different RPS and non buffer-aided cooperative transmission with XOR mapping and different RPS.

$K = 6$ users and $L = 6$ relays are adopted for a cooperative DS-CDMA system and QPSK modulation is employed. The simulation results show that a good performance gain is achieved with the introduction of the buffers. As for the RPS problem, the curves suggest that the greedy RPS can approach the exhaustive RPS with a relatively lower computational cost.

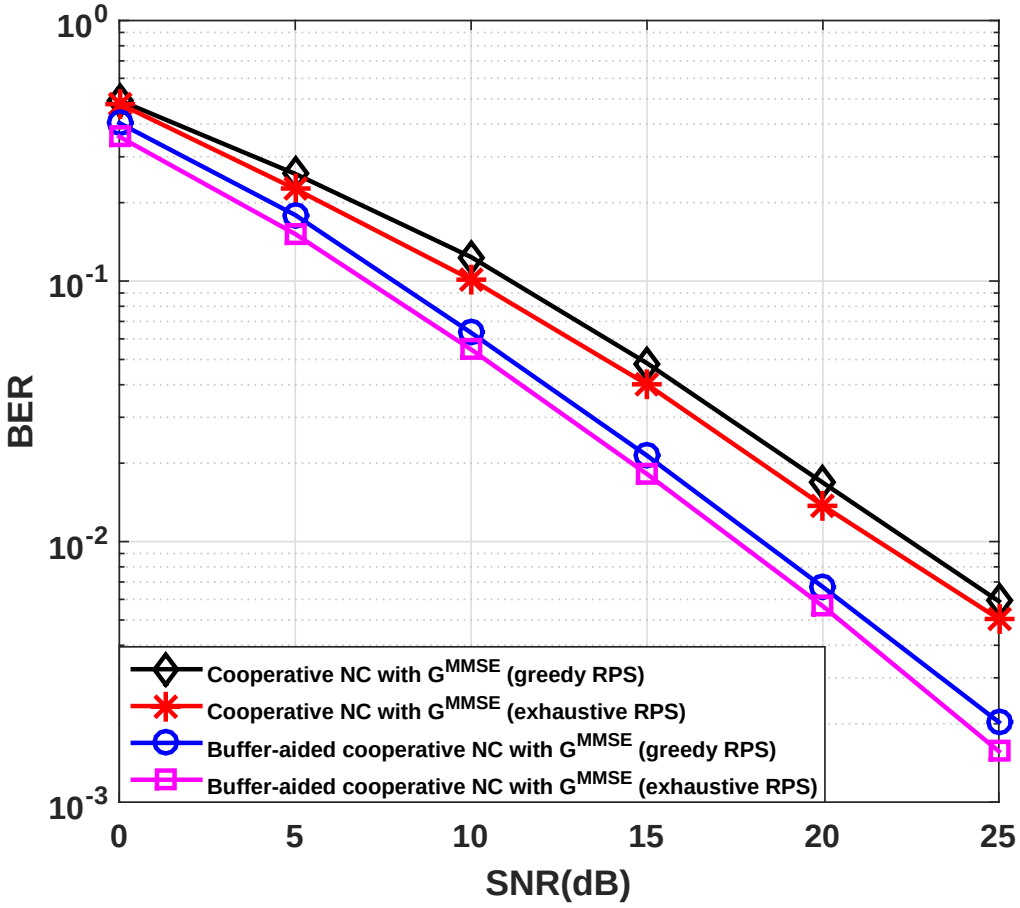

Figure 5.4: Performance comparison for buffer-aided and non buffer-aided cooperative transmissions with linear network coding and different RPS

Another example depicted in Fig. 5.4 compares the performance comparison between the proposed buffer-aided cooperative transmission with linear network coding and different RPS and non buffer-aided cooperative transmission with linear network coding and different RPS. Similarly, we have $K = 6$ users and $L = 6$ relays, QPSK modulation is employed. Clearly, with $\mathbf{G}^{\text{random}}$ applied at the relays and $\mathbf{G}^{\text{MMSE}}$ employed at the destination, the overall system performance improves when compared with Fig. 5.3 where simple XOR mapping is used. Additionally, the simulation results also reveal that

the buffer-aided designs perform better than the non-buffer aided ones. Therefore, a good balance between the BER performance and average delay can be obtained if the buffer size is carefully adjusted. Moreover, the greedy RPS can approach the exhaustive RPS quite closely, whist keeping the computational complexity reasonably low for practical utilization.

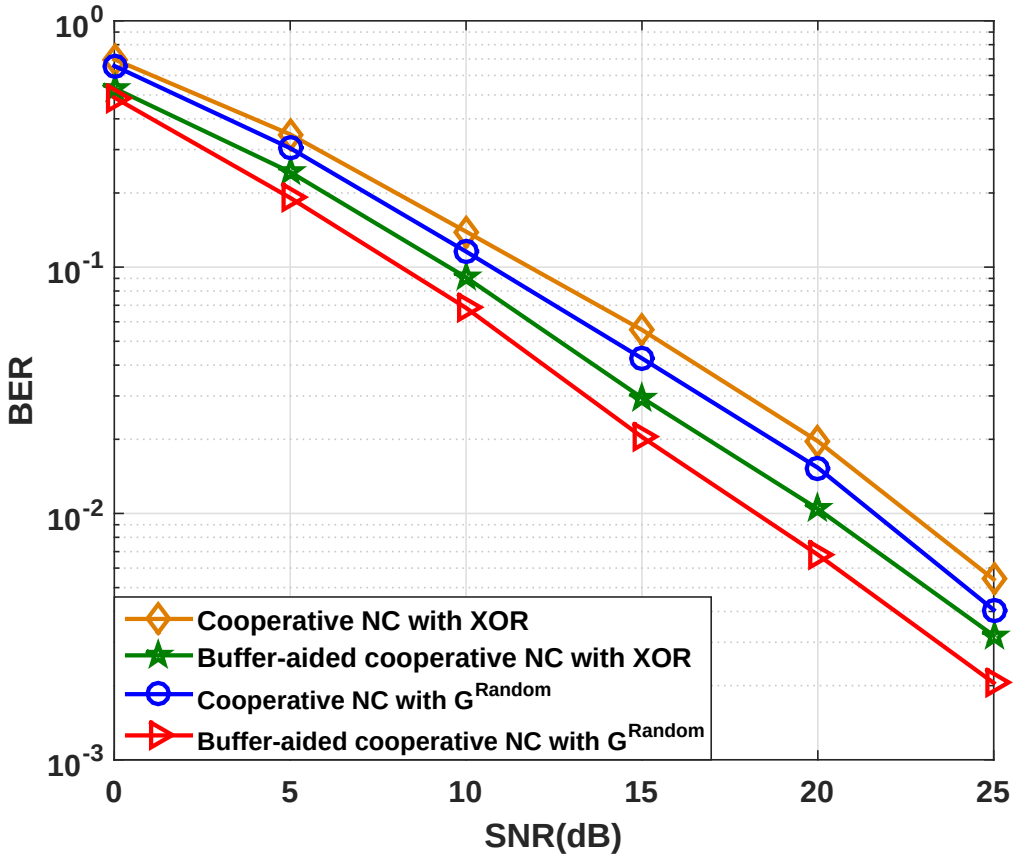

Figure 5.5: Performance comparison between different network coding techniques with buffers and without buffers

The next example shown in Fig. 5.5 illustrates the performance comparison between cooperative transmissions with $K = 6$ users, $L = 6$ relays using different network coding techniques with buffers and without buffers, both scenarios adopt an exhaustive RPS and buffer size $J = 4$. QPSK modulation is employed for all schemes. The results show that linear network coding techniques perform better than the XOR mapping even if only a binary coefficient matrix is generated randomly. Additionally, when relays are equipped with buffers, a significant performance gain is obtained as there is a high possibility that data associated with better propagation conditions or better channels are selected.

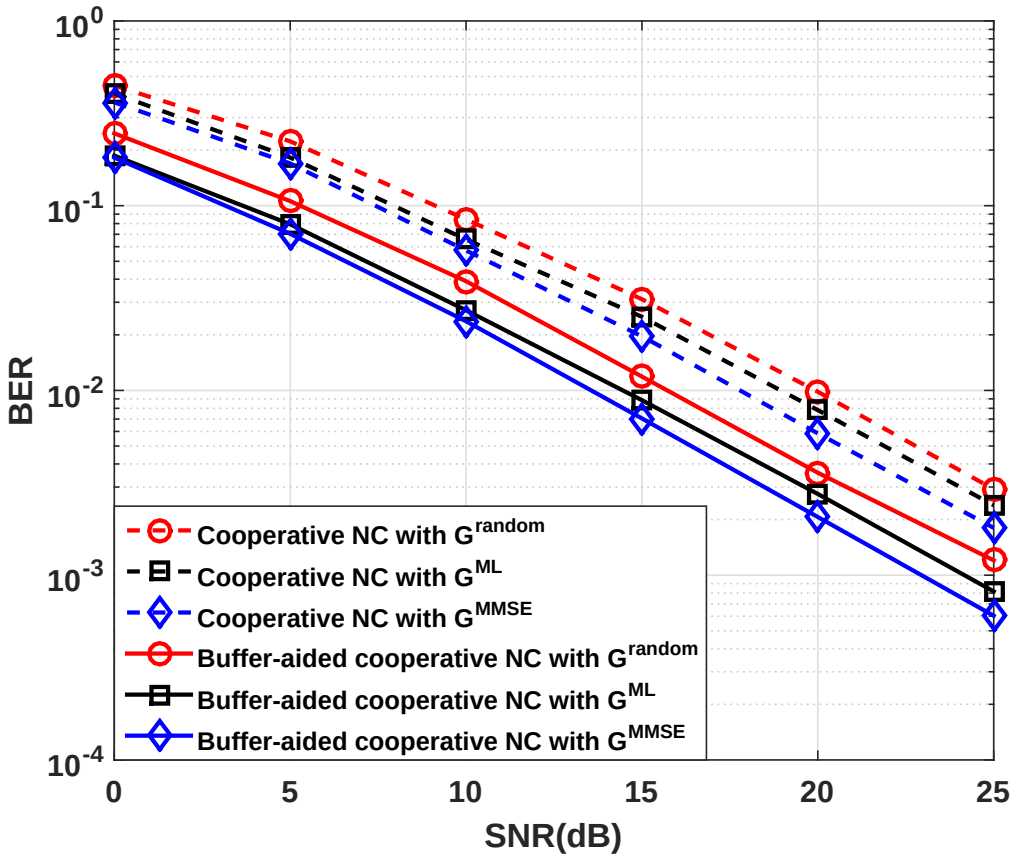

Figure 5.6: Performance comparison between different linear network coding techniques with buffers and without buffers in BPSK modulation

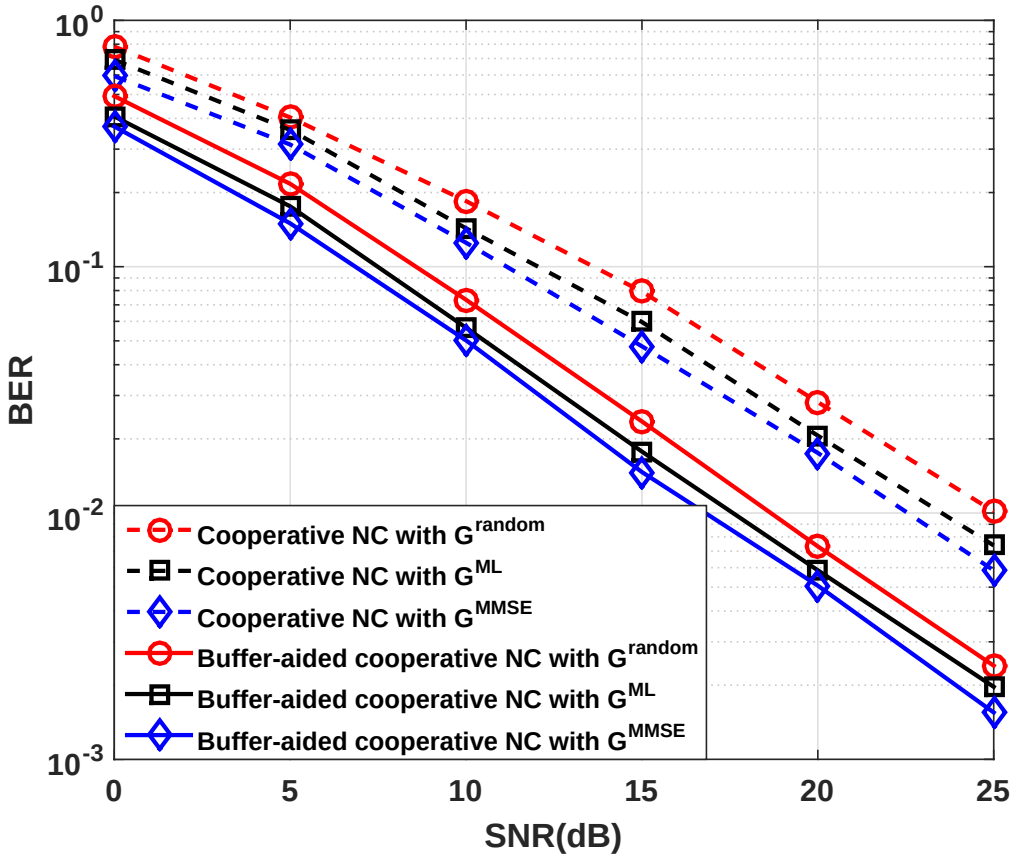

Figure 5.7: Performance comparison between different linear network coding techniques with buffers and without buffers in QPSK modulation

In the forth example shown in Fig. 5.6, the BER performance comparison of buffer-aided ($J = 4$) and non buffer-aided cooperative transmissions with various linear network coding techniques in BPSK modulation are presented. Similarly, we apply $K = 6$ users and $L = 6$ relays in the transmissions, exhaustive RPS is used. We adopted $\mathbf{G}^{\text{random}}$ at the relays for the encoding process when $\mathbf{G}^{\text{MMSE}}$ is employed at the destination for the purpose of decoding. As depicted in Fig. 5.6, the results then show that the introduction of $\mathbf{G}^{\text{MMSE}}$ provides the best performance, followed by the introduction of $\mathbf{G}^{\text{ML}}$ and $\mathbf{G}^{\text{random}}$ that are used at both the relays and the destination, respectively. On the other hand, the results also reveal that with the use of buffers, the overall system performance significantly improves.

In the fifth scenario given by Fig. 5.7, the proposed network coding (linear combination) schemes are also examined with QPSK modulation. Similarly, we apply

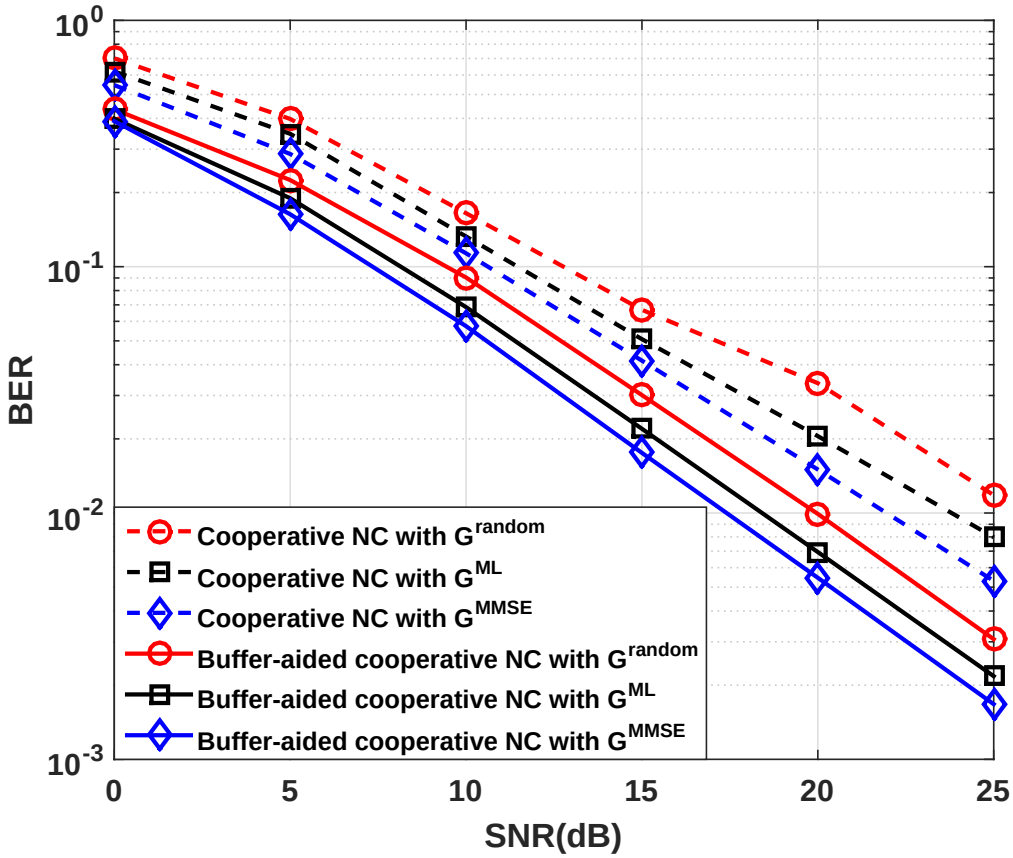

Figure 5.8: Performance comparison between different linear network coding techniques with buffers and without buffers with LS channel estimation

$K = 6$ users and $L = 6$ relays in the transmissions with exhaustive RPS applied. In Fig. 5.7, it is clear that the employ $\mathbf{G}^{\mathrm{MMSE}}$ still provides the best performance and the use of buffers also brings performance improvements with QPSK modulation.

Finally, we test the proposed network coding (linear combination) schemes in QPSK modulation with least-squares (LS) channel estimation applied in Fig. 5.8. We employ $K = 6$ users, $L = 6$ relays and exhaustive RPS is applied in the transmissions, the length of pilot sequence is 1000. Obviously, it can been seen from Fig. 5.8 that, due to the introduction of channel estimation, the performance for all algorithms are slightly degraded. But the adoption of $\mathbf{G}^{\mathrm{MMSE}}$ still has the best performance. In the meantime, extra system performance improvements can still be provided by the equipment of buffers.

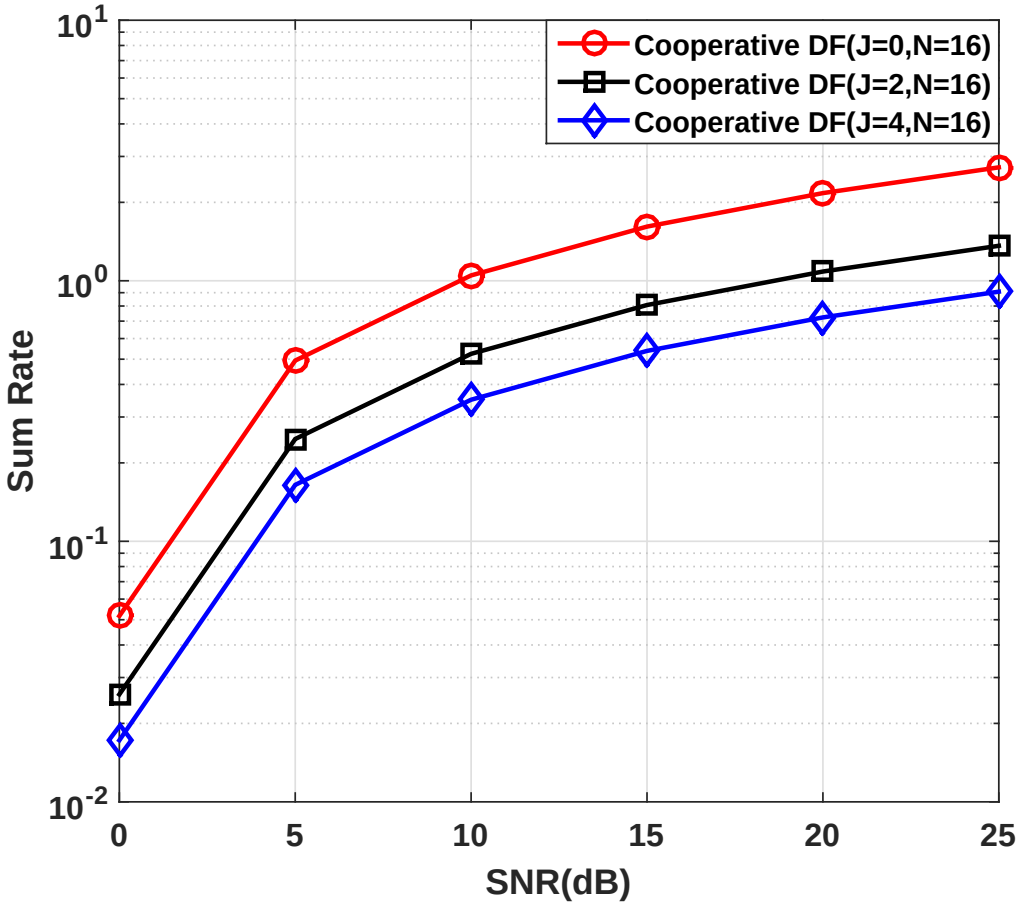

Figure 5.9: Sum rate versus SNR comparison between different buffer size for cooperative DF scheme

Sum rate versus SNR performance

In the following, we simulate the sum rate versus SNR with different buffer size and spreading sequence lengths in the cooperative DS-CDMA system with simple DF and various PNC techniques employed at the selected relays, respectively. Similarly, exhaustive RPS is used with $K = 4$ users and $L = 4$ relays adopted.

As can be seen from Fig. 5.9, the simulation curves suggest that, in a cooperative DS-CDMA system, the simple cooperative DF scheme with smaller buffer size provides the highest sum rate. This fact indicates that the size of buffer has significant influence on the transmission rate, thus, in order to achieve a good balance between the sum rate and average delay caused by the existence of buffers, the size of the buffer needs to be

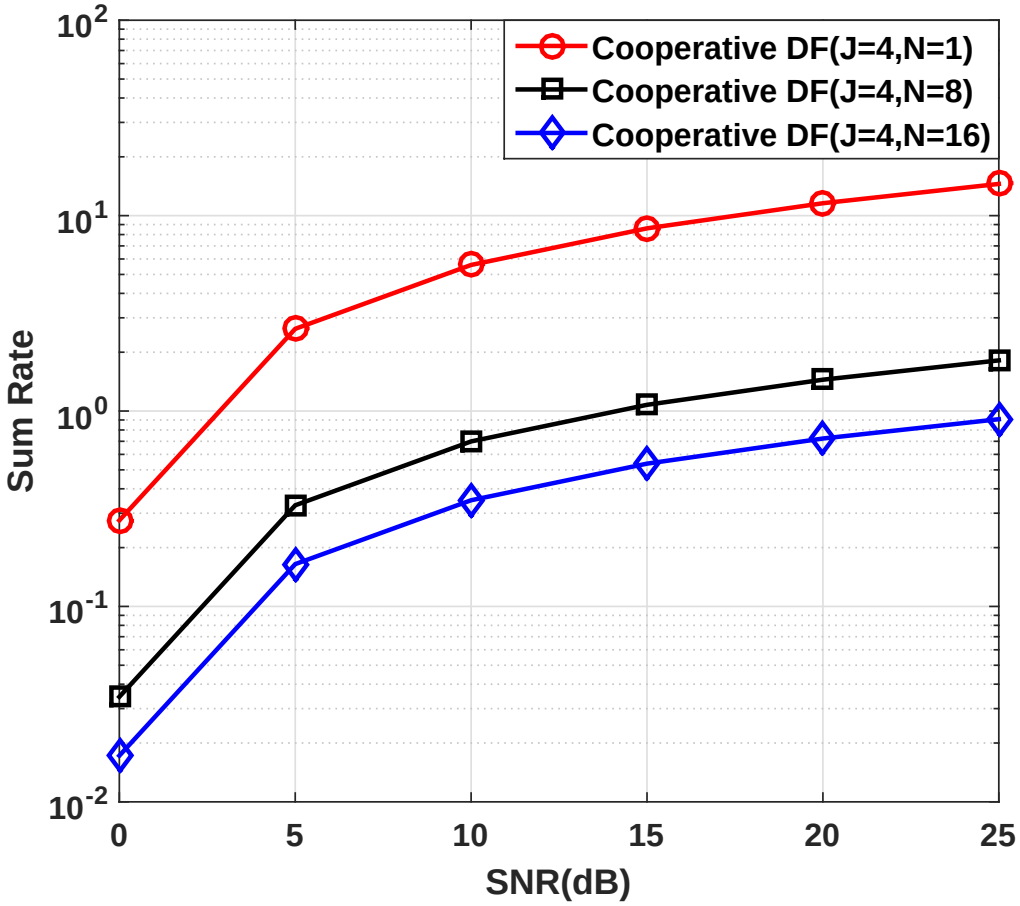

Figure 5.10: Sum rate versus SNR comparison between different spreading sequence length for cooperative DF scheme

carefully controlled and adjusted.

We then examine the effect brought by the introduction of spreading sequence with different lengths when DS-CDMA system is used. Clearly, Fig. 5.10 demonstrates that the simple cooperative DF transmission with shorter spreading sequence lengths presents the highest sum rate. Similarly, this results reveal that higher transmission rate can be achieved with lower spreading sequence or even without employing spreading but this comes at the price of less resistance to interference.

Finally, when referring to the cooperative DS-CDMA system with various PNC techniques applied at relays, we compare the corresponding sum rates versus SNR curves as shown by Fig. 5.11. The simulation results demonstrate that the LNC design

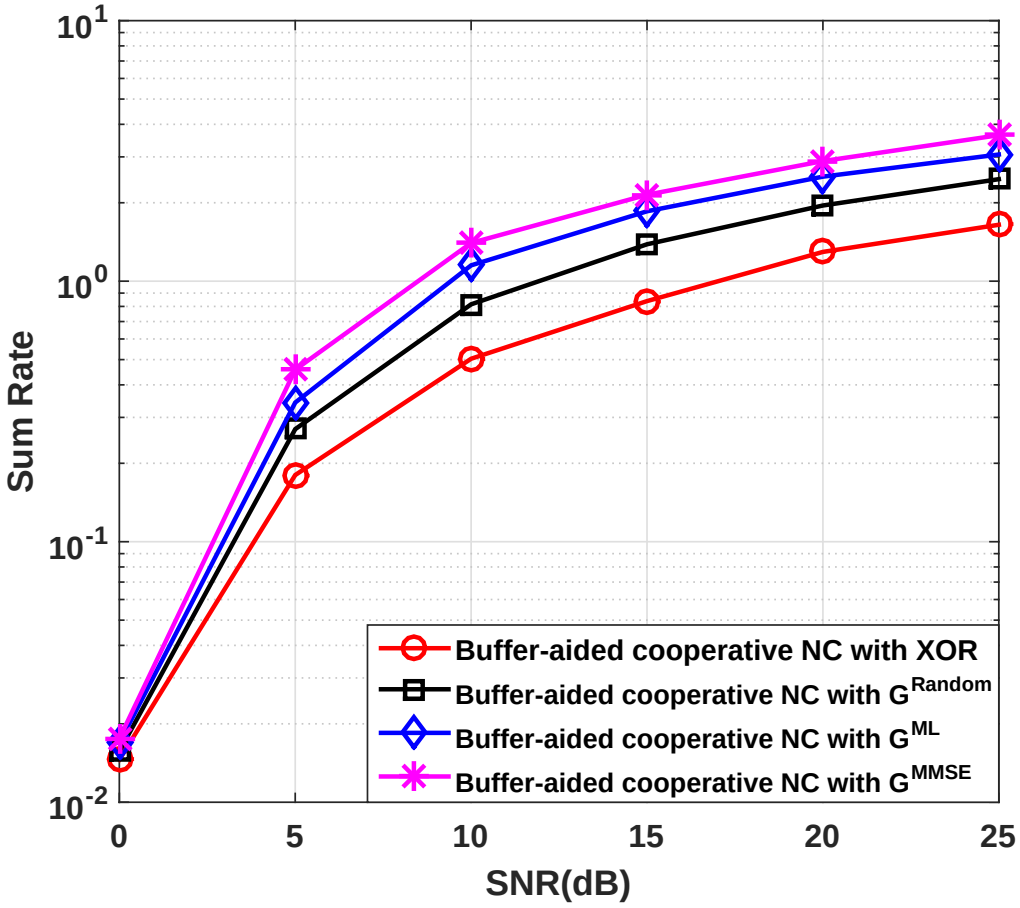

Figure 5.11: Sum rate versus SNR comparison between different network coding techniques

with $\mathbf{G}^{\mathrm{MMSE}}$ provides the highest sum rate under the same level of input SNR, followed by the LNC with $\mathbf{G}^{\mathrm{ML}}$, the LNC with $\mathbf{G}^{\mathrm{Random}}$ and the cooperative network coding design with XOR mapping applied.

5.8 Conclusions

In this chapter, we have presented a buffer-aided PNC scheme for cooperative DS-CDMA systems with different relay pair selection techniques. In particular, we have developed novel linear network coding algorithms with various code matrices according to different criteria for cooperative transmissions based on both an exhaustive search and a greedy approach. Along with the help of buffers, the transmission performance effectively improves. Simulation results show that the performance of the proposed buffer-aided scheme perform better than those without buffers, and the proposed linear network coding designs outperform the existing XOR mapping and linear mapping with randomly generations of coding coefficient. In summary, the proposed designs and algorithms can offer good gains as compared to previously reported techniques.

Chapter 6

Conclusions and Future Work

Contents

6.1 Summary of the Work

In this thesis, a number of novel relaying strategies and relay selection algorithms for dealing with interference cancellation, multipath fading mitigation and information storage are proposed for the application of the cooperative DS-CDMA system. In addition, we also combined these relaying techniques with various channel selection algorithms in order to achieve a good balance between extra performance gain and computational complexity.

In the following, we summarize the work reported in each chapter of this thesis.

In Chapter 3, a greedy list-based successive interference cancellation (GL-SIC) strategy and a greedy list-based parallel interference cancellation (GL-PIC) technique, together with a greedy multi-relay selection algorithm are presented. In particular, both interference cancellation techniques are used at both the relays and the destination in the uplink of the cooperative DS-CDMA system and the main principle of both approaches

is to divide all users into either reliable or unreliable groups for further examinations. Clearly, better detection results can be obtained and acceptable computational complexity can be achieved when the threshold for reliability check is carefully controlled. Moreover, the proposed greedy multi-relay selection algorithms select the optimum relay combination according to the SINR criterion and can approach almost the same level of exhaustive search, whist keeping the complexity reasonable low for practical utilization. Furthermore, we analyze the computational complexity required by the proposed and existing interference cancellation algorithms and the proposed greedy relay selection method, along with the investigation of the cross-layer design.

In Chapter 4, a dynamic buffer-aided cooperative distributed space-time coding (DSTC) scheme that is able to store enough data packets in the corresponding buffer entries according to different criteria is proposed and analyzed. This technique effectively improves the transmission performance by sending the most appropriate data to either the relays or destination at the suitable time instants. Clearly, with carefully control of the buffer size, a balance between good performance and long delay can be achieved. After that, we analyze the computational complexity required by the proposed relay pair selection algorithm, the problem of the average delay brought by the proposed schemes and algorithms, followed by the discussion of the proposed greedy algorithm.

In Chapter 5, a buffer-aided cooperative physical-layer network coding (PNC) scheme that can encode the detected symbols with exclusive-or (XOR) mapping and linear network coding technique at each relay is explored. Similarly, in this design, each relay is equipped with a buffer so that the most suitable symbols are sent to the encoding process when relays are under reception mode. On the other hand, the selected encoded data are sent to the destination side when the corresponding relays are in the transmission mode. Additionally, we have also developed two novel linear network coding designs according to both the ML and MMSE criteria. Finally, an analysis of the computational complexity is discussed.

6.2 Future Work

The application of many of the proposed techniques and algorithms detailed in this thesis can be extended to scenarios and systems outside the scope of this thesis, and based on the contributions of this thesis, the future avenues of relevant research are listed and summarized as below.

- The proposed dynamic buffer-aided design only changes the buffer size according to either the input SINR or the channel conditions. However, in order to broaden the application of this algorithm, there should be several other thresholds or parameters that are able to affect the transmission quality and system reliability.
- The proposed buffer-aided DSTC scheme adopts the Alamouti code for the purpose of simplicity. Clearly, this is the most basic approach, in this case, various DSTC techniques can replace the Alamouti scheme and provide higher transmission performance, including vertical Bell Laboratories Layered Space-Time (V-BLAST) scheme [29], orthogonal space-time block codes (OSTBC) [30], quasi-OSTBC (QOSTBC) [31], linear dispersion codes (LDC) [92] and adaptive DSTC [70].
- The proposed buffer-aided PNC strategy applies only the XOR mapping and two kinds of linear network coding schemes at the relays. Obviously, there are several other alternative PNC schemes such as Random Linear Network Coding [93], adaptive linear network coding [94] and Wireless Network Coding [95], that can be further explored.
- The proposed interference cancellation, buffer-aided DSTC and PNC techniques could be applied to multiple-antenna and multi-carrier systems.

Glossary

AF	**A**amplify and **F**orward
BPSK	**B**inary **P**hase **S**hift **K**eying
BER	**B**it **E**rror **R**ate
BP	**B**asis **P**ursuit
CSI	**C**hannel **S**tate **I**nformation
DS-CDMA	**D**irect **S**equence **C**ode **D**ivision **M**ultiple **A**ccess
DF	**D**ecode and **F**orward
DSTC	**D**istributed **S**pace **T**ime **C**oding
DBAE	**D**ynamic **B**uffer **A**ided **E**xhaustive
DBAG	**D**ynamic **B**uffer **A**ided **G**reedy
EM	**E**lectromagnetic **W**ave
FEC	**F**orward **E**rror **C**oding
FBAE	**F**ixed **B**uffer **A**ided **E**xhaustive
FBAG	**F**ixed **B**uffer **A**ided **G**reedy
GL-SIC	**G**reedy **L**ist-based **S**uccessive **I**nterference **C**ancellation
GL-PIC	**G**reedy **L**ist-based **P**aralle **I**nterference **C**ancellation
LNC	**L**inear **N**etwork **C**oding
MAI	**M**ultiple **A**ccess **I**nterference
MUD	**M**ultiuser **D**etection
ML	**M**aximum **L**ikelihood
MMSE	**M**inimum **M**ean **S**quare **E**rror
MSE	**M**ean **S**quare **E**rror
MF	**M**atched **F**ilter
MB	**M**ultiple **B**ranch

NCS	**N**etwork **C**oded **S**ymbol
OMP	**O**orthogonal **M**atching **P**ursuit
PIC	**P**aralle **I**nterference **C**ancellation
PNC	**P**hysical-layer **N**etwork **C**oding
PSD	**P**ower **S**pectrum **D**ensity
PN	**P**seudorandom **N**oise
QPSK	**Q**uadrature **P**hase **S**hift **K**eying
RPS	**R**elay **P**air **S**trategy
SIC	**S**uccessive **I**nterference **C**ancellation
SER	**S**ymbol **E**rror **R**ate
SINR	**S**ignal to **I**nterference plus **N**oise **R**atio
SNR	**S**ignal to **N**oise **R**atio

References

[1] K. J. R. Liu, A. K. Sadek, W. Su, and A. Kwasinski, *Cooperative Communications and Networking*, 1st ed. Cambridge University Press, 2009.

[2] E. C. Niehenke, "Wireless communications: Present and future: Introduction to focused issue articles," *IEEE Microwave Magazine*, vol. 15, no. 2, pp. 26–35, March 2014.

[3] S. Thomas, *CHAPTER FIVE: Guglielmo Marconi and the Wireless*. Communications: Sending the Message, 1997.

[4] J. G. Proakis, *Digital Communications*, 4th ed. New York, USA: McGraw-Hill, Inc, 2011.

[5] S. Verdu, *Multiuser Detection*. Cambridge, 1998.

[6] ——, "Minimum probability of error for asynchronous gaussian multiple-access channels," *IEEE Trans. Inf. Theory*, vol. IT32, no. 1, pp. 85–96, January 1986.

[7] R. Lupas and S. Verdu, "Linear multiuser detectors for synchronous code-division multiple-access channels," *IEEE Trans. Inf. Theory*, vol. 35, no. 1, pp. 123–136, January 1989.

[8] P. Patel and J. Holtzman, "Analysis of a simple successive interference cancellation scheme in DS-CDMA systems," *IEEE J. Select. Areas Commun.*, vol. 12, no. 5, pp. 796–807, June 1994.

[9] M. K. Varanasi and B. Aazhang, "Multistage detection in asynchronous code-division multiple-access communications," *IEEE Trans. Commun.*, vol. 38, no. 4, pp. 509–519, April 1990.

[10] R. C. de Lamare and R. Sampaio-Neto, "Minimum mean-squared error iterative successive parallel arbitrated decision feedback detectors for DS-CDMA systems," *IEEE Trans. Commun.*, vol. 56, no. 5, pp. 778–789, May 2008.

[11] D. G. Brenna, "Linear diversity combining techniques," *Proceedings of IRE*, vol. 47, no. 6, pp. 1075–1102, June 1959.

[12] J. N. Laneman and G. W. Wornell, "Cooperative diversity in wireless networks: Efficient protocols and outage behaviour," *IEEE Trans. Inf. Theory*, vol. 50, no. 12, pp. 3062–3080, December 2004.

[13] J. N. Laneman, G. W. Wornell, and D. N. C. Tse, "An efficient protocol for realizing cooperative diversity in wireless networks," in *Proc. IEEE Int. Symp. Information Theory (ISIT)*, 2001, p. 294.

[14] J. N. Laneman and G. W. Wornell, "Distributed space-time coded protocols for exploiting cooperative diversity in wireless networks," *IEEE Trans. Inf. Theory*, vol. 49, no. 10, pp. 2415–2425, October 2003.

[15] S. Yiu, R. Schober, and L. Lampe, "Distributed space-time block coding," *IEEE Trans. Wireless Commun.*, vol. 54, no. 7, pp. 1195–1206, July 2006.

[16] R. C. de Lamare and R. Sampaio-Neto, "Blind adaptive MIMO receivers for space-time block-coded DS-CDMA systems in multipath channels using the constant modulus criterion," *IEEE Trans. Commun.*, vol. 58, no. 1, pp. 21–27, January 2010.

[17] Y. Jing and B. Hassibi, "Distributed space-time coding in wireless relay networks," *IEEE Trans. Wireless Commun.*, vol. 5, no. 12, pp. 3524 – 3536, December 2006.

[18] T. Peng, R. C. de Lamare, and A. Schmeink, "Adaptive distributed space-time coding for cooperative MIMO relaying systems," in *2012 International Symposium on Wireless Communication Systems (ISWCS)*, August 2012, pp. 28–31.

[19] S. M. Alamouti, "A simple transmit diversity technique for wireless communications," *IEEE Journal on Selected Areas in Communications*, vol. 16, no. 8, pp. 1451 – 1458, October 1998.

[20] S. Zhang, S. C. Liew, and P. K. Lam, "Hot topic: Physical-layer network coding," *in Proc. Annual Int. Conf. on Mobile Computing and Networking(MobiCom).*, LA, USA, September 2006.

[21] R. Ahlswede, N. Cai, S. Y. R. Li, and R. W. Yeung, "Network information flow," *IEEE Trans. Inf. Theory.*, vol. 46, no. 4, pp. 1204–1216, 2000.

[22] M. Sanna and E. Izquierd, "A survey of linear network coding and network error correction code constructions and algorithms," *International Journal of Digital Multimedia Broadcasting*, vol. 2011, 2011.

[23] S. Y. R. Li, Q. T. Sun, and Z. Shao, "Linear network coding: Theory and algorithms," *Proceedings of the IEEE*, vol. 99, no. 3, pp. 372–387, March 2011.

[24] A. Burr and D. Fang, "Linear physical layer network coding for multihop wireless networks," in *22nd European Signal Processing Conference (EUSIPCO)*, September 2014, pp. 1153–1157.

[25] ——, "Linear physical-layer network coding for 5G radio access networks," in *5G for Ubiquitous Connectivity (5GU), 2014 1st International Conference on*, November 2014, pp. 116–121.

[26] H. Liu, *Signal Processing Applications in CDMA Communications*, 1st ed. Norwood, MA, USA: Artech House, Inc, 2000.

[27] J. H. Lee and C. W. Lee, "Adaptive filters for suppressing irregular hostile jamming in direct sequence spread-spectrum system," in *Military Communications Conference - Crisis Communications: The Promise and Reality, 1987. MILCOM 1987. IEEE*, vol. 1, October 1987, pp. 0118–0122.

[28] A. Jain, "Direct sequence spread spectrum signaling (ph.d. thesis abstr.)," *IEEE Transactions on Information Theory*, vol. 25, no. 3, pp. 369–369, May 1979.

[29] P.W.Wolniansky, G. J. Foschini, G. D. Golden, and R. A. Valenzuela, "V-BLAST: Architecture for realizing very high data rates over the rich-scattering wireless channel," in *Proceedings of URSI International Symposium on Signals, Systems and Electronics*, September 1998, pp. 295 – 300.

[30] V. Tarokh, H. Jafarkhani, and A. R. Calderbank, "Space-time block codes from orthogonal designs," *IEEE Trans. Inf. Theory.*, vol. 45, no. 5, pp. 1456–1467, July 1999.

[31] H. Jafarkhani, "A quasi-orthogonal space-time block code," *IEEE Trans. on Commun.*, vol. 49, pp. 1–4, 2001.

[32] A. A. Kadhim, T. A. Sarab, and H. Al-Raweshidy, "Improving throughput using simple network coding," in *Developments in E-systems Engineering (DeSE)*, December 2011, pp. 454–459.

[33] N. J. A. Harvey, "Deterministic network coding by matrix completion," *M.S. thesis, Dept. Elec. Eng. Comput. Sci., Massachusetts Inst. Technol., Cambridge, MA*, 2005.

[34] N. Jayakumar, K. Gulati, and S. K. A. Sprintson, "Network coding for routability improvement in VLSI," in *Proc. IEEE/ACM Int. Conf. Comput.-Aided Design*, San Jose, CA, November 2003, pp. 820–823.

[35] A. G. Dimakis, P. B. Godfrey, Y. Wu, M. Wainwright, and K. Ramchandran, "Network coding for distributed storage systems," in *Proc. IEEE Int. Conf. Comput. Commun.*, Anchorage, AK, May 2007, pp. 2000–2008.

[36] H. Balli, X. Yan, and Z. Zhang, "Error correction capability of random network error correction codes," in *Proc. IEEE Int. Symp. Inf. Theory*, Nice, France, June 2007, pp. 1581–1585.

[37] S. Jaggi, M. Langberg, S. Katti, D. K. T. Ho, M. Medard, and M. Effros, "Resilient network coding in the presence of byzantine adversaries," *IEEE Trans. Inf. Theory*, vol. 54, no. 6, pp. 2596–2603, June 2008.

[38] R. Dougherty, C. Freiling, and K. Zeger, "Networks, matroids, and non–shannon information inequalities," *IEEE Trans. Inf. Theory*, vol. 53, no. 6, pp. 1949–1969, June 2007.

[39] C. Fragouli, A. Markopoulou, and S. Diggavi, "Active topology inference using network coding," in *Proc. 44th Annu. Allerton Conf. Commun. Control Comput.*, Monticello, IL, October 2006, pp. 1–8.

[40] S. A. Aly and A. E. Kamal, "Network coding-based protection against link failures," in *Proc. IEEE Global Commun.*, New Orleans, LA, November 2008, pp. 1–6.

[41] D. S. Lun, N. Ratnakar, M. Medard, R. Koetter, D. R. Karger, T. Ho, E. Ahmed, and F. Zhao, "Minimum-cost multicast over coded packet networks," *IEEE Trans. Inf. Theory*, vol. 52, no. 6, pp. 2608–2623, June 2006.

[42] C. Gkantsidis, J. Miller, and P. Rodriguez, "Comprehensive view of a live network coding P2P system," in *Proc. Internet Meas. Conf.*, Rio de Janeiro, Brazil, October 2006, pp. 177–188.

[43] J. Sundararajan, M. Medard, M. Kim, A. Eryilmaz, D. Shah, and R. Koetter, "Network coding in a multicast switch," in *Proc. IEEE Int. Conf. Comput. Commun.*, Anchorage, AK, May 2007, pp. 1145–1153.

[44] S. Katti, H. Rahul, W. Hu, D. Katabi, M. Medard, and J. Crowcroft, "XORs in the air: Practical wireless network coding," in *Proc. ACM SIGCOMM*, 2006, pp. 243–254.

[45] J. He and S. C. Liew, "Building blocks of physical-layer network coding," *IEEE Trans. Wireless Commun.*, vol. 14, no. 5, pp. 2711–2728, May 2015.

[46] H. Zhang, L. Zheng, and L. Cai, "Design and analysis of heterogeneous physical layer network coding," *IEEE Trans. Wireless Commun.*, vol. 15, no. 4, pp. 2484–2497, April 2016.

[47] A. Sendonaris, E. Erkip, and B. Aazhang, "User cooperation diversity - parts I and II," *IEEE Trans. Commun.*, vol. 51, no. 11, pp. 1927–1948, November 2003.

[48] L. Venturino, X. Wang, and M. Lops, "Multi-user detection for cooperative networks and performance analysis," *IEEE Trans. Signal Processing*, vol. 54, no. 9, pp. 3315–3329, September 2006.

[49] L. Bai, L. Zhao, and Z. Liao, "A novel cooperation scheme in wireless sensor networks," in *IEEE Wireless Communications and Networking Conference*, Las Vegas, NV, April 2008, pp. 1889–1893.

[50] M. R. Souryal, B. R. Vojcic, and R. L. Pickholtz, "Adaptive modulation in ad hoc DS/CDMA packet radio networks," *IEEE Trans. Commun.*, vol. 54, no. 4, pp. 714–725, April 2006.

[51] M. Levorato, S. Tomasin, and M. Zorzi, "Cooperative spatial multiplexing for ad hoc networks with hybrid ARQ: System design and performance analysis," *IEEE Trans. Commun.*, vol. 56, no. 9, pp. 1545–1555, September 2008.

[52] Y. Jing and H. Jafarkhani, "Single and multiple relay selection schemes and their achievable diversity orders," *IEEE Trans. Wireless Commun.*, vol. 8, no. 3, pp. 1084–1098, March 2009.

[53] P. Clarke and R. C. de Lamare, "Transmit diversity and relay selection algorithms for multi-relay cooperative MIMO systems," *IEEE Trans. Veh. Technol*, vol. 61, no. 3, pp. 1084–1098, March 2012.

[54] M. Ding, S. Liu, H. Luo, and W. Chen, "MMSE based greedy antenna selection scheme for AF MIMO relay systems," *IEEE Signal Process. Lett*, vol. 17, no. 5, pp. 433–436, May 2010.

[55] S. Song and W. Chen, "MMSE based greedy eigenmode selection for AF MIMO relay channels," *IEEE Globecom*, pp. 3628–3632, Anaheim, CA, December. 2012.

[56] S. Talwar, Y. Jing, and S. Shahbazpanahi, "Joint relay selection and power allocation for two-way relay networks," *IEEE Signal Process. Lett*, vol. 18, no. 2, pp. 91–94, February 2011.

[57] J. Tropp, "Greedy is good: Algorithmic results for sparse approximation," *IEEE Trans. Inf. Theory*, vol. 50, no. 10, pp. 2231–2242, October 2004.

[58] R. Flury, S. V. Pemmaraju, and R. Wattenhofer, "Greedy routing with bounded stretch," *IEEE Infocom.*, pp. 1737–1745, Rio de Janeiro, Brazil, April. 2009.

[59] Y. Jia, E. Yang, D. He, and S. Chan, "A greedy re-normalization method for arithmetic coding," *IEEE Trans. Commun.*, vol. 55, no. 8, pp. 1494–1503, August 2007.

[60] R. C. de Lamare, "Joint iterative power allocation and linear interference suppression algorithms for cooperative DS-CDMA networks," *IET, Communications*, vol. 6, no. 13, pp. 1930–1942, September 2012.

[61] W. Chen, L. Dai, K. B. Letaief, and Z. Cao, "A unified cross-layer framework for resource allocation in cooperative networks," *IEEE Trans. Wireless Commun.*, vol. 7, no. 8, pp. 3000–3012, August 2008.

[62] Y. Cao and B. Vojcic, "MMSE multiuser detection for cooperative diversity CDMA systems," in *IEEE Wireless Communications and Networking Conference*, March 2004, pp. 42–27.

[63] P. Li and R. C. de Lamare, "Multiple feedback successive interference cancellation detection for multiuser MIMO systems," *IEEE Trans. Wireless Commun.*, vol. 10, no. 8, pp. 2434–2439, August 2011.

[64] P. Li, R. C. de Lamare, and R. Fa, "Multi-feedback successive interference cancellation with multi-branch processing for MIMO systems"," in *Vehicular Technology Conference (VTC Spring)*, May 2011, pp. 1–5.

[65] C. K. Lo, S. Vishwanath, and R. W. H. Jr., "Relay subset selection in wireless networks using partial decode-and-forward transmission," in *IEEE Vehicular Technology Conference.*, May 2008, pp. 2395–2399.

[66] S. S. Ikki and M. H. Ahmed, "Performance analysis of incremental–relaying cooperative–diversity networks over rayleigh fading channels," *IET Communications*, vol. 5, no. 3, pp. 337–349, February 2011.

[67] S. Wei, "Diversity–multiplexing tradeoff of asynchronous cooperative diversity in wireless networks," *IEEE Trans. Inf. Theory.*, vol. 53, no. 11, pp. 4150–4172, November 2007.

[68] S. Ikki and M. Ahmed, "Performance analysis of cooperative diversity with incremental-best-relay technique over rayleigh fading channels," *IEEE Trans. Commun.*, vol. 59, no. 8, pp. 2152–2161, August 2011.

[69] J. Gu and R. de Lamare, "Joint SIC and multi-relay selection algorithms for cooperative DS-CDMA systems," in *Proceedings of the 22nd European Signal Processing Conference (EUSIPCO)*, September 2014, pp. 556–560.

[70] T. Peng, R. de Lamare, and A. Schmeink, "Adaptive distributed space-time coding based on adjustable code matrices for cooperative MIMO relaying systems," *IEEE Trans. Commun.*, vol. 61, no. 7, pp. 2692–2703, July 2013.

[71] J. Gu and R. C. de Lamare, "Joint interference cancellation and relay selection algorithms based on greedy techniques for cooperative DS-CDMA systems," *EURASIP Jounal on Wireless Communications and Networking*, 2016.

[72] N. Zlatanov, A. Ikhlef, T. Islam, and R. Schober, "Buffer-aided cooperative communications: opportunities and challenges," *IEEE Communications Magazine*, vol. 52, no. 4, pp. 146–153, May 2014.

[73] N. Zlatanov, R. Schober, and P. Popovski, "Throughput and diversity gain of buffer-aided relaying," *IEEE Globecom*, pp. 1–6, Houston, TX, USA, December 2011.

[74] I. Krikidis, T. Charalambous, and J. Thompson, "Buffer-aided relay selection for cooperative diversity systems without delay constraints," *IEEE Trans. Wireless Commun.*, vol. 11, no. 5, pp. 1592–1967, May 2012.

[75] A. Ikhlef, D. S. Michalopoulos, and R. Schober, "Max-max relay selection for relays with buffers," *IEEE Trans. Wireless Commun.*, vol. 11, no. 5, pp. 1124–1135, January 2012.

[76] C. W. Tan and A. Calderbank, "Multiuser detection of Alamouti signals," *IEEE Trans. Commun.*, vol. 57, no. 7, pp. 2080–2089, July 2009.

[77] R. de Lamare and R. Sampaio-Neto, "Adaptive reduced-rank processing based on joint and iterative interpolation, decimation, and filtering," *IEEE Trans. Signal Processing*, vol. 57, no. 7, pp. 2503–2514, July 2009.

[78] ——, "Minimum mean-squared error iterative successive parallel arbitrated decision feedback detectors for DS-CDMA systems," *IEEE Trans. Commun.*, vol. 56, no. 5, pp. 778–789, May 2008.

[79] T. Islam, R. S. A. Iklef, and V. Bhargava, "Diversity and delay analysis of buffer-aided BICM-OFDM relaying," *IEEE Trans. Wireless Commun.*, vol. 12, no. 11, pp. 5506 – 5519, November 2013.

[80] D. P. Bertsekas and R. G. Gallager, *Data Networks*, 2nd ed. Englewood Cliffs, N.J.: Prentice-Hall, Inc, December, 1991.

[81] M. Bouanen, W. Ajib, and H. Boujemaa, "Throughput and delay analysis of truncated cooperative ARQ protocols using DSTC," in *7th International Wireless Communications and Mobile Computing Conference (IWCMC)*, July 2011, pp. 731–736.

[82] Y. Gong and K. Letaief, "Performance evaluation and analysis of space-time coding in unequalized multipath fading links," *IEEE Trans. Commun.*, vol. 48, no. 11, pp. 1778–1782, November 2000.

[83] Z. Sheng, Z. Ding, and K. Leung, "Transmission delay analysis with finite coding length in wireless cooperative networks," in *IEEE Global Telecommunications Conference*, November 2009, pp. 1–6.

[84] L. Yang, T. Tang, Y. Xie, J. Yuan, and J. An, "Linear physical-layer network coding and information combining for the k-user fading multiple-access relay network," *IEEE Trans. Wireless Commun.*, vol. 15, no. 8, pp. 5637–5650, August 2016.

[85] M. Nokleby and B. Aazhang, "Cooperative compute-and-forward," *IEEE Trans. Wireless Commun.*, vol. 15, no. 1, pp. 14–27, January 2016.

[86] P. A. Chou and Y. Wu, "Network coding for the internet and wireless networks," in *Tech. Rep.,Microsoft Research*, 2007.

[87] N. Cai and T. Chan, "Theory of secure network coding," *Proceedings of the IEEE*, vol. 99, no. 3, pp. 421–437, March 2011.

[88] R. W. Yeung and N. Cai, "Network error correction. I. basic concepts and upper bounds," *Communications in Information & Systems*, vol. 6, no. 1, pp. 19–35, 2006.

[89] K. Jain, L. Lovasz, and P. A. Chou, "Building scalable and robust peer-to-peer overlay networks for broadcasting using network coding," *Distributed Computing*, vol. 19, no. 4, pp. 301–311, March 2007.

[90] M. Huemer, C. Hofbauer, and J. B. Huber, "Non-systematic complex number RS coded OFDM by unique word prefix," *IEEE Trans. Signal Processing*, vol. 60, no. 1, pp. 285–299, January 2012.

[91] I. E. Telatar, "Capacity of multi-antenna gaussian channels," *AT&T Bell Laboratories, Internal Tech. Memo*, June 1995.

[92] B. Hassibi and B. Hochwald, "High-rate codes that are linear in space and time," *IEEE Trans. Inf. Theory*, vol. 48, no. 7, pp. 1804–1824, July 2002.

[93] T. Ho, R. Koetter, M. Medard, D. R. Karger, and M. Effros, "The benefits of coding over routing in a randomized setting," in *Proceedings. IEEE International Symposium on Information Theory*, June 2003, p. 442.

[94] A. Burr and D. Fang, "Performance of adaptive linear physical layer network coding," in *Proceedings of 20th European Wireless Conference*, Barcelona, Spain, May 2014, pp. 1–6.

[95] M. H. Firooz, Z. Chen, S. Roy, and H. Liu, "Wireless network coding via modified 802.11 MAC/PHY: Design and implementation on SDR," *IEEE J. Select. Areas Commun.*, vol. 31, no. 8, pp. 1618–1628, August 2013.